CHARACTERIZATION OF IMPREGNATED COMMERCIAL RICE HUSKS ACTIVATED CARBON WITH MONOETHANOLAMINE (MEA) AND DIETHANOLAMINE (DEA) AS POTENTIAL CO_2 ADSORBENT

SITI NORAISHAH BINTI MASOUM RAMAN

BACHELOR OF CHEMICAL ENGINEERING

UNIVERSITI MALAYSIA PAHANG

CHARACTERIZATION OF IMPREGNATED COMMERCIAL RICE HUSKS ACTIVATED CARBON WITH MONOETHANOLAMINE (MEA) AND DIETHANOLAMINE (DEA) AS POTENTIAL CO_2 ADSORBENT

SITI NORAISHAH BINTI MASOUM RAMAN

A thesis submitted in fulfilment of the
requirements for award of the degree of
Bachelor of Chemical Engineering

Faculty of Chemical Engineering & Natural Resources
Universiti Malaysia Pahang

JULY 2014

SUPERVISOR'S DECLARATION

"I hereby declare that I have checked this thesis and in my opinion, this thesis is adequate in terms of scope and quality for the award of the degree of Bachelor of Chemical Engineering"

Signature : ……..

Name of Supervisor : Nur Aminatulmimi Ismail

Position : URP Supervisor

Date : 1 July 2014

STUDENT'S DECLARATION

I declare that thesis entitle *"Characterization of Impregnated Commercial Rice Husks Activated Carbon with Monoethanolamine (MEA) and Diethanolamine (DEA) as Potential CO_2 Adsorbent"* is the result of my own research except as cited in the references. The thesis has not been accepted for any degree and is not concurrently submitted in candidature of any other degree.

Signature : ……...

Name : Siti Noraishah Binti Masoum Raman

Date : 1 July 2014

To my wonderful life,

Thanks for the enjoyment and happiness,

Sorry for the hardship and tears.

ACKNOWLEDGEMENT

Bismillahirrahmanirrahim and Alhamdulillah. Praise to Allah S.W.T. for His help and guidance that I finally able to complete this Undergraduate Research Project.

First and foremost I would like to thank my supervisors; Madam Nur Aminatulmimi Ismail for giving me the opportunity to work on this interesting project and also, willingness in overseeing the progress of my works from its initial phases till the completion of it. I do believe that all her advice and comments are for the benefit of producing the best thesis quality.

I am also very thankful to my beloved father, my lovely mother and all my family members for their support and motivation. Without their support, the completion of this thesis will be more difficult. I am grateful to everybody that involves directly or indirectly helping me completing this thesis.

I would also like to take this opportunity to thank all lecturers who involved directly and indirectly in helping me to complete this research. For personnel at FKKSA technical staffs, thank you very much for your guidance, trust and assistance.

To my friends and course mates, that giving endless helps and support, thank you very much, especially during the experimental works in the laboratory. Thanks to former and present colleagues at Universiti Malaysia Pahang for making an enjoyable working environment and giving me ideas, opinions and advices. Thank you again.

PENCIRIAN PERCANTUMAN KARBON AKTIF SEKAM PADI KOMERSIAL DENGAN MONOETANOLAMINA (MEA) DAN DIETANOLAMINA (DEA) YANG BERPOTENSI SEBAGAI PENJERAP KARBON DIOKSIDA

ABSTRAK

Kajian daripada pencirian percantuman karbon aktif dengan monoethanolamine (MEA) dan dietanolamina (DEA) sebagai kebolehan penjerap karbon dioksida (CO_2) telah dijalankan. Kapasiti penjerapan karbon aktif boleh ditingkatkan dengan memperkenalkan kumpulan amina pada permukaan bahan penjerap tersebut. MEA dan DEA telah dipilih sebagai sebatian amino untuk proses percantuman permukaan karbon aktif. Sintesis karbon aktif yang tercantum telah disediakan mengikut kepekatan dan nisbah campuran. Ciri fizikokimia karbon aktif yang tercantum telah disifatkan oleh *X-Ray Diffraction* (XRD), *Brunauer, Emmett and Teller* (BET), *Fourier Transform Infrared Spectroscopy* (FTIR) dan *Field Emission Scanning Electron Microscopy* (FESEM). Analisis XRD telah digunakan untuk menentukan kehadiran jenis sebatian pada permukaan karbon aktif. Hasil kajian menunjukkan bahawa sudut pembelauan sekitar 21.66º 22.18º yang dihubungkan untuk pyrazole, ethanolamine dan dietanolamina membuktikan kehadiran hidrokarbon dan amina pada permukaan karbon aktif. Daripada analisis BET, jumlah luas permukaan dan isipadu liang menurun dengan peningkatan kepekatan MEA dan DEA. Kehadiran kumpulan amida dalam analisis FTIR pada jalur 3288 cm^{-1} dan 1651 cm^{-1} untuk karbon aktif yang tercantum membuktikan terdapat satu tindak balas berlaku antara kumpulan karboksil pada permukaan karbon aktif dengan amina terikat. Bagi analisis FESEM, ia menunjukkan bahawa morfologi karbon aktif tanpa cantuman mengandungi banyak liang di permukaannya manakala liang di karbon aktif tercantum dengan MEA dan DEA telah dipenuhi dengan amina mengikut kepekatan yang dipilih. Penemuan dari penyelidikan ini memberitahu terdapat potensi yang tinggi untuk kapasiti penjerapan CO_2 apabila hasil pencirian menunjukkan maklum balas yang positif terhadap kuantiti MEA dan DEA dalam sampel percantuman karbon aktif.

CHARACTERIZATION OF IMPREGNATED COMMERCIAL RICE HUSKS ACTIVATED CARBON WITH MONOETHANOLAMINE (MEA) AND DIETHANOLAMINE (DEA) AS POTENTIAL CO_2 ADSORBENT

ABSTRACT

The studies characterization of impregnated activated carbon with monoethanolamine (MEA) and diethanolamine (DEA) as potential carbon dioxide (CO_2) adsorbent was successfully performed. The adsorption capacity of the activated carbon can be increased by introducing the amine group on the surface of the adsorbent. MEA and DEA were selected as amino compounds for the binding process on the activated carbon surface. The synthesis of the impregnated activated carbon was prepared according to the concentration and mixture ratio. The physicochemical properties of the impregnated activated carbon were characterized by X-Ray Diffraction (XRD), Brunauer, Emmett and Teller (BET), Fourier Transform Infrared Spectroscopy (FTIR) and Field Emission Scanning Electron Microscopy (FESEM). The XRD analysis was used to determine the type of compound presence on the activated carbon surface. The result reveals that the diffraction angles around 21.66º to 22.18º were linked for pyrazole, ethanolamine and diethanolamine which prove the presence of hydrocarbon and amine on the activated carbon surfaces. From the BET analysis, the total surface area and pore volume decreased with the increase of concentration of MEA and DEA. The presence of amide functional groups in FTIR analysis at 3288 cm^{-1} and 1651 cm^{-1} band for the impregnated activated carbon proved that there was a reaction occurs between carboxyl groups on the activated carbon surfaces with amine bonded. As for FESEM analysis, it was shown that the morphology of the non-impregnated activated carbon contains many pores on its surface while the pores on the impregnated activated carbon with MEA and DEA were filled with amines according to the selected concentration. The findings signify the high potential of CO_2 adsorption capacity as the characterization results shows a positive feedback towards the quantity of MEA and DEA in the impregnated activated carbon samples.

TABLE OF CONTENTS

LIST OF TABLES

LIST OF FIGURES

LIST OF ABBREVIATIONS

AC	Activated carbon
BET	Brunauer, Emmett and Teller isotherm
DEA	Diethanolamine
FESEM	Field Emission Scanning Electron Microscopy
FTIR	Fourier Transform Infrared Spectroscopy
MEA	Monoethanolamine
XRD	X-Ray Diffraction

LIST OF SYMBOLS

^{o}	Degree.
C	Constant value, characteristics of the adsorbate.
N_A	Avogadro constant.
m	Mass of test powder.
θ	Fraction of surface of covered by adsorbed molecules.
P	Gas pressure.
P_0	Saturated pressure of adsorbate gas.
S	Surface area of solid.
V_a	Volume of gas adsorbed at standard temperature and pressure.
V_m	Volume of gas adsorbed at STP to produce an apparent monolayer on the sample surface.

LIST OF APPENDICES

CHAPTER 1

INTRODUCTION

The topic for this research is Characterization of Impregnated Commercial Rice Husks Activated Carbon with Monoethanolamine (MEA) and Diethanolamine (DEA) as Potential CO_2 Adsorbent. Activated carbon is a form of carbon processed which is known to have a large surface area for adsorption process. This research investigates the characterization of activated carbon for adsorption process with and without the aid of MEA and DEA.

1.1 Background of Study

Global warming is the term used to describe a gradual increase in the average temperature of the Earth's atmosphere and its oceans, a change that is believed to be

permanently changing the Earth's climate. The major contribution of this problem is because of the release of acidic gases such as carbon dioxide (CO_2), sulphur dioxide (SO_2) and hydrogen sulphide (H_2S) from human's activity like industrial revolution and destruction of forests. U.S. Department of State (2007) states that many industrial processes emit CO_2 through fossil fuel combustion and several processes produce CO_2 emissions through chemical reactions that do not involve combustion, for example, the production and consumption of mineral products such as cement, the production of metals such as iron and steel, and the production of chemicals. By increasing the concentration of CO_2 gases, the infrared energy emitted by the surface will be increased and being absorbed by the atmosphere. The extra energy from the warmer atmosphere will radiates back to the Earth's surface thus, increase the surface temperature.

The present of adsorbent may help in reducing the CO_2 level in the atmosphere. In commercial processes, the adsorbent is usually in the form of small particles (solid) in a fixed bed and the fluid (liquid or gas) passed through the bed before being adsorbed by the solid particles (Geankoplis, 2003). Adsorption is systematic in most natural physical, biological, and chemical aspect, and is widely used in industrial applications such as activated charcoal, synthetic resins and water purification. There are many types of physical and chemical adsorbent that can be used to adsorb acidic gas such as activated carbons and zeolites for physical adsorbent while alkali metal carbonates and amine-based material for chemical adsorbent. Zeolites have a high capacity for CO_2 capture but it is expensive whereas carbon-based materials are abundant, cheap, easy to make, and chemically and hydrothermally stable, but their selectivity for CO_2 is low in the presence of other gases such as Nitrogen (N_2), Hydrogen (H_2) and Methane (CH_4) (Wang et al., 2010). However, the basic amine group is an ideal functionality to strongly interact with acidic CO_2 molecules (Lin et al., 2013).

There are many primary raw materials that have high carbon content that can be used as activated carbon such as coal, wood, palm shell and coconut shell. Activated carbon is the most versatile and frequently used sorbent for environmental control in the form of a fixed bed due to its large internal surface area and pore volume, and its ability to adsorb organic vapors at low cost (Jahangiri et al., 2013). The huge surface area of activated carbon gives it many bonding sites which can be used to trapped chemical for adsorption process. The carbon-based material is converted to activated carbon by thermal decomposition in a furnace using a controlled atmosphere and heat (Deithorn & Mazzoni, 2013). The heating process is called pyrolysis which means thermochemical decomposition of organic material at elevated temperatures in the absence of oxygen (or any halogen).

One of the carbon-based materials that can be used as activated carbon is rice husk. Rice husk is one of the main agriculture wastes in many rice producing countries. Rice husk is the outermost layer of paddy grain which is produced in the first step of milling process and makes up about 20% of the rice (paddy). The rice husk is then undergoing the activation process with used of furnace and steam boiler to become an activated carbon. In Malaysia, the production of rice is increases annually from 2.7 million tonnes in 1985 to 4 million tonnes in 2009 because of the increasing population (Arshad et al., 2011). With the high number of rice produced, the rice husk activated carbon production will also be increased.

1.2 Problem Statement

Acidic gases such as CO_2 gas can lead to environmental problem such as greenhouse effect and global warming. The CO_2 gas does not only elevate global temperature; it also

gives negative impact to human health because its higher concentrations can affect respiratory function and thus, resulting in lower concentrations for breathing (Subki et al., 2011). Therefore it is important to control the release of CO_2 gas to the atmosphere to minimise the environmental problem. The rice husk ash, if properly been treated can be a good source of activated carbon that can be used to adsorb the CO_2 gas. In Malaysia, the production of rice is increases annually as the demand for rice is increasing within country and outside the country. Generally, farmers and rice processor often burn the rice husk as wastes and most of the rice husks are not commercially used. Burning of rice husk in ambient atmosphere leaves a residue, called rice husk ash which will cause damage to land and surrounding area where it is dumped (Kumar et al., 2012).

1.3 Research Objective

The objective of this research is to study the comparison between the non-impregnated activated carbon with the impregnation of MEA and DEA with activated carbon at different concentration and mixture ratio.

1.4 Scopes of Study

The activated carbon being used in this research is made from rice husk ash. The rice husk ash is produced with used of furnace and steam boiler. The research is conducted according to three main variables that is the absent of MEA and DEA with activated carbon,

impregnation of MEA and DEA with activated carbon at different concentration and impregnation of MEA and DEA mixture with activated carbon at different mixture ratio. The characterization of the activated carbon with and without the impregnation of MEA and DEA will be observe by using several methods such as X-Ray Diffraction (XRD) analysis, Brunauer, Emmett and Teller's (BET) isotherm, Fourier Transform Infrared Spectroscopy (FTIR) analysis and Field Emission Scanning Electron Microscopy (FESEM) analysis.

1.5 Significance of Study

This research is done to produce an adsorbent from the rice husk activated carbon. The activated carbon is impregnated with MEA and DEA to increase the adsorption capacity of acidic gases such as CO_2. The adsorption of these acidic gases will help to reduce the environmental problem such as global warming greenhouse effect. The study is done with different concentration and mixture ratio of MEA and DEA to identify the optimum concentration and mixture ratio of the adsorbent that going to be used. This research provides several benefits such as reduce the amount of acidic gas in air and improve the environment air quality. With a good quality of air, human health and environment problems can be reduced. It is hope that this research may give a good impact for environment, especially and therefore, will give benefits to the community.

CHAPTER 2

LITERATURE REVIEW

This chapter provides the general ideas on the subject that are going to be study including the background and introduction of rice husk, activated carbon as adsorbent, impregnation of activated carbon with amine and characterization of impregnated and non-impregnated activated carbon.

2.1 Rice Husk as Activated Carbon

Each year, approximately 600 million tons of rice paddy is produced globally and there are more than seventy countries in the world produce rice including China, India, and Indonesia (Kumar et al., 2013). 20% of the rice paddy is husk, giving an annual total production of 120 million tons (Shelke et al., 2010). Rice husk is a by-product of the rice milling process and usually treated as agricultural waste (Kermani et al., 2006). Rice husks

are the hard protecting coverings of grains of rice which is made from hard materials such as opaline silica and lignin in order to protect the seed during the growing season (Subki et al., 2011). The presence of large amount of hydrocarbon such as cellulose and lignin content made the rice husk to be used as a raw material for preparation of activated carbons that contain complex porous structures (Kumar et al., 2012). The high silica content also contributes the formation of residual carbon in the rice husk (Javed et al., 2010). Porous carbon derived from the rice husks has wide availability, has fast kinetics and appreciable adsorption capacities too (Chen et al., 2011). At the temperature from 500 to 700°C, rice husk may be carbonized for a certain period of time and after the thermal decomposition, rice husk would become granular charcoal (Chien, C. C., 2013). The thermal decomposition enables the formation of pores on the surface of the activated carbon. An increase on number of pores and the size of pores made the surface area of the activated carbon larger. According to Allwar (2012), an activated carbon usually consists of three types of pores which are micropores (diameter < 2 nm), mesopores (diameter 2 – 50 nm), and macropores (diameter > 50 nm). The function of micropores and mesopores is to give the carbon its adsorptive capacity whereas micropores allow the access of adsorbate into the micropores and mesopores (Mdoe & Mkayula, 2002). The rice husk that has been processed as activated carbon can be used widely in many applications such as chemical adsorbent and fuel in power plant. The high availability and low price makes extra benefit towards the use of this material in many industries.

2.2 Activated Carbon as Adsorbent

Gas adsorption is a separation process in which a gaseous component is separated from a gas stream with the use of a solid material known as adsorbent (Spigarelli & Kawatra, 2013). Activated carbon is usually used as adsorbent for environmental control in the form of a fixed bed due to its large internal surface area and pore volume, and its ability to adsorb organic vapors at low cost (Jahangiri et al., 2013). Specific surface area, size and porosity are some of the physical properties of carbons while surface functional groups such as carboxyl and anhydrides are the chemical properties of activated carbon (Meng et al., 2009). Large surface area is a result of creation of additional micropores and probably widening of the existing one, hence, increase in active sites as well as accessibility to the sites (Mdoe & Mkayula, 2002). The types of activated carbon that usually being used as adsorbent is granular (0.2 – 5 mm) and palletised (> 5 mm) because of their low pressure drop and high mechanical strength (Dali et al., 2012). Activated carbon has a very large pore volume especially in the mesopore range resulting from the activation process. Activation process of carbon would tend to increase the number of active sites, and in turn the surface activity, similar to observed reactions with higher activates (Cameron Carbon Incorporated, 2006). Physical adsorption occurs when weak Van der Waals force of attraction hold the organic molecules on the surface and in the pores of the adsorbent and is generally characterized by low heat absorption (Ray & Altshuer, 2013). Harmful gas such as CO_2 and H_2S is usually being adsorbed before released to the atmosphere. Adsorption is considered to be one of the most promising methods of mitigating fossil fuel CO_2 emissions and it has accepted recently nationwide (Snape et al., 2004). CO_2 gas is known as the major greenhouse gas which means it absorbs and emits radiation in the infrared range. The CO_2 gas does not only increase global temperature; it also gives drawbacks to human health because its higher concentrations

can affect respiratory function and thus, resulting in lower concentrations for breathing (Subki et al., 2011). Therefore it is important to adsorb the harmful gas especially CO_2 gas before it been released to the atmosphere to minimise the environmental problem.

2.3 Impregnation of Amine with Activated Carbon

Carbon-based materials are abundant, cheap, easy to make, and chemically and hydrothermally stable, but their selectivity for CO_2 and other acidic gases is low in the presence of other gases such as N_2, H_2 and CH_4 (Wang et al., 2010). The carbon-based materials sorption capacity can be improved by using amine solution as the impregnator of the porous materials as the amine is characterized by a high absorption capacity in relation to CO_2 (Bukalak et al., 2013). CO_2 adsorption capacity also can be enhanced by impregnation of amine and ammonia on the surface of adsorbent (Boonpoke et al., 2011). The carbon based material is high in alkalinity and the amine will be stabilized on the surface so that the amine can be prevented from dissociating (Liang et al., 1995). In the direct method, amine will condense with carboxyl group on the activated carbon to form amide which is used in CO_2 captured (Houshmand et al., 2011). The impregnation of large amounts of amines is good on the mesoporous carbons having high surface area, large pore volumes and specific surface properties (Wang et al., 2012). The common amine used to make adsorbent is MEA, DEA and Polyethlenimine and Piperazine. Aqueous solutions of amines such as MEA have been used by industry as absorbents for acid gas such as CO_2 and H_2S (Drage et al., 2006). However, liquid amine is not a good choice for absorbent of the acidic gas as it needs high cost and creates several issues such as solvent leakage and corrosion. The integration of

organic amines into porous material such as activated carbon may help to reduce these problems. Solid-supported amine sorbents offer many advantages for CO_2 capture such as potential elimination of corrosion problems and lower energy cost for sorbent regeneration (Qi et al., 2010). The impregnated activated carbon with MEA would develop many active sites on the surface and inside the pores of the activated carbon particles through chemisorption, thus the probability to adsorb CO_2 molecules is higher (Khalil et al., 2011). DEA is a secondary amine and superior absorbents compared to MEA, a primary amine (Warudka, S. S., 2011). According to Kim et. al. (2013), the breakthrough curve of MEA absorption rate is more than DEA absorption rate. This means that the DEA absorption rate and capacities is faster than MEA.

2.4 Impregnated and Non-Impregnated Activated Carbon

In the previous research, it is shown that impregnated activated carbon has a higher adsorption capacity than the non-impregnated activated carbon. Jahangiri et al. (2013) stated that the activated carbon impregnated with a nickel nitrate catalyst precursor and carbon nanofibers lasted about 50% longer than those activated carbon alone with a same weight of adsorbent. Activated carbon consists of acidic and basic surfaces. Figure 1 shows the acidic groups and basic groups on the surface of activated carbon.

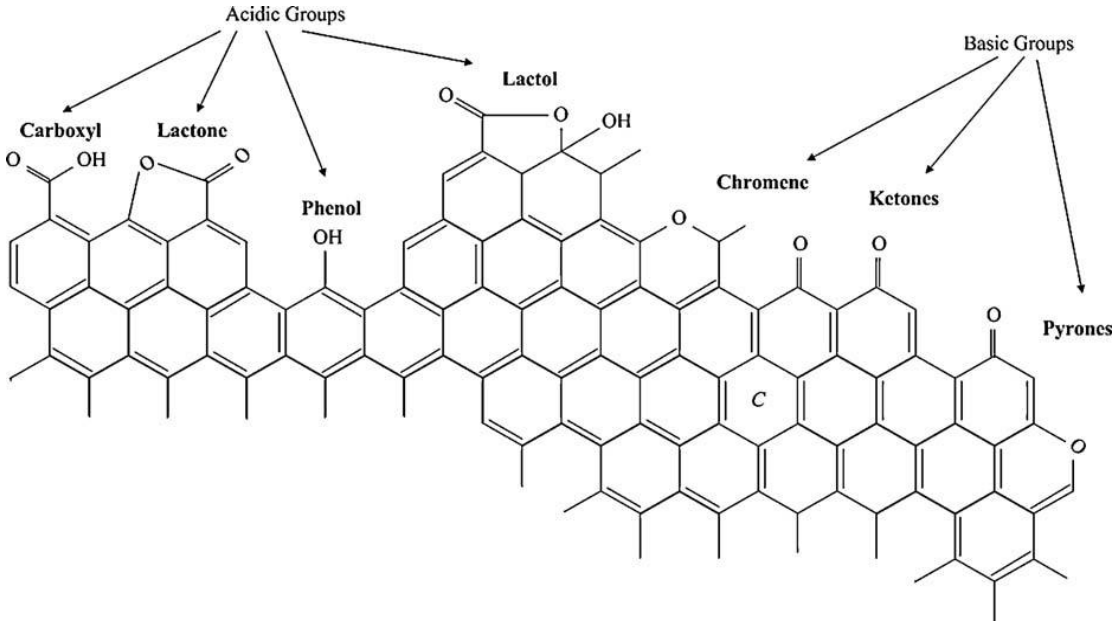

Figure 2.1: Acidic and basic surface functionalities on a carbon basal plane.

(Source: Shafeeyan et al., 2010)

Carbon dioxide is an acidic gas. As the CO_2 gas interact with activated carbon, the basic groups of activated carbon will be attract to adsorb the CO_2 gas. Ammonia will decompose to free radicals such as NH_2, NH, and atomic hydrogen and nitrogen when the carbon materials are treated with ammonia at high temperatures (Shafeeyan et al., 2010). The monoethanolamine (MEA) is a primary amine while diethanolamine (DEA) is a secondary amine. Below is the reaction of primary and secondary amine with CO_2:

Primary Amines: $CO_2 + R_1NH_2 \rightleftharpoons R_1NHCOO^- + H^+$ (2.1)

Secondary Amines: $CO_2 + 2R_1R_2NH \rightleftharpoons R_1R_2NCOO^- + R_1R_2NH_2^+$ (2.2)

The effectiveness of the impregnation of the sample modified with DEA has been confirmed that the impregnation of porous materials using amine solutions can help to improve their sorption capacity and the research carried out at 25°C (Bukalak et al., 2013).

2.5 Characterization of Impregnated and Non-Impregnated Activated Carbon

After the process of impregnation of amine on the activated carbon, a series of analysis being done to determine the physical and chemical characteristics of the experiment. The analysis includes the use of equipment such as XRD, BET, FTIR and FESEM.

2.5.1 X-Ray Diffraction (XRD)

Based on the study carried out by Kumar et al. (2012), it shows that the pyrolysis process of rice husk produces 75-90% organic matter such as cellulose and lignin. Based on Figure 2.2, the presence of carbon in the analysis indicates that the rice husk ash can be used as activated carbon and adsorbent.

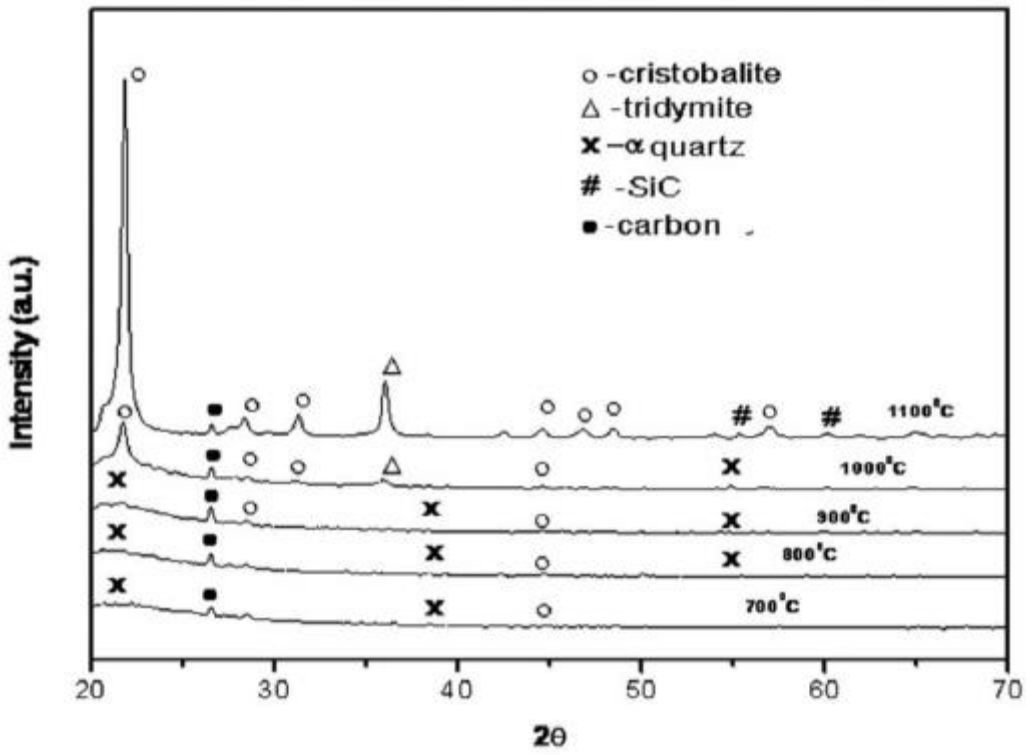

Figure 2.2: XRD analysis of rice husk pyrolysed at different temperature.

(Source: Kumar et al., 2012)

According to Lee et al. (2013), the diffraction peaks located at 2θ = 6.0 – 6.5º can clearly be observed, as the higher intensity of diffraction peak shows a lower amine concentration. The type of amine used also shows different diffraction peak where isopropanol amine (IPA) has a lower peak compared to tetraethylenepent amine (TEPA) and monoethanolamine (MEA). This shows that IPA has better adsorption capacity than TEPA and MEA. The weaker intensity of the diffraction patterns with increasing amine loading suggests the filling of the mesoporous pores with amine (Qi et al., 2010)

2.5.2 Brunauer, Emmett and Teller (BET)

Figure 2.4 shows the nitrogen adsorption/desorption isotherms at 77K for activated carbon and modified activated carbon with monoethanolamine (MEA) and triethanolamine (TEA). Based on Bezerra et al. (2010), the non-modified activated carbon showed smooth type I isotherms, with increase in pore volume from relatively low pressures up to $P/P_0 = 1$, which indicates a larger pore distribution. MEA impregnated activated carbon shows a slightly steeper slope in the low pressure range, which indicates its high fraction of micropores.

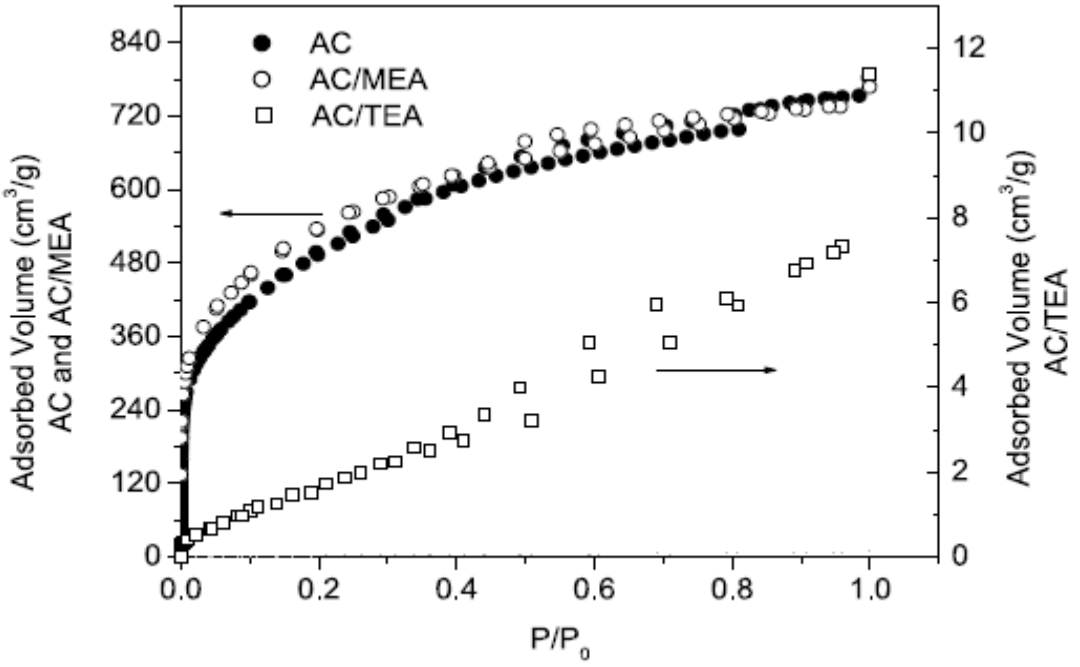

Figure 2.3: Nitrogen adsorption/desorption isotherms at 77K for parent and modified activated carbon.

(Source: Bezerra et al., 2010)

According to Meng et al. (2009), the surface area decrease significantly upon amine functionalization due to the initial part of the adsorption isotherm corresponds to adsorption in the micropores. Figure 2.5 shows a type IV shape isotherm according to IUPAC classification. The pore volume and surface area decreased dramatically after the amine loading (Lin et al., 2013).

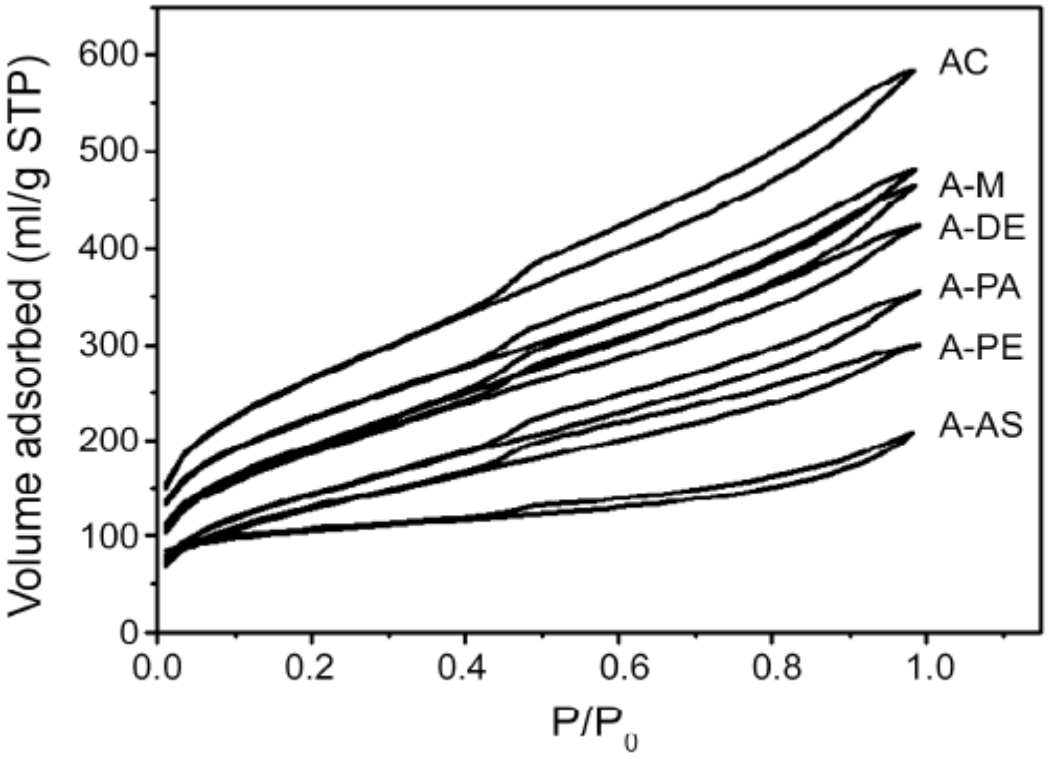

Figure 2.4: The N_2 full isotherms of the pristine and amine functionalized ACs.

(Source: Meng et al., 2009)

Based on the study carried out by Kangwanwatana et al. (2013), there is a decrease in the surface area and pore volume of the micropore thus, indicates that there was some amount

of piperazine blocking in the micropore. Table 2.1 shows the surface area analysis of non-impregnated activated carbon and impregnated activated carbon. The BET analysis indicates substantial decrease in surface area and pore volume as the amine molecules have clogged the pores (Yin et al., 2007).

Table 2.1: Surface area analysis of non-impregnated activated carbon and impregnated activated carbon.

Adsorbing Bed	Total surface area (m^2/g)	Mesopore surface area (m^2/g)	Micropore surface area (m^2/g)	Total pore volume (cc/g)e-01	Mesopore volume (cc/g) e-01	Micropore volume (cc/g) e-01	Average pore diameter (Å)
Non-impregnated activated carbon	801.9	745.2	764.0	4.43	2.57	3.79	22.10
40 wt % piperazine-activated carbon	570.9	734.5	535.3	3.25	2.60	2.65	22.10

(Source: Kangwanwatana et al., 2013)

2.5.3 Fourier Transform Infrared Spectroscopy (FTIR)

From Aroua et al. (2008), the FTIR transmission spectra of non-impregnated activated carbon and impregnated activated carbon is shown in Figure 2.6. From the figure, the absorbance of impregnated activated carbon with polyethyleneimine is higher compared to the absorbance of non-impregnated activated carbon. The N-H bending vibration was shown clearly at 1570 cm^{-1} for the pure amine solution (Lin et al., 2013). The NH_2 deformation band

at ~1600 cm^{-1} decreases as the loss in CO_2 adsorption capacity is connected with a loss of primary amine groups (Wagner et al., 2013).

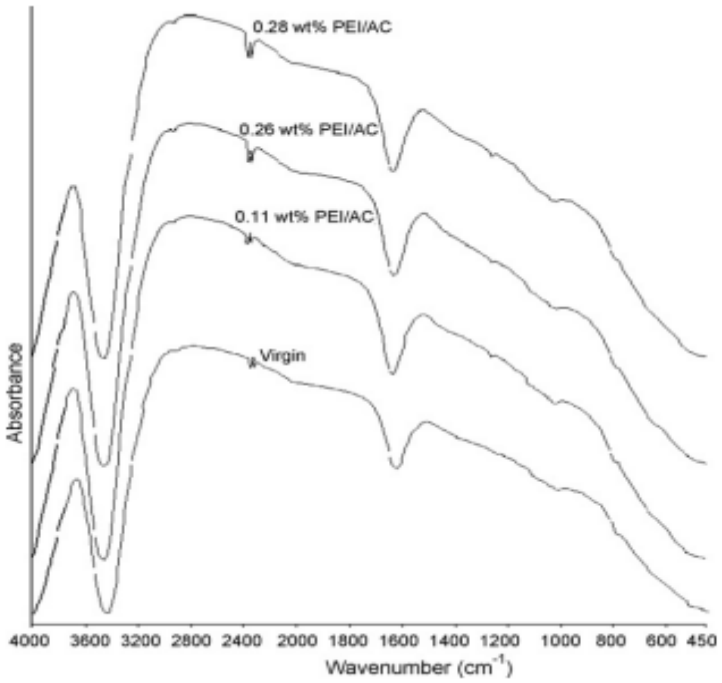

Figure 2.5: FTIR transmission spectra for non-impregnated and impregnated activated carbon.

(Source: Aroua et al., 2008)

From this research, the increase in absorbance is affected by the weight percent of amine used. An increase in weight percent will results in higher absorbance in FTIR analysis. Based on the research done by Lee et al. (2013), the integration of amine inside the adsorbent is confirmed as the adsorption peaks at 1530-1560 cm^{-1} and 3300-3500 cm^{-1} were associated

with the stretching vibrations of $–NH_2$. This study also shows IPA has a high $–NH_2$ content compared to TEPA and MEA.

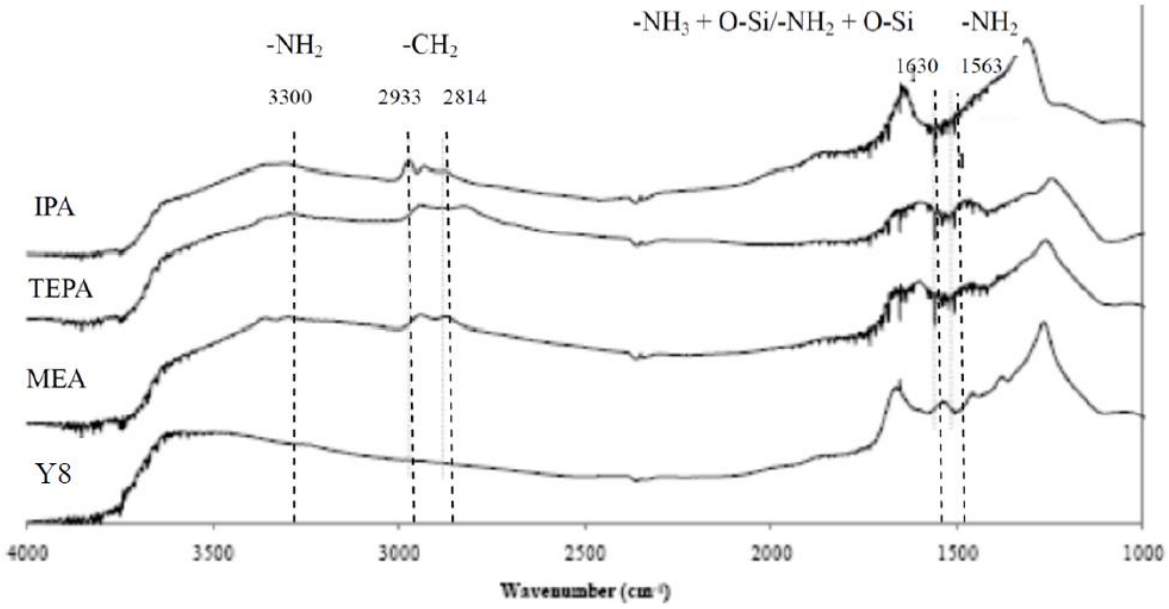

Figure 2.6: FTIR transmission spectra for Y8 (adsorbent), MEA, TEPA and IPA impregnated with Y8.

(Source: Lee et al., 2013)

2.5.4 Field Emission Scanning Electron Microscopy (FESEM)

Figure 2.8 shows the surface morphology of impregnation of PEI on adsorbent by using FESEM analysis. From this research by Lin et. al. (2013), the stacking of the octahedral particle size shows the impregnated of PEI occurs. The number of particle increases when the

loading of PEI increases. This indicates that higher weight percent will increases the binding of amine on the adsorbent surface.

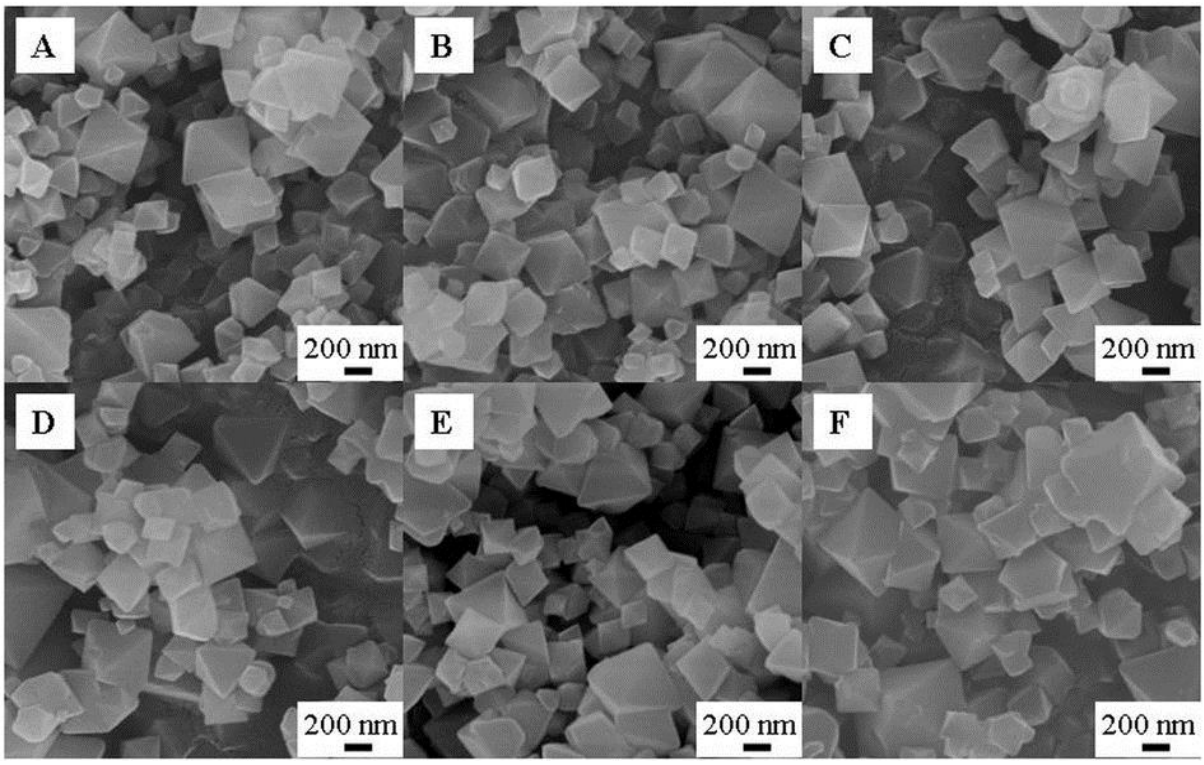

Figure 2.7: The FESEM images of (A) non-impregnated adsorbent, (B) 50 wt% PEI loaded, (C) 75 wt% PEI loaded, (D) 100 wt% PEI loaded, € 125 wt% PEI loaded and (F) 160 wt% PEI loaded.

(Source: Lin et al., 2013)

According to Kangwanwatana et al. (2013), there is slight difference in the surface morphology of the non-impregnated activated carbon and 40 wt % piperazine-activated carbon at magnification of 100,000 times. The impregnated activated carbon shows that the activated carbon was thickened by the piperazine coating which indicates there is a blockage of mesopores of the activated carbon.

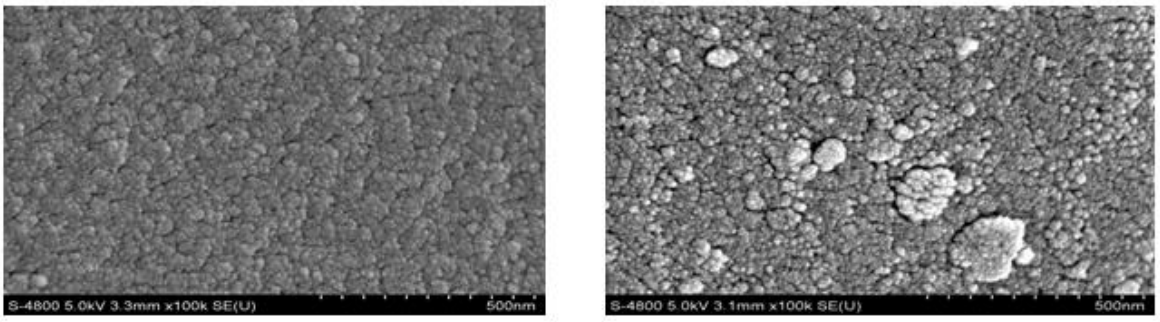

Figure 2.8: The non-impregnated activated carbon (left) and 40 wt % piperazine-activated carbon (right).

(Source: Kangwanwatana et al., 2013)

CHAPTER 3

METHODOLOGY

3.1 Introduction

This chapter provides a list of chemicals used for the preparation of the impregnation of activated carbon, including their supplier, grade, physical and chemical properties. Additionally, the operational procedures of the catalyst characterization instruments also presented in this chapter. The first stage of the experimental work is the synthesis of the non-impregnated activated carbon and impregnated activated carbon. The activated carbon impregnated with MEA and DEA was prepared based on the concentration and weight ratio. The samples were then characterized using X-Ray Diffraction (XRD), Brunauer, Emmett and Teller (BET) isotherm, Fourier Transform Infrared Spectroscopy (FTIR) and Field Emission Scanning Electron Microscopy (FESEM) in order to obtain their physicochemical properties. The result obtained was compared with other previous researches. Finally, conclusions will be drawn based on the findings obtained from this study. The overall experimental work was summarized in Figure 3.1.

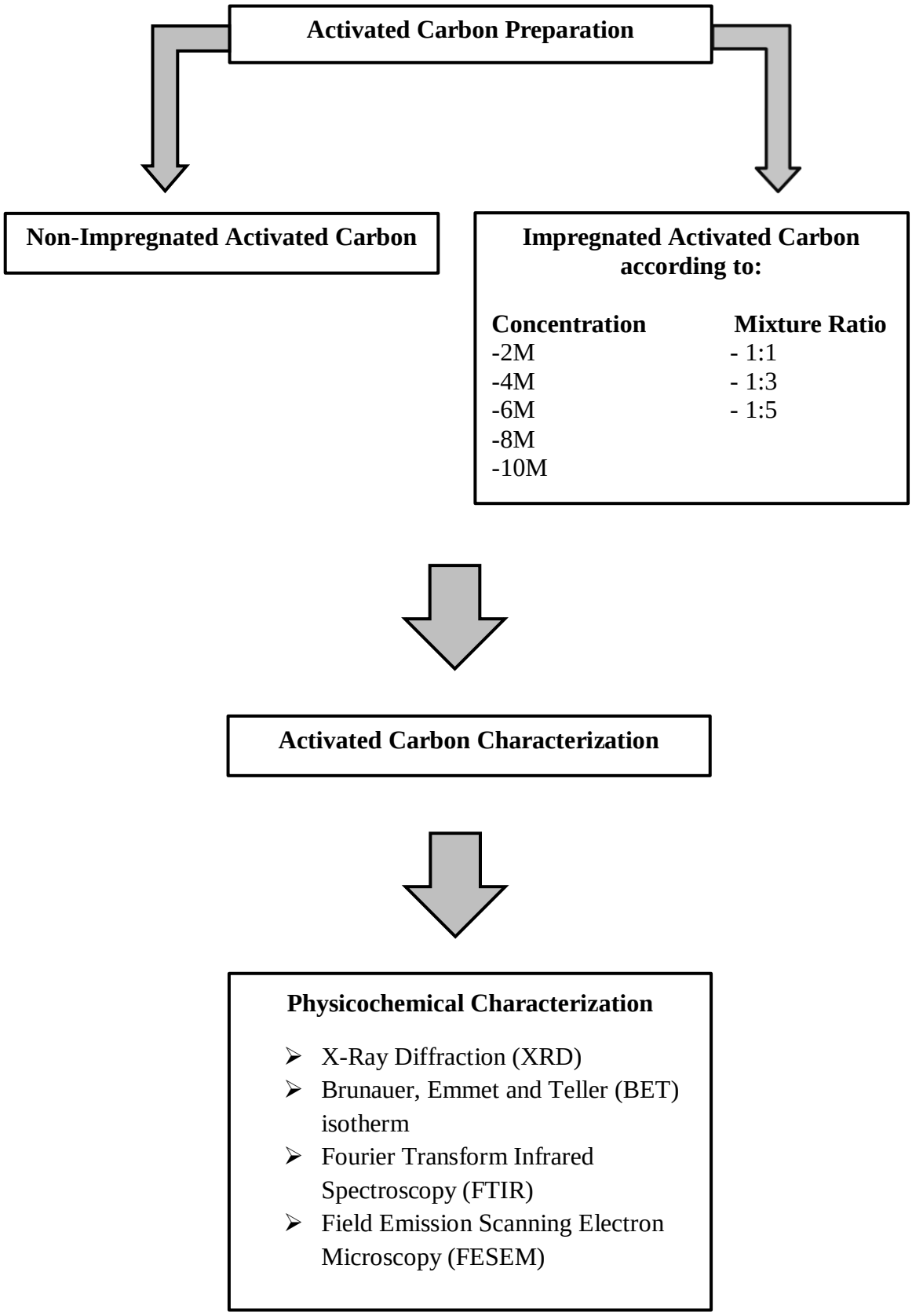

Figure 3.1: Flowchart of overall experimental work.

3.2 Materials and Chemicals

All chemicals and material used in this research are provided in Table 3.1.

Table 3.1: List of chemicals and material.

Chemicals	Molecular Formula	Supplier	Molecular Weight (g/mol)	Purity (%)
Monoethanolamine	C_2H_7NO	MERCK	61.08	99
Diethanolamine	$C_4H_{11}NO_2$	MERCK	105.14	99
Activated Carbon	-	Sin Guan Hup Oil & Rice Mill	-	-

3.3 Activated Carbon Preparation

3.3.1 Non-Impregnated Activated Carbon

The non-impregnated activated carbon was act as a control in this study. The control experiment was carried out with absent of impregnation of activated carbon by the method describe by Kangwanwatana et al. (2013). The activated carbon particle's size was sifted using 1 mm sieve. The prepared activated carbon particles were rinsed with deionized water followed by heating in a 70°C oven for 6 hours. The sample is then being kept in a desiccator at room temperature to avoid the moisture effect. Figure 3.2 shows the preparation of the non-impregnated activated carbon sample.

Figure 3.2a: Activated carbon before sieve.

Figure 3.2b: Activated carbon after sieve.

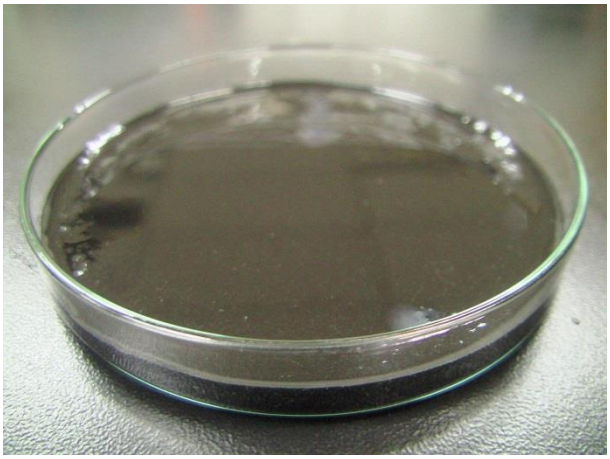

Figure 3.2c: Activated carbon rinsed with deionized water.

Figure 3.2d: Activated carbon was heated at 70ºC for 6 hours in an oven.

Figure 3.2e: Non-impregnated activated carbon.

3.3.2 Impregnated Activated Carbon with MEA and DEA

The impregnation of activated carbon was done with the presence of MEA and DEA. First, the activated carbon particle's size was sifted using 1 mm sieve. The concentration of MEA and DEA being used are 2M, 4M, 6M, 8M and 10M. 50 g of activated carbon was used for preparation of one sample. The volume of the MEA and DEA with deionized water

used was calculated by using the dilution equation. The mixture ratio being used is based on the weight percent of both MEA and DEA mixture to activated carbon. The mixture ratio that will be used is 1:1, 1:3 and 1:5 of activated carbon to MEA mixture and DEA. The activated carbon was impregnated with MEA and DEA based on the concentration and mixture ratio as mentioned above. The mixture was mixed in a beaker and magnetically stirred at 500 rpm for one hour at room temperature. The slurry is then being heated at 70°C at 1 atm for 6 hours to dry completely without any trace of moisture left within its particles and will be keep in a desiccator at room temperature (Khalil et al., 2011). Figure 3.3 shows the impregnation step for the activated carbon with MEA and DEA.

Figure 3.3a: Activated carbon before sieve.

Figure 3.3b: Activated carbon after sieve.

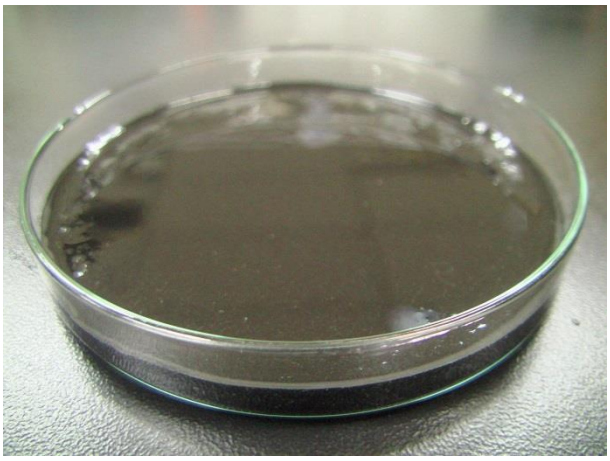

Figure 3.3c: Activated carbon mixed with MEA and DEA.

Figure 3.3d: Impregnated activated carbon was heated at 70ºC for 6 hours in an oven.

Figure 3.3e: Impregnated activated carbon with MEA and DEA.

Figure 3.4 demonstrates the step by step methods for preparation of non-impregnated activated carbon and impregnated activated carbon with MEA and DEA.

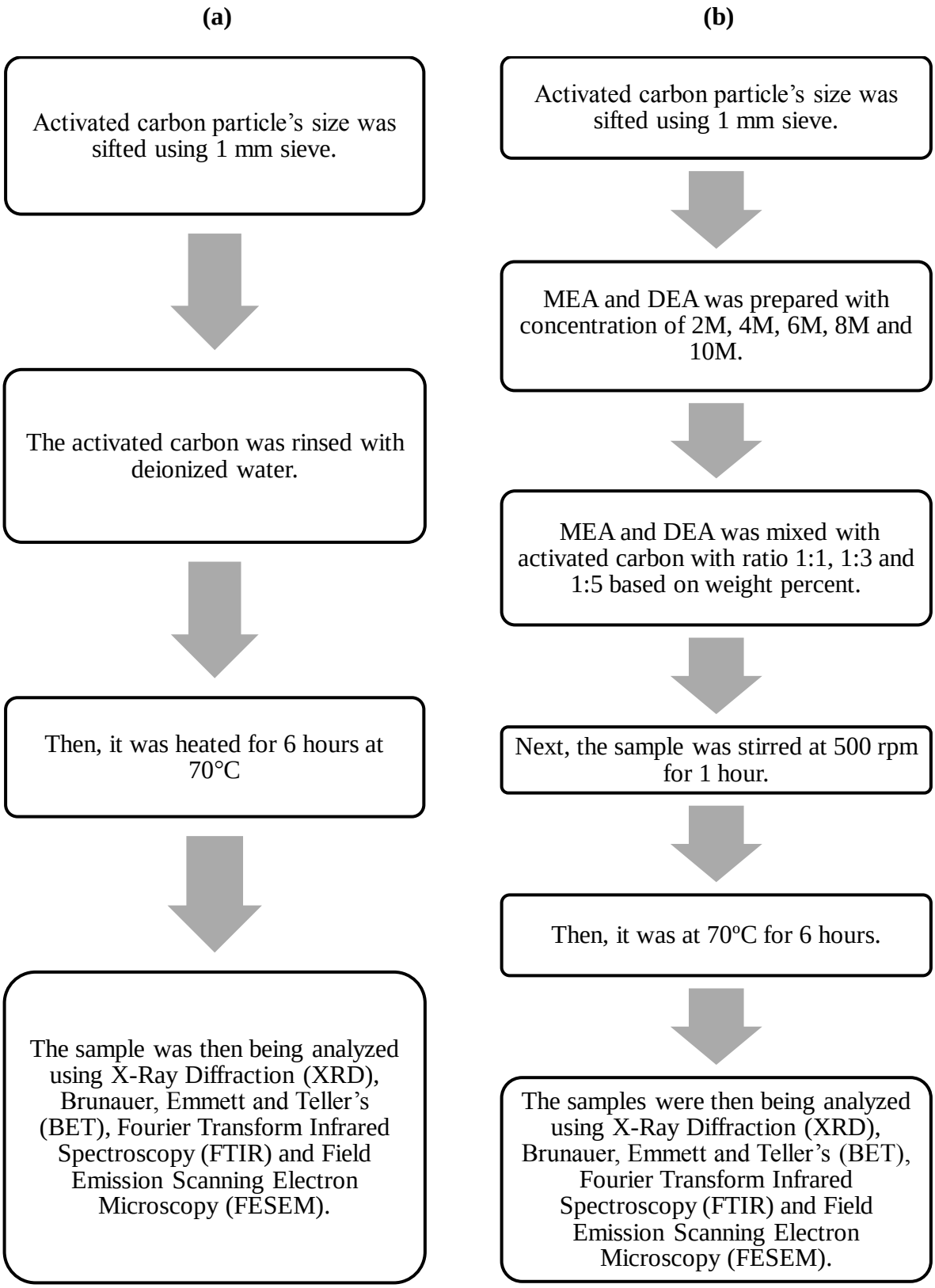

Figure 3.4: The experimental procedure for the preparation of (a) non-impregnated activated carbon and (b) impregnated activated carbon with MEA and DEA.

3.4 Activated Carbon Characterization

Activated carbon characterization provides the information on the physicochemical characteristics of the activated carbon. Analytical techniques such as spectroscopic, microscopic and diffraction can be effectively used to investigate the surface properties of the activated carbon. This section describes the basic and important concepts of various characterization techniques used for this study.

3.4.1 X-Ray Diffraction (XRD)

The crystalline phases and structure of the non-impregnated activated carbon and impregnated activated carbon were determined using X-Rray Diffraction (XRD) techniques. XRD is a rapid analytical technique primarily used for phase identification of a crystalline material and can provide information on unit cell dimensions. The analysed material is finely ground, homogenized, and average bulk composition is determined. XRD is a Desktop Powder Diffractometer capable of measuring powder diffraction patterns from 3 to 145 degrees in two-theta scanning range. It can be used for phase identification, qualitative and quantitative analysis and quality control of raw materials and products. The types of samples can be multi-phase microcrystals of powdered materials, metal and ceramic plates. The Rigaku Miniflex X-Ray Diffractometer of the CuKα radiation filtered by a Ni filter has a wavelength of 1.54 Å at 30 kV and 15 mA.

The activated carbon samples were initially crushed to a fine powder (< 200 µm). The specimens was placed on the glass specimen holder and pressed using a glass slide. Scanning

of samples was performed starting from 3º to 80º at a speed of 1º min^{-1}. The peaks obtained from the analysis were identified using PDLX software. PDXL provides various analysis tools such as automatic phase identification, quantitative analysis, crystallite-size analysis, lattice constants refinement and Rietveld analysis.

3.4.2 Brunauer, Emmett and Teller (BET)

The Brunauer-Emmett-Teller (BET) equation is used primarily to determine the surface area from the physical adsorption of a gas (N_2 or CO_2) on a solid surface. Adsorbed gas molecules tend to form a thin layer that covers the entire solid surface. The BET instrument provides single sample surface area and pore size distribution analysis. Physical adsorption results from relatively weak forces (van der Waals forces) between the adsorbate gas molecules and the adsorbent surface area of the test powder. The determination is usually carried out at the temperature of liquid nitrogen. The amount of gas adsorbed can be measured by a volumetric or continuous flow procedure.

The data are treated according to the Brunauer, Emmett and Teller (BET) adsorption isotherm equation:

$$\frac{1}{Va\left(\frac{P_0}{P}-1\right)} = \frac{C-1}{V_m C} \times \frac{P}{P_0} + \frac{1}{V_m C} \qquad (3.1)$$

Where:

P = partial vapour pressure of adsorbate gas in equilibrium with the surface at 77.4 K (b.p. of liquid nitrogen), in pascals,

P_0 = saturated pressure of adsorbate gas, in pascals,

V_a = volume of gas adsorbed at standard temperature and pressure (STP) [273.15 K and atmospheric pressure (1.013 × 105 Pa)], in millilitres,

V_m = volume of gas adsorbed at STP to produce an apparent monolayer on the sample surface, in millilitres,

C = dimensionless constant that is related to the enthalpy of adsorption of the adsorbate gas. on the powder sample.

A value of Va is measured at each of not less than 3 values of P/Po. Then the BET value:

$$\frac{1}{\mathrm{Va}\left(\frac{\mathrm{P_0}}{\mathrm{P}}-1\right)} \tag{3.2}$$

The equation is plotted against P/Po according to equation (3.1). This plot should yield a straight line usually in the approximate relative pressure range 0.05 to 0.3. The data are considered acceptable if the correlation coefficient, r, of the linear regression is not less than 0.9975; that is, r^2 is not less than 0.995. From the resulting linear plot, the slope, which is equal to $(C - 1)/V_mC$, and the intercept, which is equal to $1/V_mC$, are evaluated by linear regression analysis. From these values, V_m is calculated as 1/(slope + intercept), while C is calculated as (slope/intercept) + 1. From the value of V_m so determined, the specific surface area, S, in $m^2 \cdot g^{-1}$, is calculated by the equation:

$$S = \frac{V_m N_a}{m \times 22400} \tag{3.3}$$

Where:

V_m = volume of gas adsorbed at STP to produce an apparent monolayer on the sample

surface, in millilitres,

N_a = Avogadro constant ($6.022 \times 1023\ mol^{-1}$),

m = mass of test powder, in grams.

And for N_2 the usual cross-section area is 16.2 $Å^2$ ($1Å^2 = 10^{-20}\ m^2$) (Gregg & Sing, 1991).

Firstly, around 0.3 g of activated carbon was packed in the U-sample tube. The sample was degassed at 70 ºC at overnight and cool down to ambient temperature. The N_2 adsorption/desorption process is done by using Thermo Scientific (Surfer) equipment. Once the TCD signal has stabilized, the sample tube was immersed in a flask fill up with liquid N_2. As a result, nitrogen will be physisorbed on the support surface. When the adsorption has reached the equilibrium, the sample was shifted back to ambient temperature by let the sample exposed to ambient temperature for 15 minutes. The surface area was determined by Equation 3.3. The effect of surface porosity and pore size can be determined by the surface area calculated.

3.4.3 Fourier Transform Infrared (FTIR)

Fourier Transform Infrared Spectroscopy (FTIR) offers quantitative and qualitative analysis for organic and inorganic samples. FTIR identifies chemical bonds in a molecule by producing an infrared absorption spectrum. The spectra produce a profile of the sample, a distinctive molecular fingerprint that can be used to screen and scan samples for many different components. FTIR is an effective analytical instrument for detecting functional groups and characterizing covalent bonding information. The wavelength of light absorbed is

characteristic of the chemical bond as can be seen in this annotated spectrum. By interpreting the infrared absorption spectrum, the chemical bonds in a molecule can be determined. By interpreting the infrared absorption spectrum, the chemical bonds in a molecule can be determined.

The analysis on the non-impregnated activated carbon and impregnated activated carbon were conducted by FTIR (Thermo Scientific) using KBr/Ge mid-infrared optimized technique. The wavelength used was in range 500 – 4000 cm^{-1}.

3.4.4 Field Emission Scanning Electron Microscopy (FESEM)

Field emission scanning electron microscopy (FESEM) provides topographical and elemental information at magnifications of 10x to 300,000x, with virtually unlimited depth of field. Electrons are liberated from a field emission source and accelerated in a high electrical field gradient. Within the high vacuum column these so-called primary electrons are focussed and deflected by electronic lenses to produce a narrow scan beam that bombards the object. As a result secondary electrons are emitted from each spot on the object. The angle and velocity of these secondary electrons relates to the surface structure of the object. A detector catches the secondary electrons and produces an electronic signal. This signal is amplified and transformed to a video scan-image that can be seen on a monitor or to a digital image that can be saved and processed further.

The activated carbon was analysed by using JEOL field emission scanning electron microscope at the magnifications of 60x and 100,000x. The accelerating voltage is 5.0 kV during image capture using the secondary electron and dark field detectors.

CHAPTER 4

RESULTS AND DISCUSSION

4.1 Introduction

This chapter discusses the data obtained from the experimental work that had been done throughout this research. The result is described based on the characterization analysis of the non-impregnated activated carbon and impregnated activated carbon with MEA and DEA. The characterization of the samples was performed using X-Ray Diffraction (XRD), Brunauer, Emmett and Teller (BET) isotherm, Fourier Transform Infrared Spectroscopy (FTIR), and Field Emission Scanning Electron Microscopy (FESEM). The details were described in next section and the conclusions were drawn based on the findings obtained from the study.

4.2 Characterization of Non-Impregnated Activated Carbon and Impregnated Activated Carbon

The past studies have shown the difference between non-impregnated and impregnated activated carbon from many perspectives such as the types of activated carbon and the types of amine used for the impregnation purpose. The activated carbon has a high porosity on its structures containing many types of functional group such as carboxyl and ketone groups which can react with acidic gas, for example, CO_2 gas. The activated carbon adsorption capacity can be increased with the aid of amine such as MEA and DEA which bonded to the activated carbon surfaces. The impregnated activated carbon with amine would develop many active sites on the surface and inside the pores of the activated carbon particles through chemisorption, thus the probability to adsorb CO_2 molecules is higher.

In this section, the characteristics of the non-impregnated activated carbon and impregnated activated carbon were investigated through the observations from four main techniques. Firstly, the differences in type of compound present on the surface and crystalline phase of both types of activated carbons was examined using XRD analysis. Besides, the N_2-physisorption result of BET reflects the changes in surface area and pore size. The functional groups present in both samples were identified using FTIR analysis. Lastly, the surface morphology of the activated carbons were analysed by using FESEM analysis.

4.2.1 X-Ray Diffraction (XRD) Analysis

X-Ray diffraction (XRD) was used to reveal information about the crystallographic structure and chemical composition of the non-impregnated activated carbon and impregnated activated carbon with MEA and DEA. Figure 4.1 shows the diffraction peaks for the non-impregnated activated carbon. The peaks of pyrazole can be observed at the diffraction angle around 21.54º and 36.25º. Shafeeyan et al. (2010) has proved that there are presence of pyrazole, pyridine and pyridone in the activated carbon surfaces.

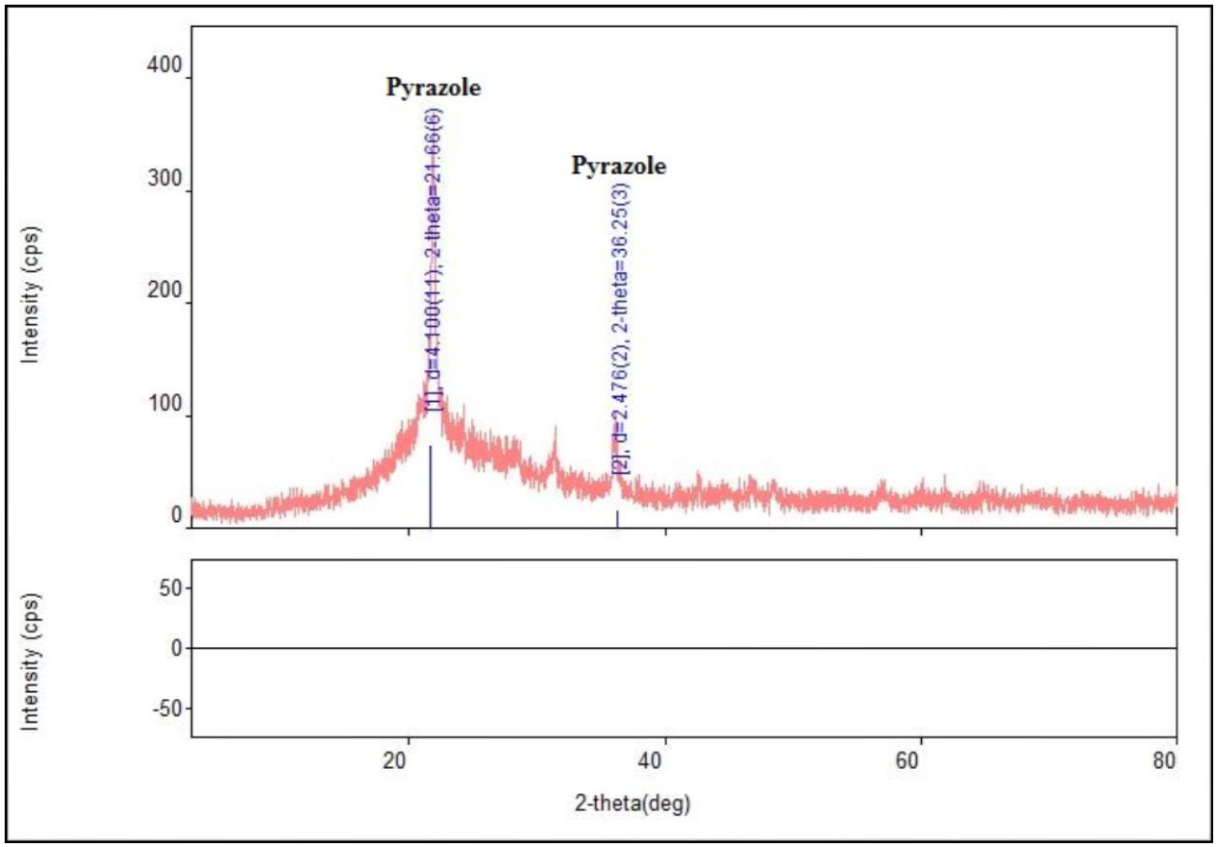

Figure 4.1: XRD pattern for the non-impregnated activated carbon.

Figure 4.2a and 4.2b show the diffraction peaks for the impregnated activated carbon with MEA which were heated at 70ºC for 6h. Figure 4.2a shows a lower concentration of MEA used for the impregnation process which is 4M while Figure 4.2b shows a concentration of 10M of MEA impregnated sample. Both figures show the presence of ethanolamine at different diffraction angle. For the lower concentration of MEA, the diffraction angle for ethanolamine can be seen at 22.11º and 36.34º while for higher concentration of MEA, the diffraction angles are around 21.66º and 36.1º.

From the results obtained in both figures, it was clearly seen that there are presence of different compounds at different concentration of MEA. At lower concentration of MEA, the pyrazole are still present on the surface of impregnated activated carbon. This indicates that the concentration used is still low and the MEA are not fully covered on the activated carbon surfaces. At concentration of 10M MEA, the compound named 2,6-diaminopyridine is present on the activated carbon surfaces resulted from the reaction between MEA and pyridine that was present on the activated carbon surfaces (Scheiman, M. A., 1962). The reaction between MEA and pyridine is shown as follows:

$$\underset{\text{(Monoethanolamine)}}{C_5H_5N} + \underset{\text{(Pyradine)}}{2C_2H_7NO} \longrightarrow \underset{\text{(2,6-diaminopyradine)}}{C_5H_7N_3} + \underset{\text{(oxybismethane)}}{C_4H_{12}O_2}$$

As the reaction above occurs in the impregnated sample of MEA, it can be proved that the modification of the activated carbon with MEA has changes the surface content which caused the pores being filled and the MEA coating on the outer surface of the activated carbon.

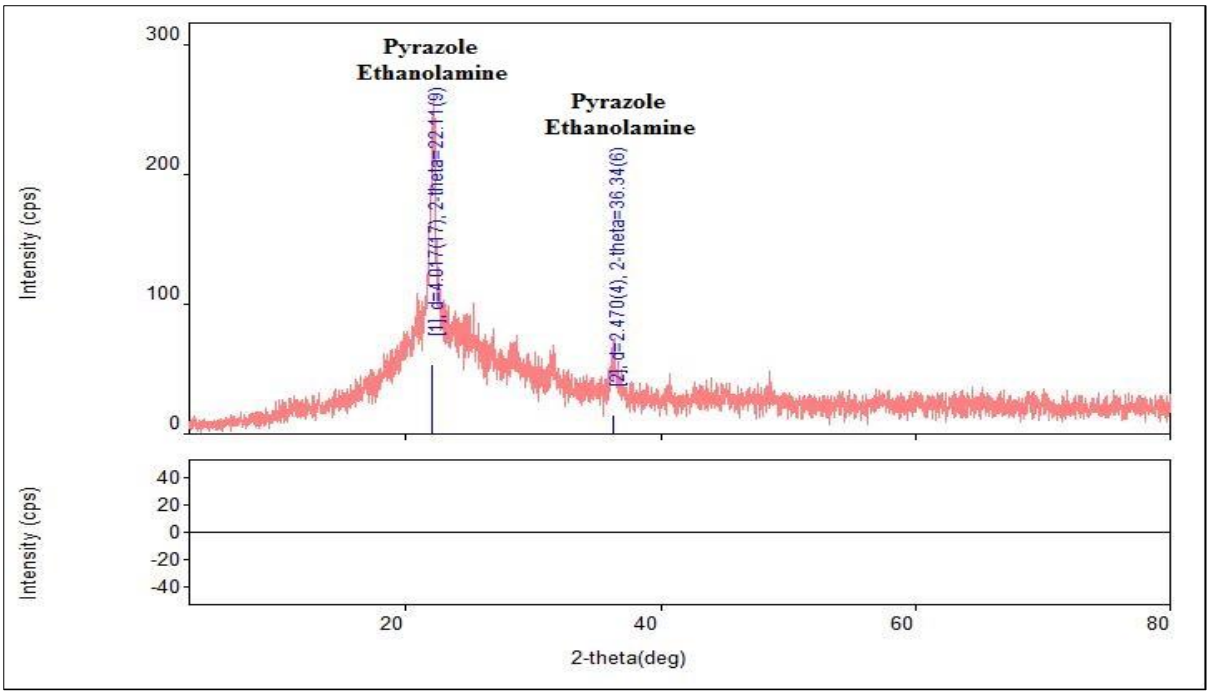

Figure 4.2a: XRD pattern for impregnated activated carbon with 4M of MEA.

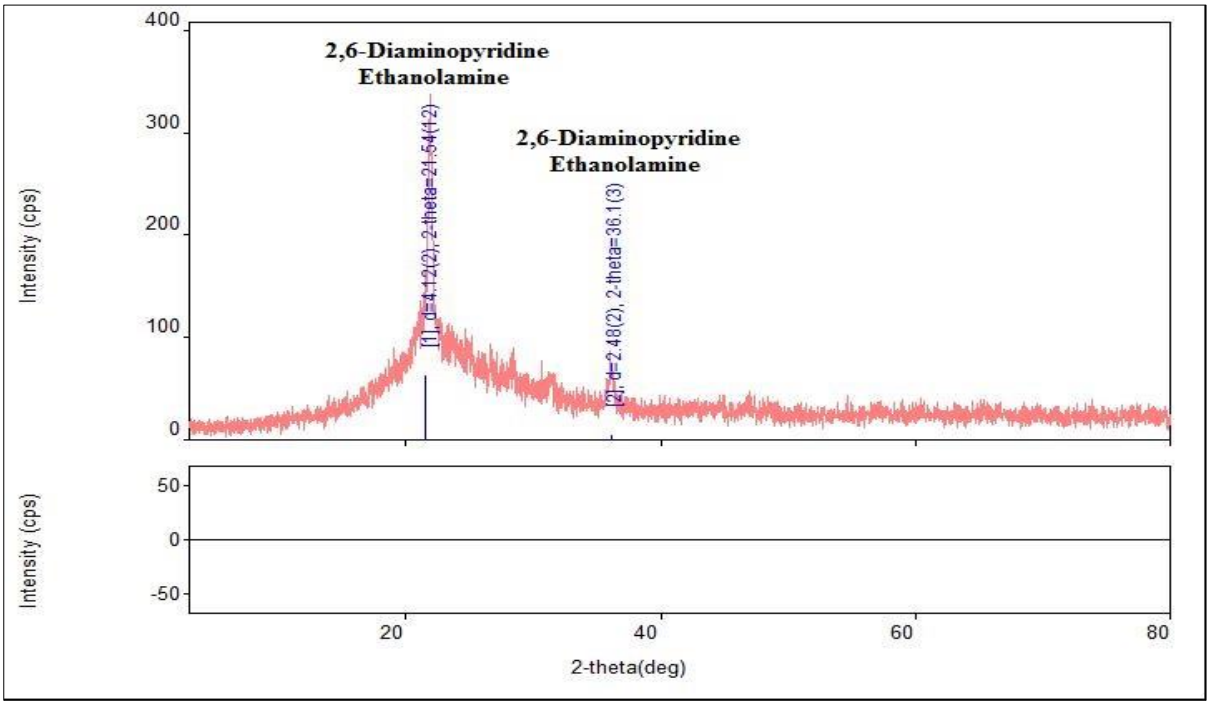

Figure 4.2b: XRD pattern for impregnated activated carbon with 10M of MEA.

.

The diffraction peaks for the impregnated activated carbon with DEA were shown in the Figure 4.3a and Figure 4.3b. The diffraction peaks of the low concentration of DEA which is 4M was presented in Figure 4.3a while Figure 4.3b shows the diffraction peaks for the concentration of 10M of DEA impregnated on the activated carbon. Both figures show the presence of diethanolamine at slightly different diffraction angle. At the concentration of 4M of DEA used, the diffraction angle is around 22.13º while at higher concentration, the diffraction angle is at 22.18º.

From the figures obtained, there were different types of compound present at concentration of 4M and 10M of DEA. For a lower concentration which is 4M, there was a presence of 4-aminopyradine on the surface of the impregnated activated carbon. This can be concluded that there was a reaction between the surface content of the activated carbon with the DEA. Based on the previous studies, the alcohol containing amine is able to react with the other amine by nucleophilic reactions (Brotzel, F., & Mayr, H., 2007). For the higher concentration of DEA which is 10M, the presence of benzalazine on the sample surface is detected. Benzalazine is an aromatic unsaturated hydrocarbons containing nitrogen functional group in it (Binkley, R. W., 1969). It can be assumed that the aromatic compound presence in the non-impregnated activated carbon such as pyridine and imine undergo further reactions with DEA to produce benzalazine as benzalazine contains more nitrogen functional groups than pyridine and imine.

Modification of the activated carbon with DEA has been achieved as the presence of the reaction product can be clearly seen based on the XRD results. The surface content for the impregnated activated carbon with DEA was highly coated with the reaction product as well as DEA itself.

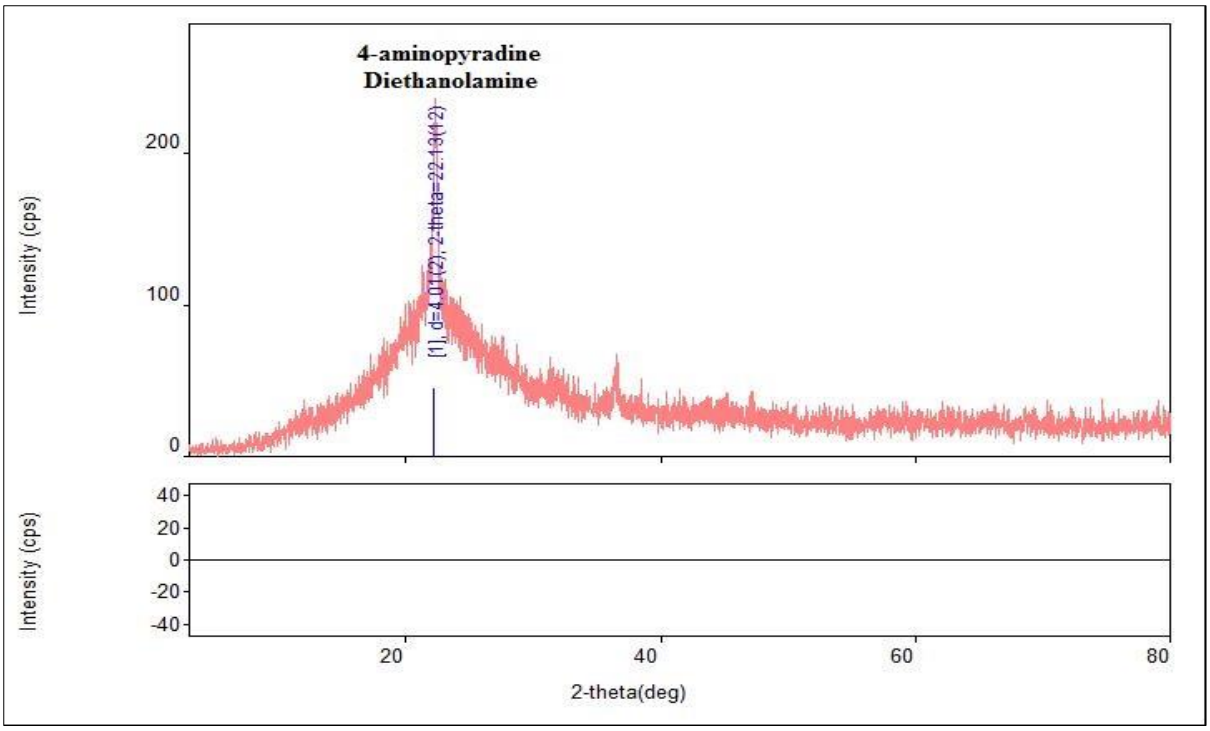

Figure 4.3a: XRD pattern for impregnated activated carbon with 4M of DEA.

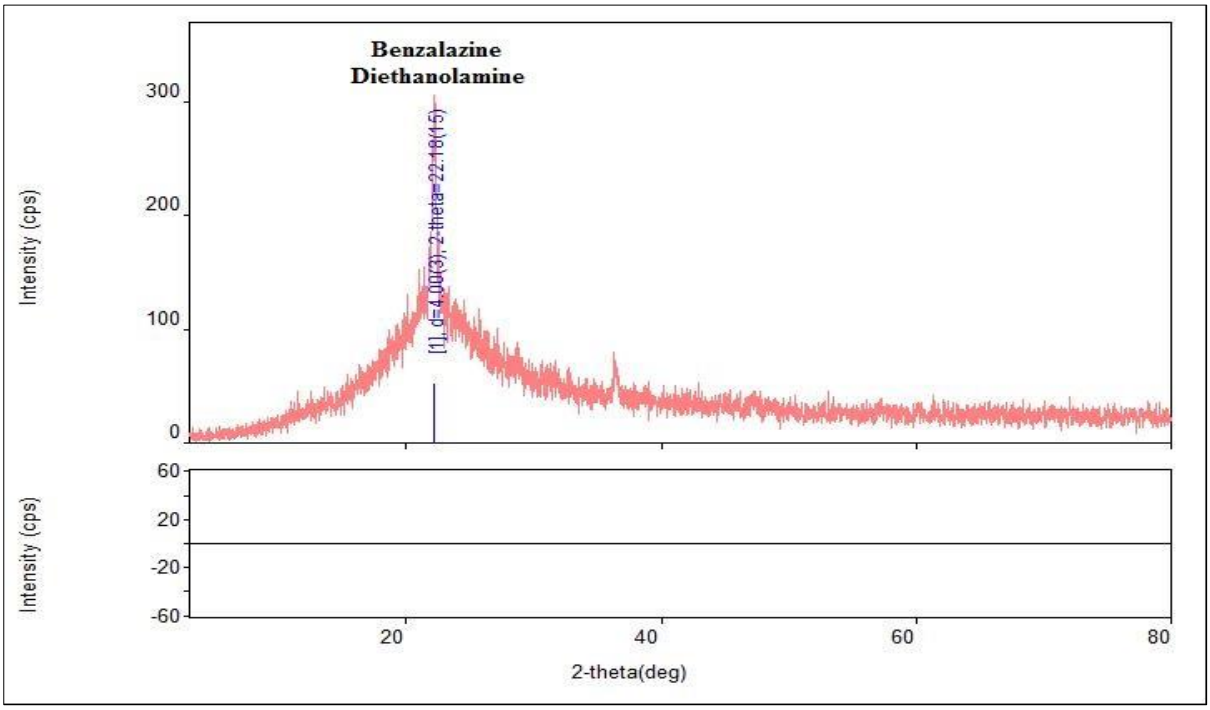

Figure 4.3b: XRD pattern for impregnated activated carbon with 10M of DEA.

The peaks characteristics of the impregnated activated carbon with MEA and DEA were shown in Table 4.1. The diffraction angles are different according to the selected components. From the table, the intensity of the component varies with the difference in sample concentration. The intensity of the component is inversely proportional to the sample concentration. MEA, for instance, has a lower intensity at higher concentration and the same goes to DEA. The intensity of the diffraction does decrease at higher MEA and DEA loadings caused by the filling of the mesoporous pores with MEA and DEA (Qi et al., 2010).

Table 4.1: XRD peaks characteristics for non- impregnated activated carbon and MEA and DEA impregnated activated carbon.

Component	Sample concentration	Diffraction angles, 2θ (º)	Height (cps)	Intensity (cps¥deg)	Detected compound
Blank	-	21.54	63	509	Pyrazole
MEA	4M	22.11	54	460	-Pyrazole -Ethanolamine
	10M	21.66	74	395	-Ethanolamine -2,6-Diaminopyradine
DEA	4M	22.13	46	327	-4-aminopyradine -Diethanolamine
	10M	22.18	53	321	-Benzalazine -Diethanolamine

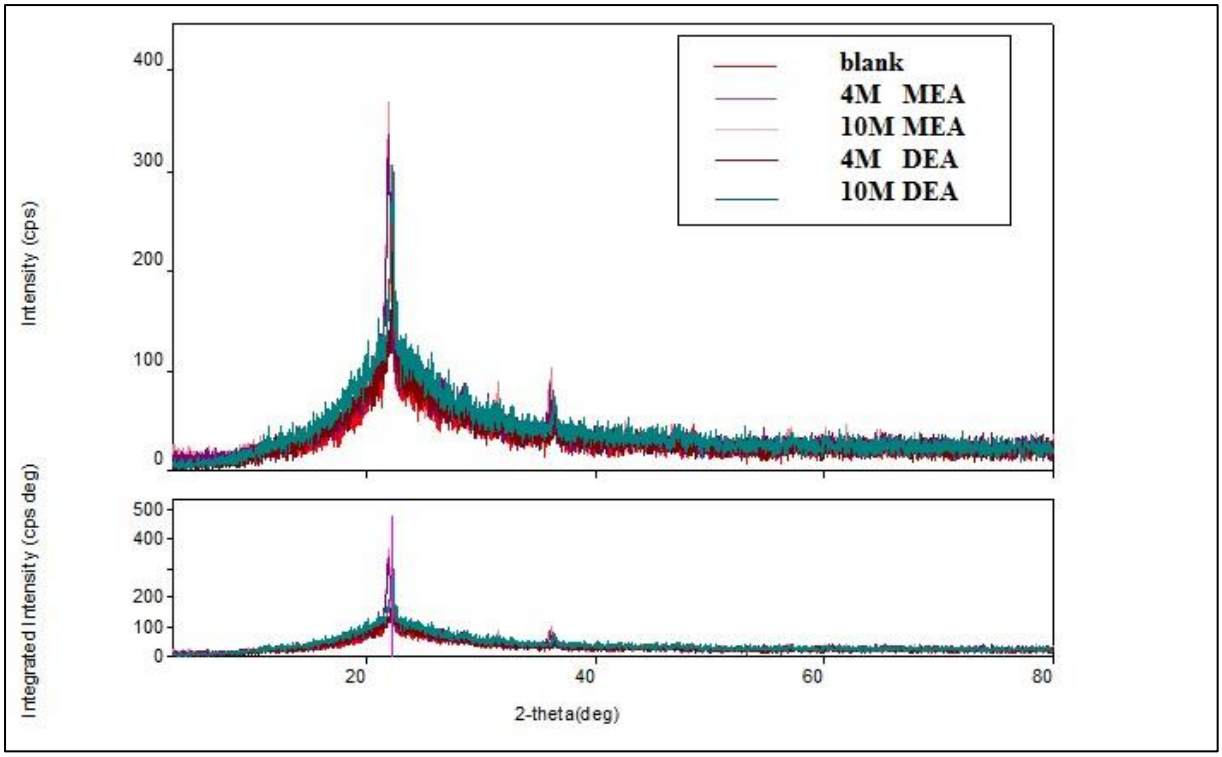

Figure 4.4: XRD pattern for non-impregnated activated carbon and impregnated activated carbon with MEA and DEA.

4.2.2 N_2 – Physisorption Analysis

The analysis for the physical adsorption of gas molecules on a solid surface serves as the basis for an important analysis technique for the measurement of the specific surface area, pore volume and pore diameter of a material. In this study, the isothermal adsorption and desorption of N_2 at -196.3 ºC (77.3 K) were measured as function of the change in relative pressure (P/P_0). Figure 4.5 shows the standard isotherm profile which includes six main categories. Brunauer et al. classified types I – V from this standard isotherms in 1940 and been add on later by Gregg and Sing (1982).

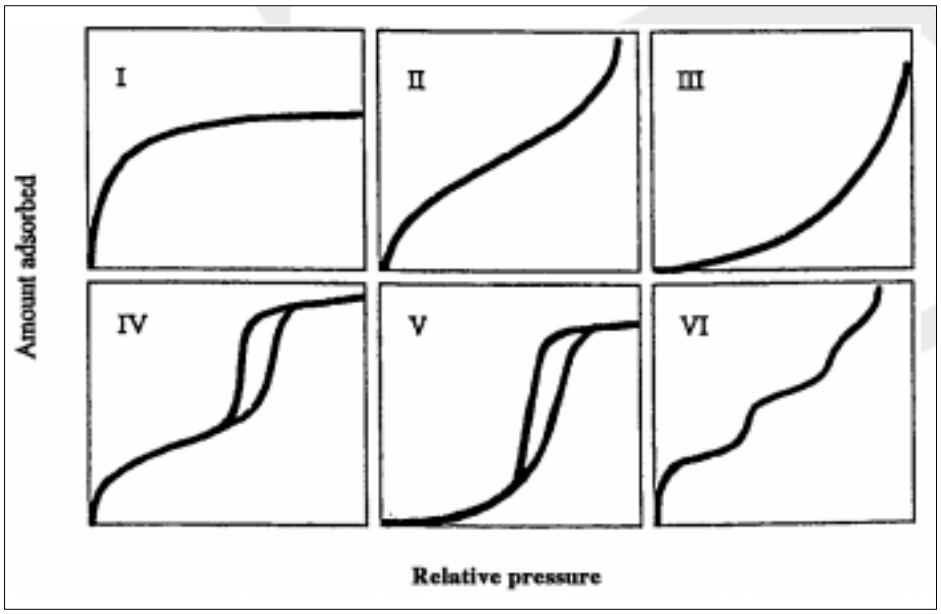

Figure 4.5: Standard isotherms for absorption and desorption profile.

(Source: Donohue, M., 2004)

The simulated isotherms for nitrogen adsorption and desorption profile for non-impregnated activated carbon and impregnated activated carbon with MEA and DEA at 77.3 K were analysed. These simulated isotherms were used to calculate the BET surface area as tabulated in Table 4.2.

In this study, the isothermal profile for the non-impregnated activated carbon and the impregnated activated carbon were found to be slightly different based on the isotherm profile in Figure 4.5. The non-impregnated activated carbon shows *Type I* isotherm which is for adsorbents with a predominantly micropore particles (< 2 nm). In micropore, the adsorption potential may be enhanced when the pore walls overlap, creating more adsorption sites. The adsorption potential increase and creates bigger adsorption energy as the pore

width of the activated carbon is small which causes the adsorption process starts immediately as the N_2 molecules contact the surface of the activated carbon (Bezerra et al., 2011).

Meanwhile, the modified activated carbon with MEA and DEA show *Type II* isotherm which describes adsorption on macroporous adsorbents with weak adsorbate-adsorbent interactions. The weak connections between the adsorbate and adsorbent were created due to the large amount of the activated carbon particles pores blocked by the MEA and DEA. As the partial pressure of N_2 increases towards the atmospheric pressure, the quantity adsorbed of N_2 is also increases due to higher pressure exerted on the samples (Meng et al., 2009).

Table 4.2 shows the summary of the surface area and pore volume of the non-impregnated activated carbon and impregnated activated carbon with 10M MEA and 10M DEA. The BET total surface area of the non-impregnated activated carbon is 0.0458 m^2g^{-1}. The value is higher compared to the total surface area of the impregnated activated carbon with MEA and DEA which is only 0.0086 and 0.0071 m^2g^{-1} correspondingly. The BET total surface area of the impregnated activated carbon shows 5 to 6 times less than BET total surface area of the non-impregnated activated carbon suggesting that the pores were blocked by the MEA and DEA molecules which also resulted in the decrease in pore volume. The decrease in surface area and pore volume indicates that there are many active sites for the CO_2 binding on the surface of the activated carbon as the adsorption process was chemisorption in nature. From the results, it can be assumed that the activated carbon impregnated with DEA is a better adsorbent as the surface area and pore volume is the smallest and this indicates that the active sites for CO_2 adsorption is largest in this type of adsorbent.

Table 4.2: Surface area and pore volume analysis for non-impregnated activated carbon and impregnated activated carbon with MEA and DEA

	Surface Area (m^2g^{-1})			Pore Volume (cm^3g^{-1})			
Adsorbing bed	Total	Mesopore	Micropore	Total	Mesopore	Micropore	Average pore diameter (Å)
Non-impregnated activated carbon	0.0458	0.0172	0.0313	63.791	14.159	72.441	35.858
Impregnated activated carbon with 10M MEA	0.0086	0.0091	0.0014	4.2134	6.7359	1.2908	30.114
Impregnated activated carbon with 10M DEA	0.0071	0.0077	0.0012	1.4774	5.665	0.85	34.288

The difference between the pore size of the non-impregnated activated carbon and impregnated activated carbon with MEA and DEA were observed through Horvath & Kawazoe desorption pore size. There was a large difference between the pore sizes of the non-impregnated activated carbon and the impregnated activated carbon. The non-modified activated carbon has a very high pore size which is around 0.03 cm^3g^{-1} while the impregnated activated carbon with MEA and DEA has around 0.0012 cm^3g^{-1} and 0.0006 cm^3g^{-1} respectively. This shows that the pore of the impregnated activated carbon has been filled with MEA and DEA. The pore size of MEA is more than the pore size of DEA because of the amine functional group present in DEA is more than in MEA and the reactions occurs between the activated carbon surfaces and amine is more rapid with DEA compared to MEA. Based on Kangwanwatana et al., (2013), the average pore diameter should be the same for all

type of samples. In this study, the average pore diameter is slightly different from each other because of the exact size of the sieved activated carbon may be varied.

4.2.3 Fourier Transform Infrared Spectroscopy (FTIR)

4.2.3.1 Comparison between Non-Impregnated Activated Carbon and Impregnated Activated Carbon with MEA and DEA

The Fourier Transform Infrared (FTIR) spectra of the non-impregnated activated carbon and the impregnated activated carbon with MEA and DEA are depicted in Figure 4.6. The samples have a transmission range from 4000 - 500 cm^{-1} but the sensitive transmission of the samples were divided into different sensitive transmission regions. The sensitive transmission regions required in this study is the amides regions which include several regions from the range of 3500 - 1500 cm^{-1}. The formation of amides can be explained from the reaction between the carboxylic acid with amine. In this study, the carboxyl functional groups are present on the activated carbon surfaces and the MEA and DEA were introduced to the activated carbon thus, caused the reaction between the carboxyl and amine groups on the activated carbon surfaces. The reaction is as follows:

$$\underset{\text{(amine)}}{ROHNH_2} + \underset{\text{(carboxylic acid)}}{RCOOH} \longrightarrow \underset{\text{(amide)}}{RONH_2RCO} + \underset{\text{(water)}}{H_2O}$$

Based on the Figure 4.6, the difference in transmittance peaks can be clearly seen according to the type of amine used. The activated carbon with the absent of amines does not form peaks at amide transmission regions as there is no reaction occurs on the activated

carbon surfaces. For MEA impregnated activated carbon, the transmittance peaks can be observed at 3287.73 cm^{-1} and 1651.95 cm^{-1} which confirmed that there was a presence of amide on the activated carbon structure as shown in Figure 4.7b. The modified activated carbon with DEA also shows the presence of amide that can be seen at 3288.44 cm^{-1} and 1651.60 cm^{-1} band. The transmittance percentage peaks of DEA are lower than the transmittance percentage peaks of MEA for both amide regions. This can be explained by the presence of amides are more in DEA because DEA have more amine functional groups (secondary amine) compared to MEA which have less nitrogen functional groups (primary amine) (Kim et al., 2013).

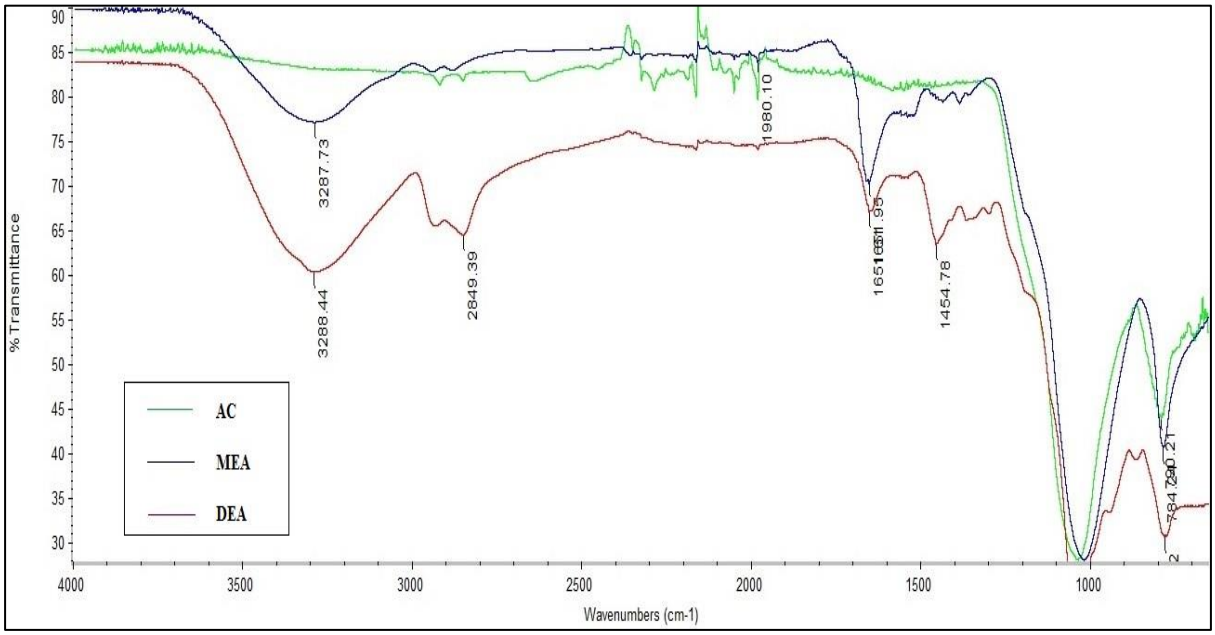

Figure 4.6: FTIR spectrum of non-impregnated activated carbon and impregnated activated carbon with MEA and DEA.

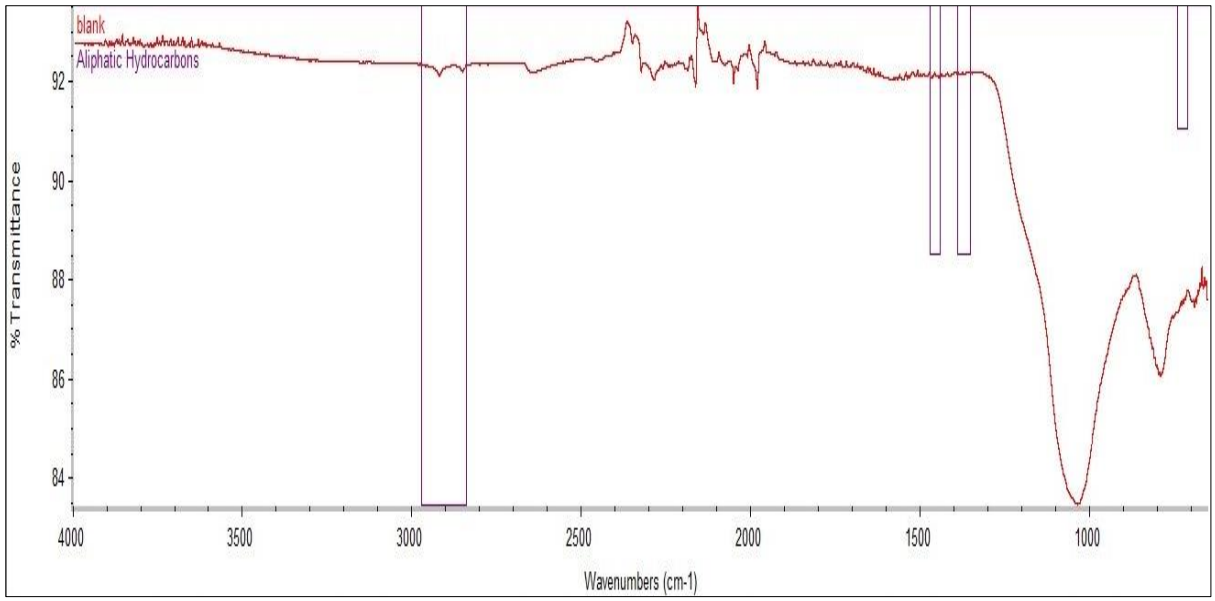

Figure 4.7a: The functional group presence in non-impregnated activated carbon sample.

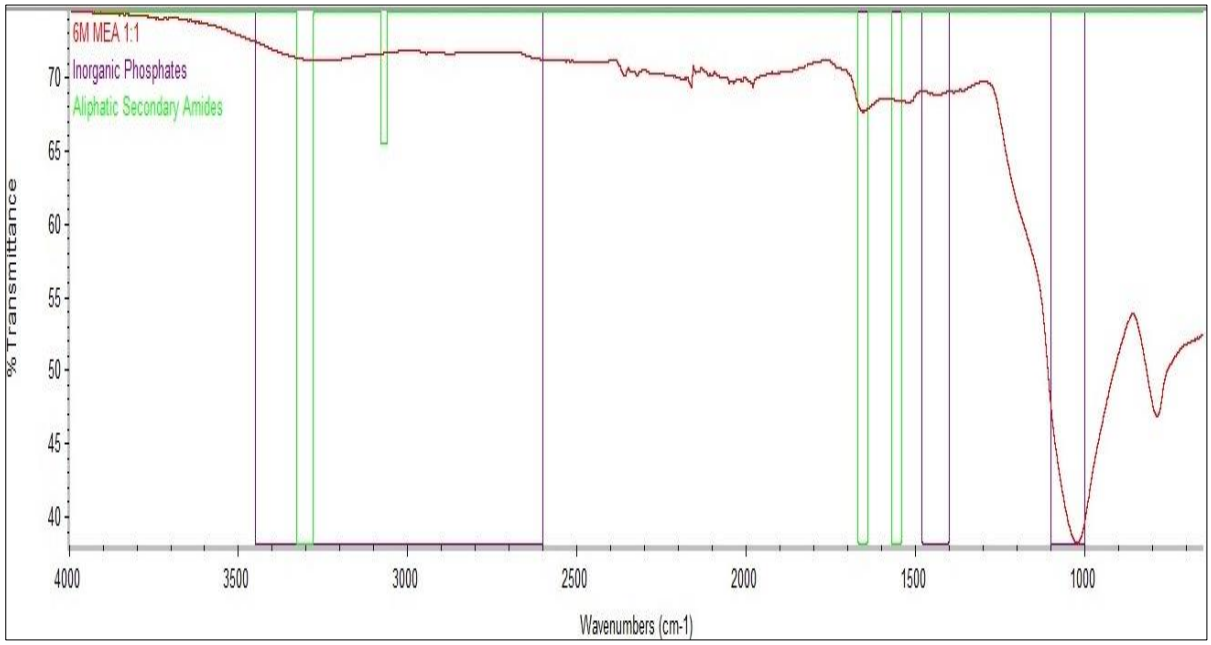

Figure 4.7b: The functional group presence in MEA impregnated activated carbon sample.

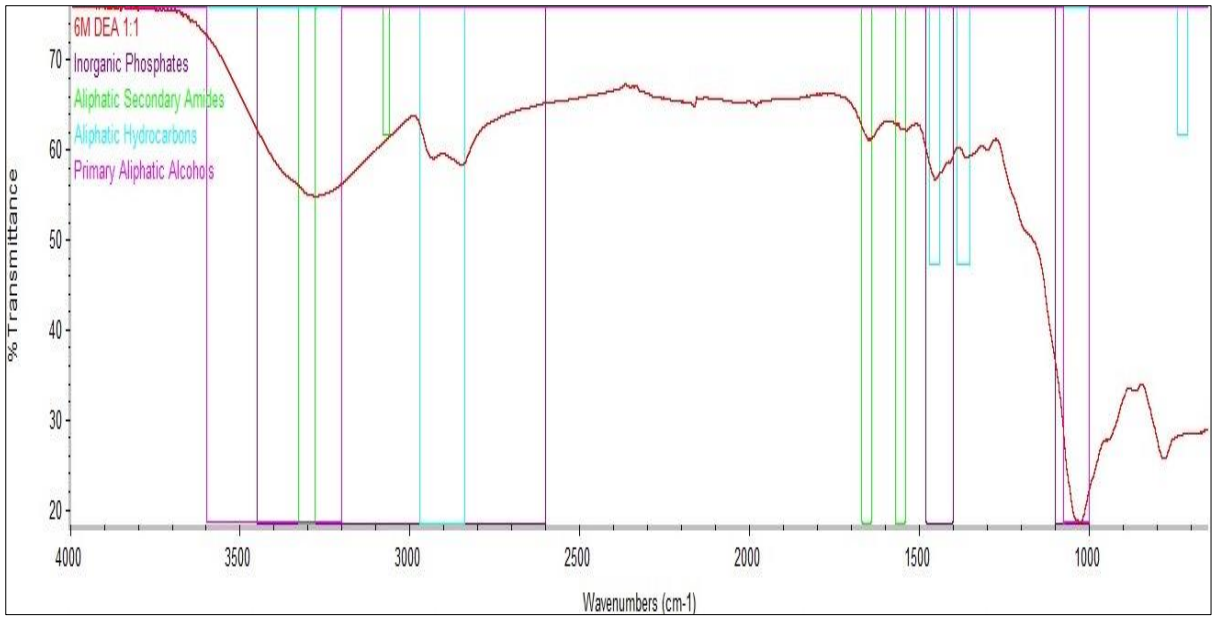

Figure 4.7c: The functional group presence in DEA impregnated activated carbon sample.

4.2.3.2 Effect on Concentration of Impregnated Activated Carbon with MEA and DEA

The effect of concentration of MEA and DEA on the impregnation of activated carbon can be observed in Figure 4.8a and Figure 4.8b. Figure 4.8a shows a variation of MEA concentration used in the impregnation process of the activated carbon. All concentrations which is 2M, 4M, 6M, 8M and 10M show there was an imprint of amides as the transmittance peaks being formed in the amides sensitive regions. The bands at 3287.73 cm^{-1} and 1656.10 cm^{-1} were formed and indicate the presence of amides in all samples. From the results, we can see that the transmittance percentage decreased with increasing concentration of MEA and the amount of amide formed in higher concentration of amine is larger than the less concentrate amine (Havens, M., 1989).

Figure 4.8b shows the transmittance percentage of the DEA impregnated activated carbon with different concentration. The amides formed at 3285.08 cm^{-1} – 3272.66 cm^{-1} and at 1651.68 cm^{-1} band. Based on the transmittance percentage obtained from the analysis, the patterns for DEA impregnated activated shows similar pattern with MEA impregnated activated carbon. The increasing concentration of DEA resulted in decreasing transmittance percentage as the quantity of amide increasing with the increased DEA concentration.

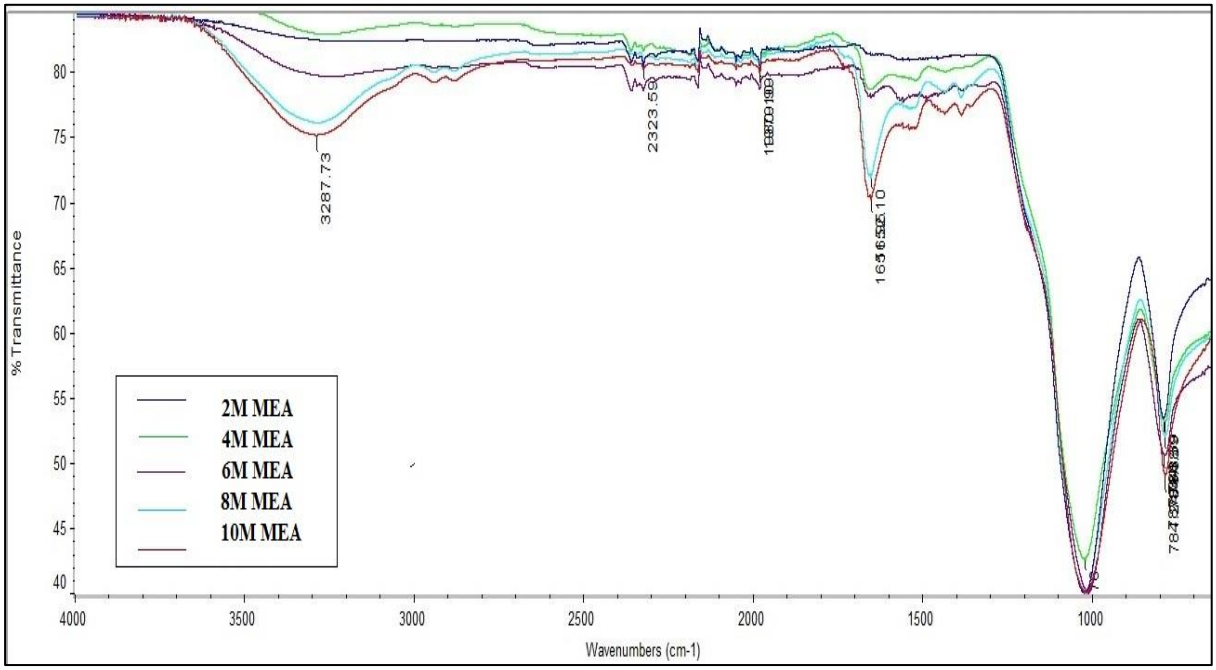

Figure 4.8a: FTIR spectrum of impregnated activated carbon with different concentration of MEA.

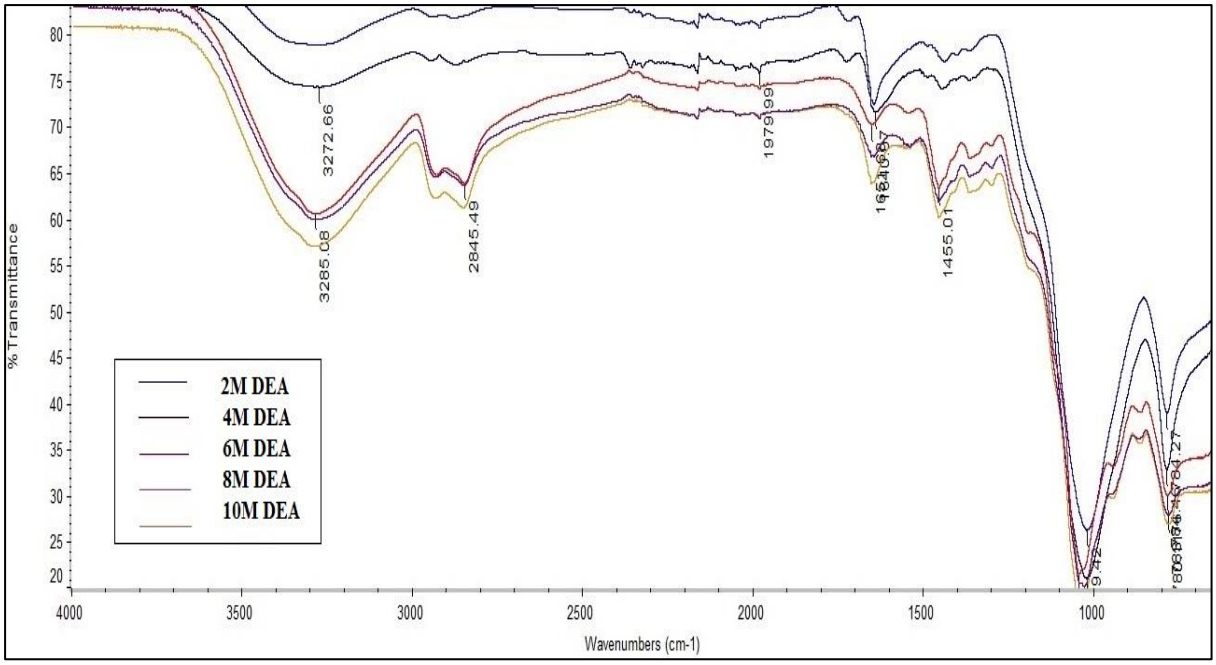

Figure 4.8b: FTIR spectrum of impregnated activated carbon with different concentration of DEA.

4.2.3.3 Effect on Mixture Ratio (Weight Percent) of Impregnated Activated Carbon with MEA and DEA

Figure 4.9a and Figure 4.9b show the impregnated activated carbon with different mixture ratio. The mixture ratio is based on the weight of activated carbon to the weight of MEA and DEA. The spectra of the MEA impregnated activated carbon with different mixture ratio can be observed in Figure 4.9a. The mixture ratio with the same quantity of activated carbon and MEA shows the highest transmittance percentage while the highest mixture ratio of MEA which is 5 times the weight of activated carbon shows the lowest transmittance percentage. The bands formed are parallel with the amide sensitive regions which are 3288.96 cm^{-1} and 1651.85 cm^{-1}.

The DEA impregnated activated carbon with different mixture ratio is shown in Figure 4.9b. Equal weight of activated carbon and DEA shows the least amide content whereas high mixture ratio of DEA shows a low transmittance percentage. The amide content for the 3 types of mixture ratio is from the range 3289.41 – 3277.35 cm^{-1} and 1647.86 – 1651.67 cm^{-1} band which indicates the amide regions.

From the results obtained, the higher amount of MEA and DEA produced a lower transmittance peak compared to the lower or equal amount of MEA and DEA to activated carbon. These results proved that the amount of amine impregnated with the activated carbon is higher with the increase in mixture ratio of MEA and DEA. These results also indicate there are many reactions between the carboxyl group and the amine group as high amount of amide formed on the surface of the activated carbon (Hayley. C., 2012).

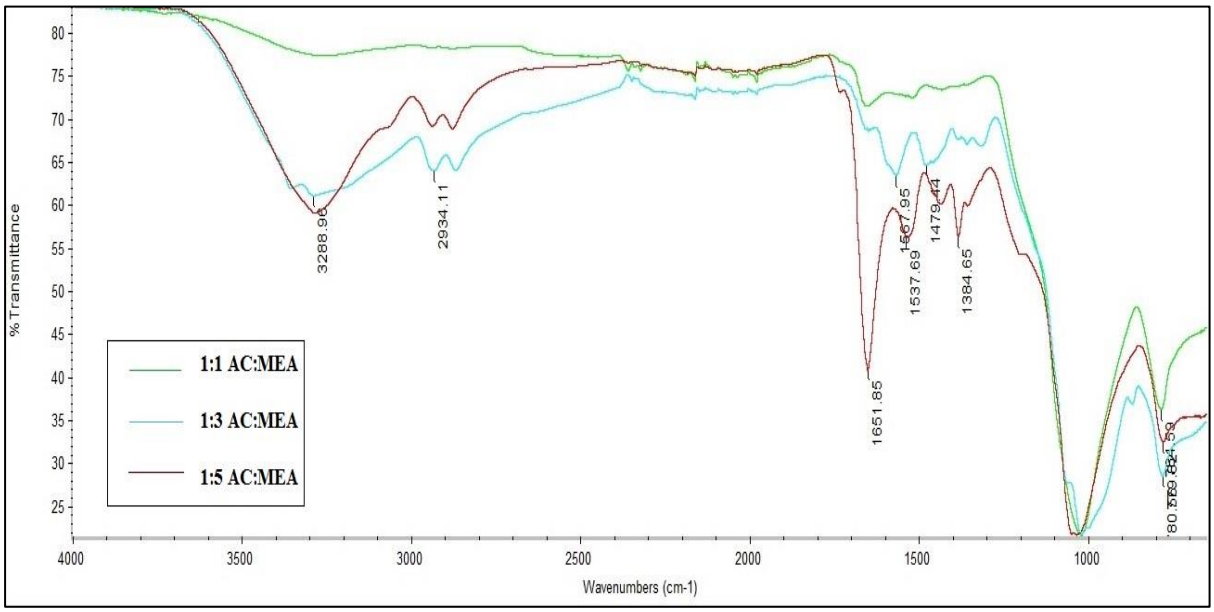

Figure 4.9a: FTIR spectrum of MEA impregnated activated carbon with different mixture ratio.

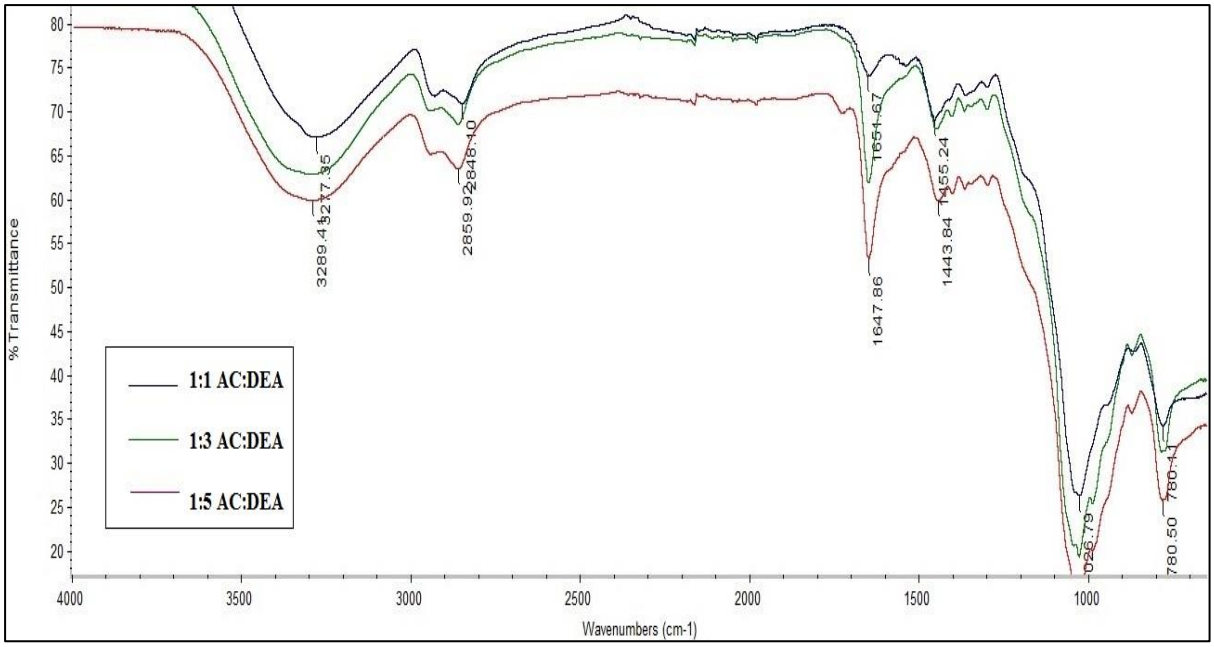

Figure 4.9b: FTIR spectrum of DEA impregnated activated carbon with different mixture ratio.

Table 4.3 shows the result summary for FTIR analysis of non-impregnated activated carbon and impregnated activated carbon with MEA and DEA.

Table 4.3: Result summary for FTIR analysis.

Type of AC	Concentration/ Mixture Ratio	Characteristics			
		Band (cm^{-1})	Transmittance (%)	Band (cm^{-1})	Transmittance (%)
Non-impregnated activated carbon	-	2849.39	81	-	-
Impregnated activated carbon with MEA	**2M** **4M** **6M** **8M** **10M**	3287.73	83 82 79 76 74	1656.10	82 79 78 72 70
Impregnated activated carbon with DEA	**2M** **4M** **6M** **8M** **10M**	3285.08 - 3272.66	79 74 61.5 61 57	1651.68	72 71 70 66 63
Impregnated activated carbon with MEA	**1:1** **1:3** **1:5**	3288.96	77 61 58	1651.85	71 68 41
Impregnated activated carbon with DEA	**1:1** **1:3** **1:5**	3289.41 - 3277.35	67.5 63 60	1647.86- 1651.67	74 63 54

4.2.4 Field Emmision Scanning Electron Microscopy (FESEM)

Figures 4.10a and 4.10b show the surface morphology of the non-impregnated activated carbon and impregnated activated carbon with MEA and DEA. The impregnated activated carbon varies in concentration which consist of 4M MEA, 10M MEA, 4M DEA and 10M DEA. The activated carbons (1 mm in size) are magnified at 60 times and 100,000 times. It can be seen that the activated carbon surface shows it is irregular with some smooth

surfaces and large pore size. An activated carbon usually consists of three types of pores which are micropores (diameter < 2 nm), mesopores (diameter 2-50 nm), and macropores (diameter > 50 nm).

At magnification of 60 times, a major difference can be seen in the surface structure and pore size of the macropores. The non-impregnated activated carbon has larger pore size compared to the impregnated activated carbon while the impregnated activated carbon with MEA has larger pore size than DEA impregnated activated carbon. The pore sizes for the impregnated activated carbon are also different according to the concentration of MEA and DEA. A higher concentration of MEA and DEA resulted in decrease of pore size. The decrease in pore size indicates that there was some amount of MEA and DEA blocking in the macropores of the activated carbon. A higher concentration of MEA and DEA will cause the increment in amount of MEA and DEA loaded in the macropores.

At magnification of 100,000 times, there is a slight difference in the surface structure and pore size of the mesopores. The loading of MEA and DEA on the activated carbon increased with the increase of concentration. A higher concentration of MEA and DEA cause the coating on the activated carbon to be thickened. The highest concentration of MEA and DEA which is 10M shows that all the pores were blocked and the activated carbon was fully covered by MEA and DEA. As in macropores, the mesopores also show that DEA has better attachment and coating on the activated carbon compared to MEA. The coating of DEA is thicker and larger than the coating of MEA on the activated carbon.

The different magnification of the sample which is 1000 times, 2000 times and 50,000 times are also shown in Figure 4.10c, Figure 4.10d and Figure 4.10e.

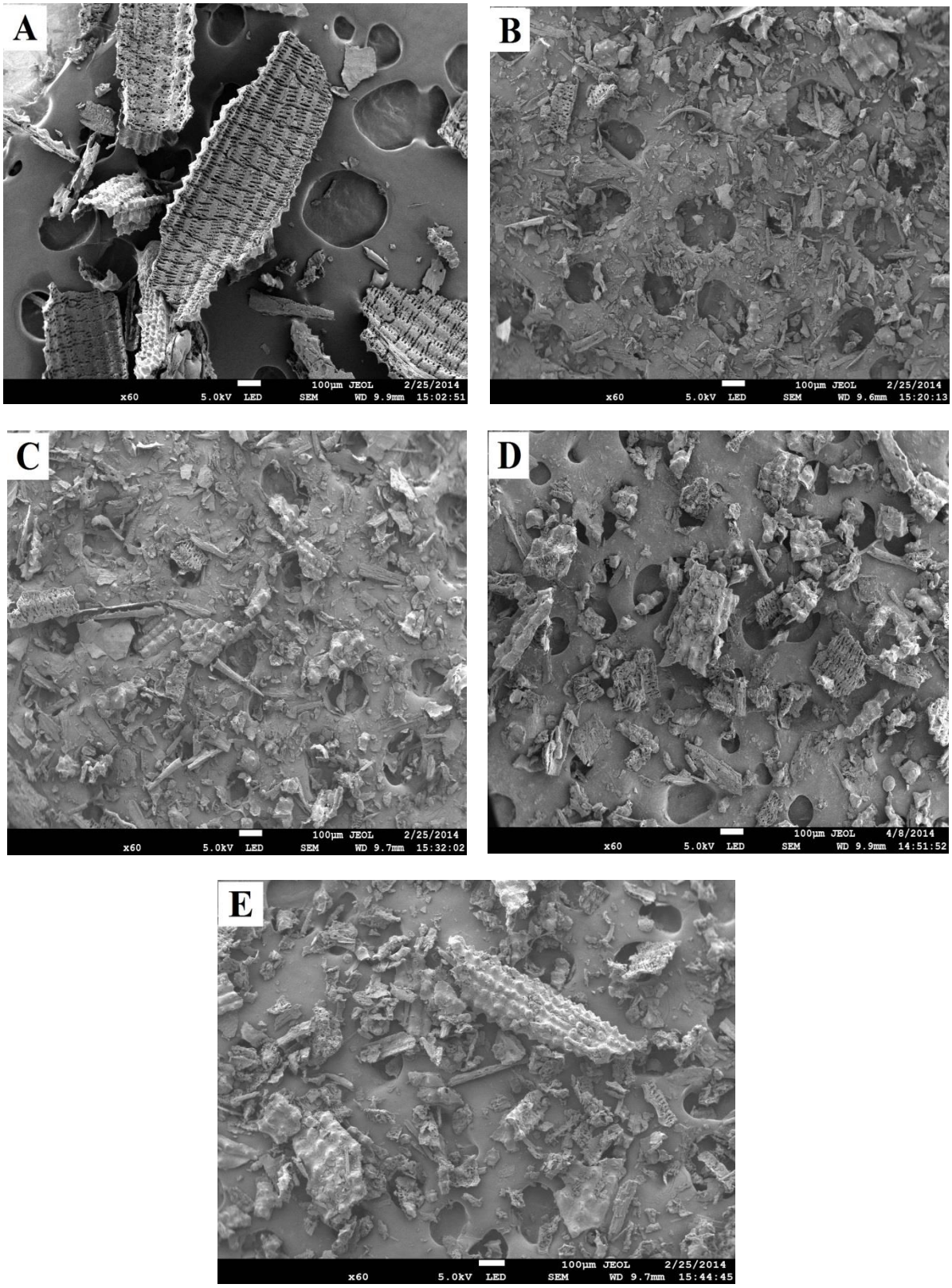

Figure 4.10a: The FESEM images magnified 60 times of (A) non-impregnated AC, (B) AC impregnated with 4M MEA, (C) AC impregnated with 10M MEA, (D) AC impregnated with 4M DEA and (E) AC impregnated with 10M DEA.

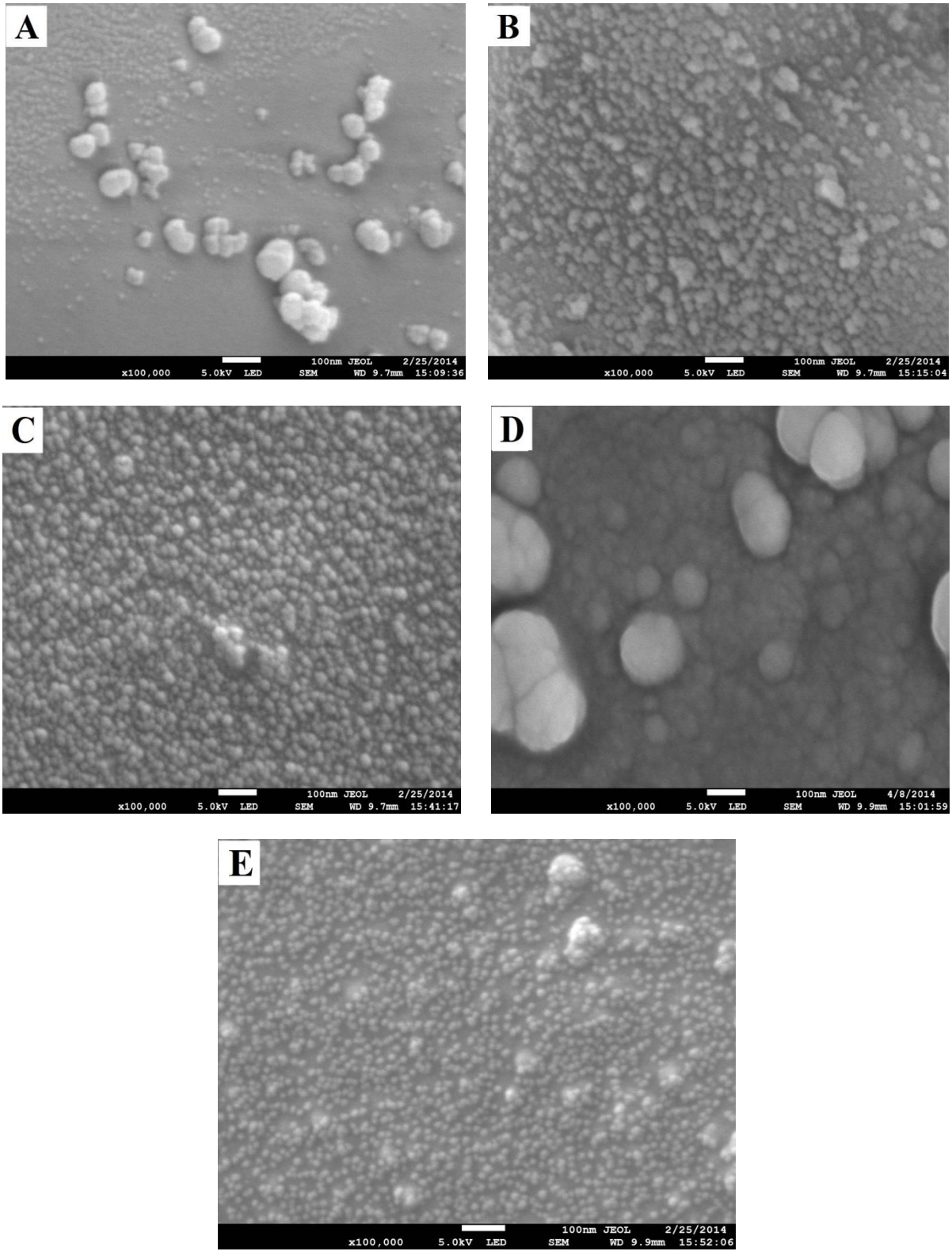

Figure 4.10b: The FESEM images magnified 100,000 times of (A) non-impregnated AC, (B) AC impregnated with 4M MEA, (C) AC impregnated with 10M MEA, (D) AC impregnated with 4M DEA and (E) AC impregnated with 10M DEA.

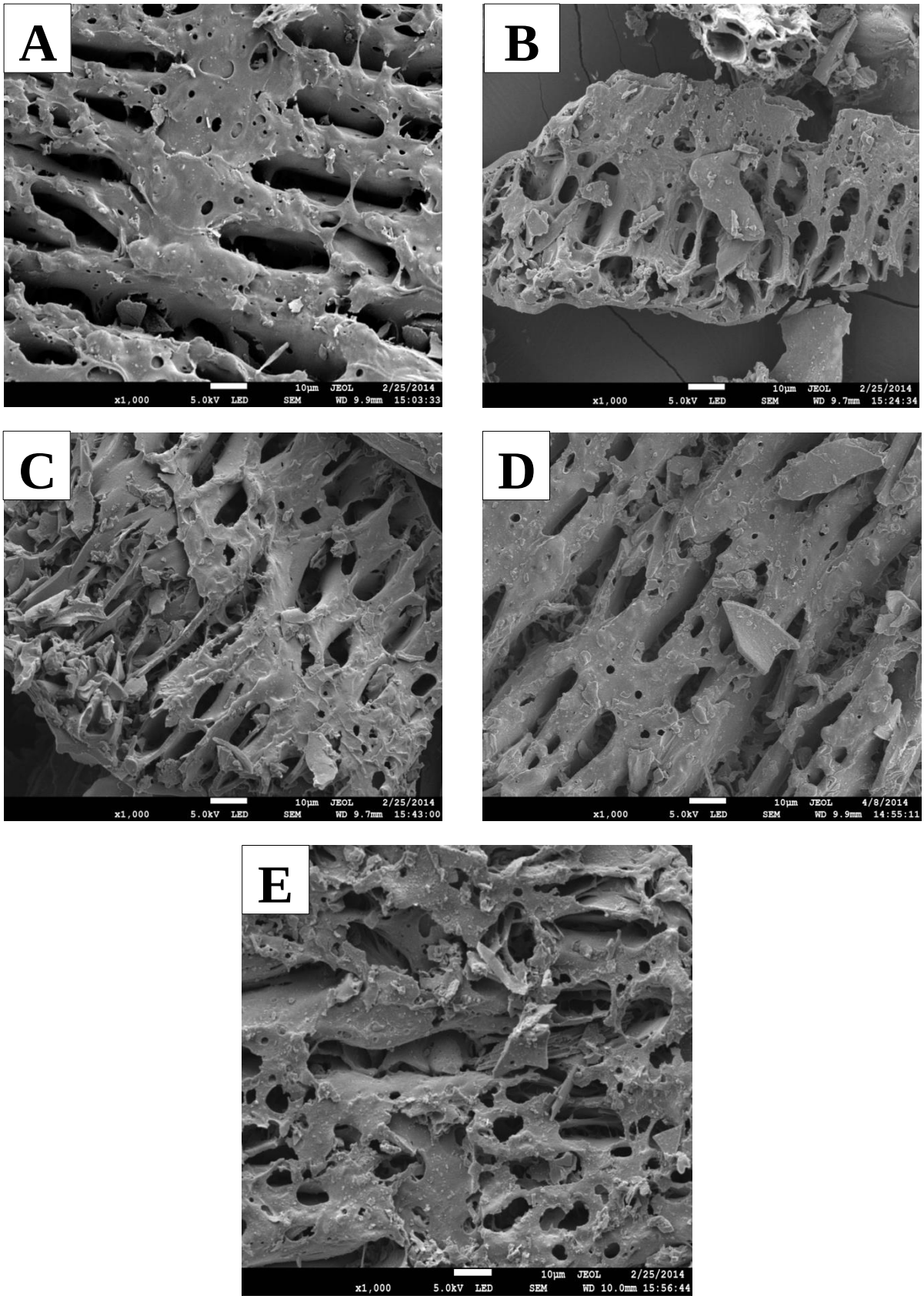

Figure 4.10c: The FESEM images magnified 1,000 times of (A) non-impregnated AC, (B) AC impregnated with 4M MEA, (C) AC impregnated with 10M MEA, (D) AC impregnated with 4M DEA and (E) AC impregnated with 10M DEA.

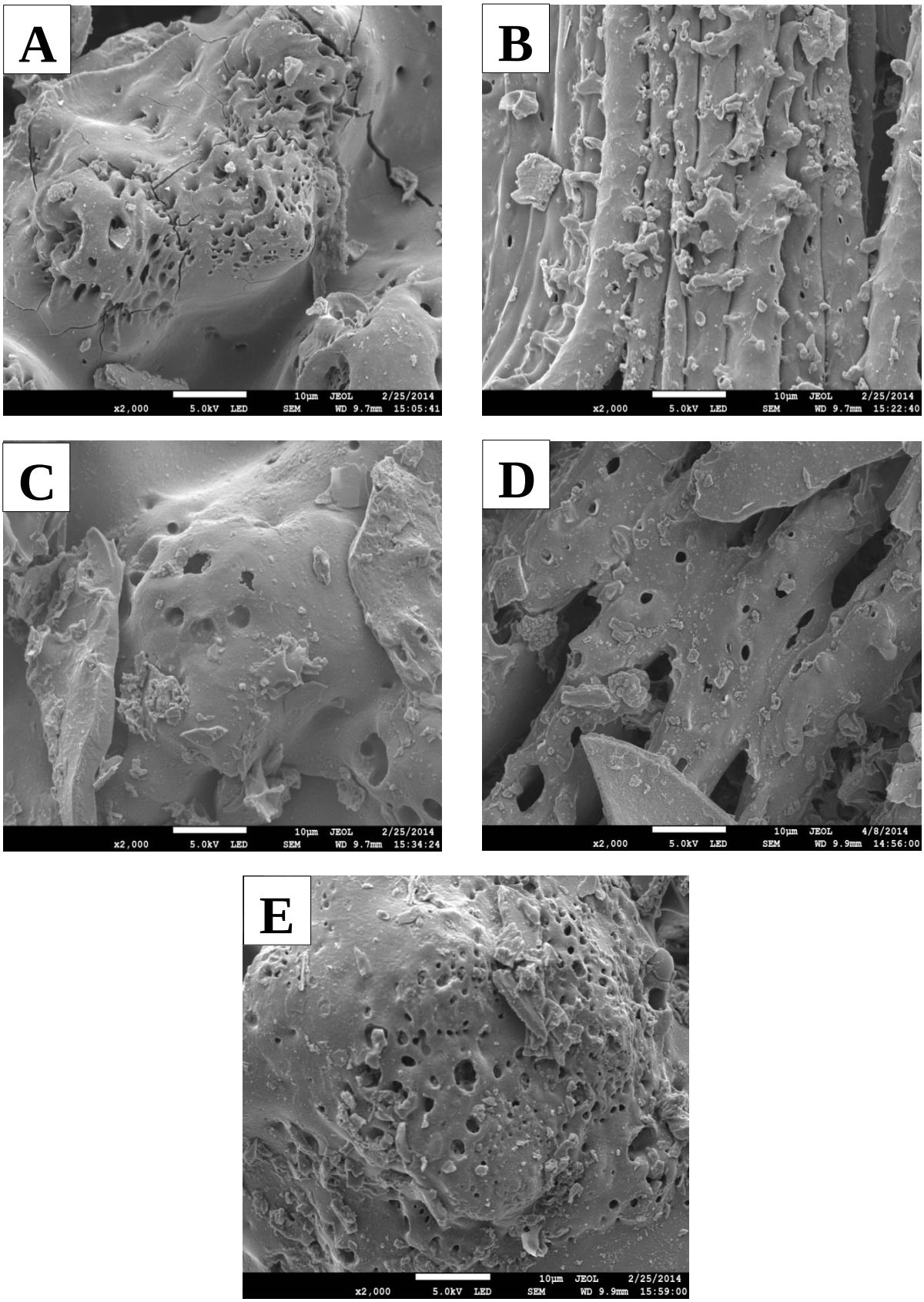

Figure 4.10d: The FESEM images magnified 2,000 times of (A) non-impregnated AC, (B) AC impregnated with 4M MEA, (C) AC impregnated with 10M MEA, (D) AC impregnated with 4M DEA and (E) AC impregnated with 10M DEA.

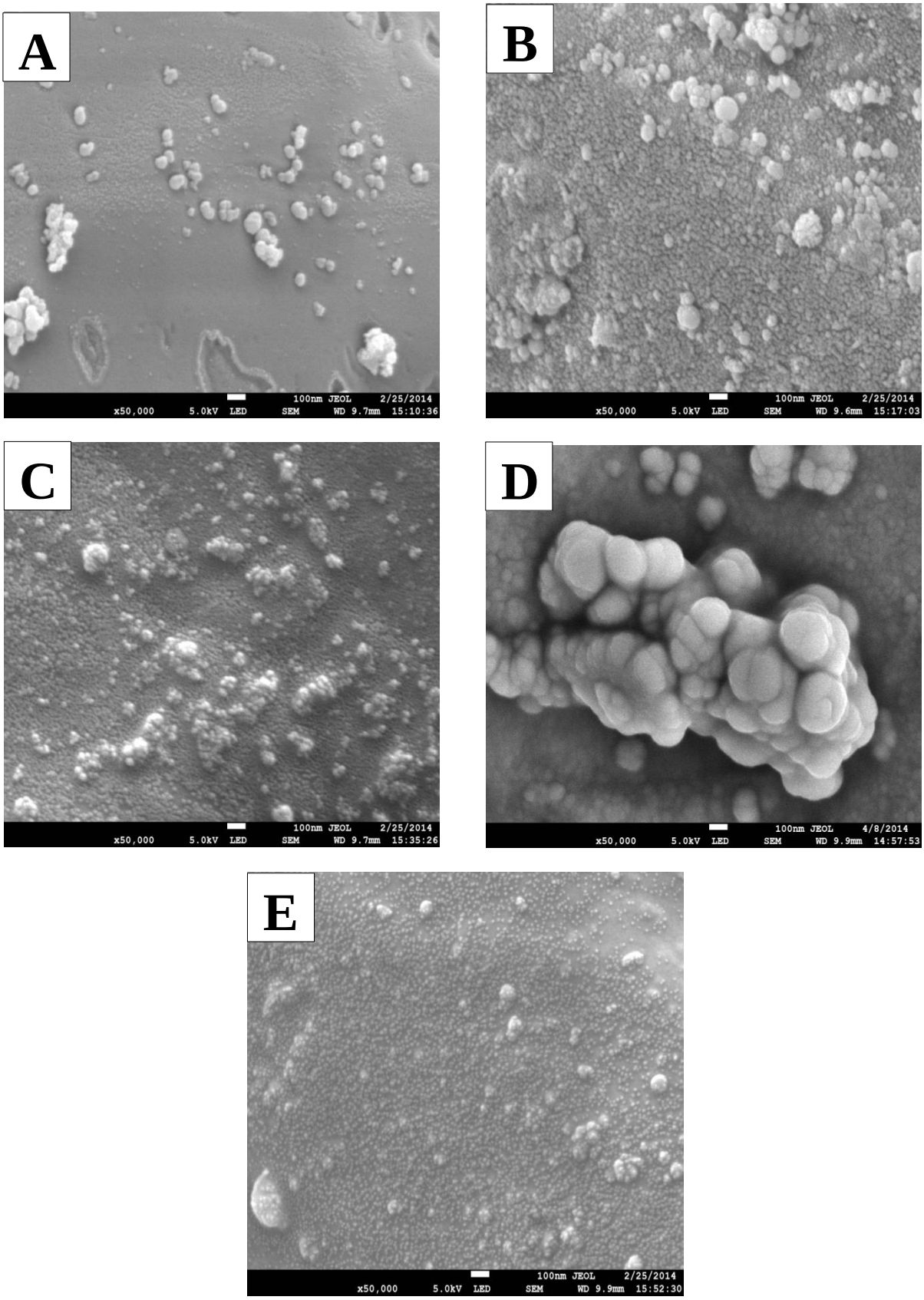

Figure 4.10e: The FESEM images magnified 50,000 times of (A) non-impregnated AC, (B) AC impregnated with 4M MEA, (C) AC impregnated with 10M MEA, (D) AC impregnated with 4M DEA and (E) AC impregnated with 10M DEA.

Activated carbon consists of acidic and basic surfaces. According to Houshmand et. al. (2011), amine groups were able to condense with carboxyl groups on activated carbon to generate surface consist of amide groups. Below is the reaction between carboxyl group with MEA and DEA.

MEA:

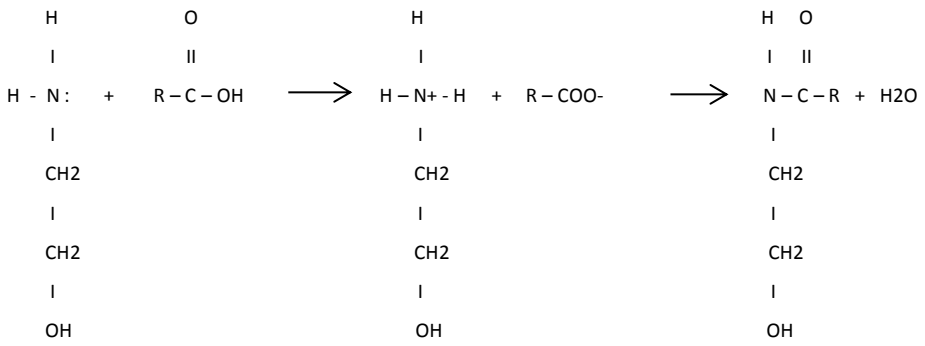

MEA + carboxylic acid ⟶ substituted-ammonium carboxylate salt ⟶ amide + water

Figure 4.11a: The reaction between carboxyl group with MEA.

DEA:

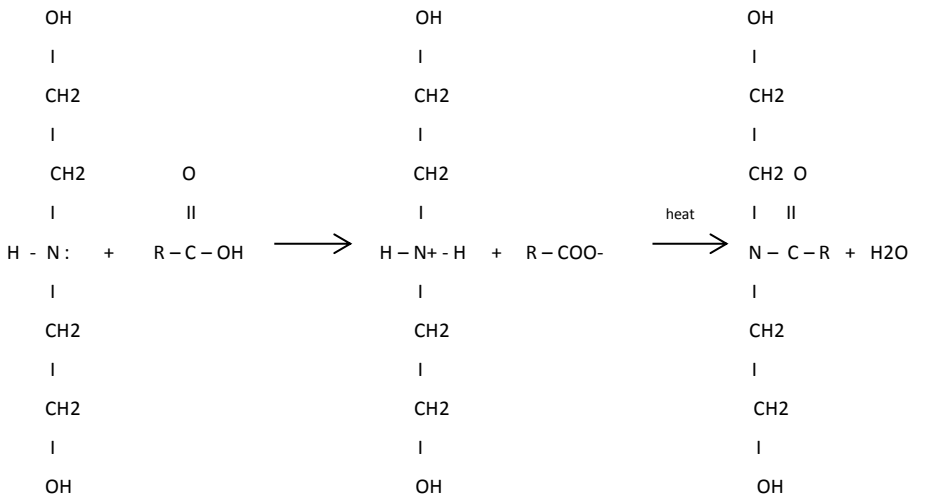

DEA + carboxylic acid ⟶ substituted-ammonium carboxylate salt ⟶ amide + water

Figure 4.11b: The reaction between carboxyl group with DEA.

As the drying of activated carbon impregnated with MEA and DEA is the part of methodology of the experiment, the reaction between carboxyl groups on activated carbon with MEA and DEA will produce amide. It was also proof that activated carbon containing oxygen has several basic functionalities such as chromene, ketone and pyrone (Shafeeyan et. al., 2010). Below is the reaction between ketone with MEA and DEA.

MEA:

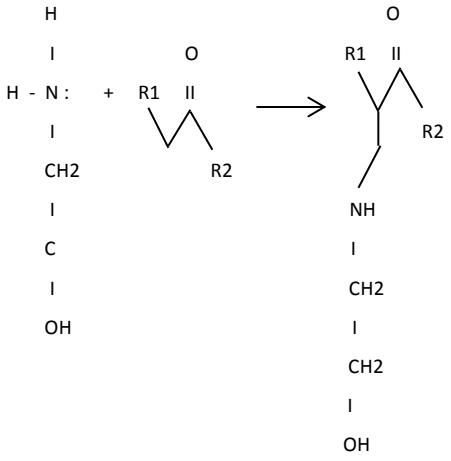

MEA + ketone ⟶ aminomethylated

Figure 4.12a: The reaction between ketone with MEA.

DEA:

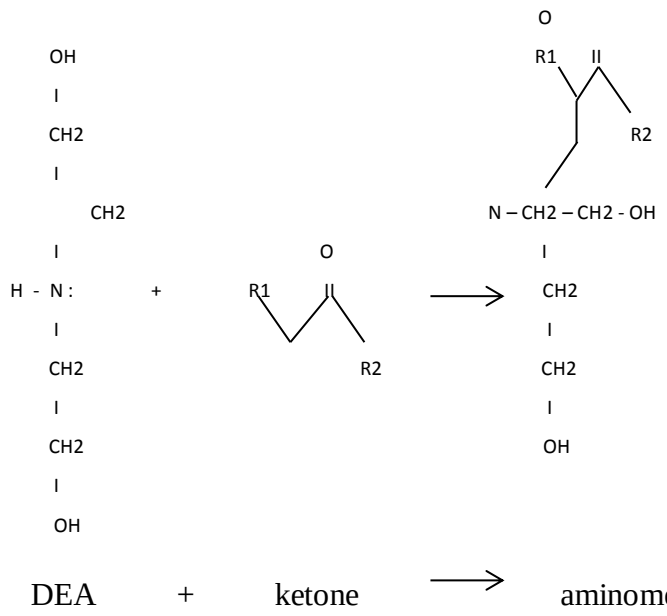

Figure 4.12b: The reaction between ketone with DEA.

The reaction of MEA and DEA with carboxylate acid and ketone facilitated the reduction of the pore size and the changing of the surface structure of activated carbon depending on the concentration of MEA and DEA used. The reactions occur also will cause the MEA and DEA attached strongly on the activated carbon surface.

4.3 Concluding Remarks

The findings tell the high potential of CO_2 adsorption capacity as the characterization results shows a positive feedback towards the quantity of MEA and DEA in the impregnated activated carbon samples. Table 4.4 summarized the findings from all the analysis done.

Table 4.4: Result summary for XRD, BET, FTIR and FESEM analysis.

Analysis	Non-Impregnated AC	Impregnated AC with MEA	Impregnated AC with DEA
XRD	• Presence of Pyrazole • Has highest intensity	• Presence of Ethanolamine • The intensity decrease with increase concentration	• Presence of Diethanolamine • The intensity is less compared to MEA
BET	Has the highest surface area and pore volume	Has higher surface area and pore volume compared to DEA but less than non-impregnated AC	Has the lowest surface area and pore volume
FTIR	• Presence of hydrocarbon • Has the highest transmittance	• Presence of amides • The transmittance decreases with increase in concentration and mixture ratio • The transmittance is low compared to non-impregnated AC but high compared to DEA	• Presence of amides • The transmittance decreases with increase in concentration and mixture ratio • Has the lowest transmittance
FESEM	Has the largest pore size	• Has smaller pore size compared to non-impregnated AC but larger pore size than DEA impregnated AC • The pore size decrease with increase in concentration	• Has the smallest pore size • The pore size decrease with increase in concentration

CHAPTER 5

CONCLUSION AND RECOMMENDATION

5.1 Conclusions

The preparation of non-impregnated activated carbon and impregnated activated carbon with MEA and DEA was successfully carried out in this research. The effects of concentration and mixture ratio on physical and chemical characteristics for both types of activated carbon were investigated by using various techniques which are XRD, BET, FTIR and FESEM.

The verification of the compound present on the non-impregnated activated carbon and impregnated activated carbon with MEA and DEA was done by XRD analysis. In XRD pattern analysis, diffraction angle around 21.66º to 22.18º were linked for pyrazole, ethanolamine and diethanolamine. Besides, there were also other compound present with a the higher concentration of MEA and DEA such as 2,6-diaminopyridine, 4-aminopyradine and benzalazine.

The adsorption isotherm for the non-impregnated activated carbon showed a *Type I* isotherm while the impregnated activated carbon showed a *Type II* isotherm. The total surface area, pore volume and pore size distribution in the non-impregnated activated carbon is higher than the impregnated activated carbon. The modified activated carbon with MEA showed higher surface area, pore volume and pore size compared to the impregnated activated carbon with DEA.

The FTIR analysis of the non-impregnated activated carbon showed that there are absent of amide functional group while there was a presence of amide functional groups on the impregnated activated carbon with MEA and DEA. The transmittance percentage of MEA is less than DEA which indicates that DEA contains more amines functional group compared to MEA. The higher concentration and mixture ratio resulted in lower transmittance percentage for both MEA and DEA.

The morphology of the non-impregnated activated carbon and modified activated carbon with MEA and DEA was studied using FESEM analysis. The pores were clearly seen in the non-impregnated activated carbon sample while the impregnated activated carbon with MEA and DEA showed the pores were being filled with amines. The higher concentration of MEA and DEA caused more pores closure and the distribution of DEA on the activated carbon surface is better compared to MEA.

From all the analysis done, it can be concluded that the DEA is the best amine for the impregnation purpose as it is secondary amine and contains more nitrogen functional group compared to MEA. The best concentration for both MEA and DEA in this study is 10M as it shows the most effectiveness such as lowest pore volume and surface area. It also shows the lowest transmittance which indicates a high quantity of amine in the sample. From FTIR analysis, it shows that the mixture ratio of 1:5 has the lowest transmittance value compared

to other mixture ratio. This indicates that the high amount of MEA and DEA were present in the sample and hence, will improve the CO_2 adsorption capacity.

5.2 Recommendations

Based on the outcomes of this research and plenty of ideas reported in the literature, the following remarks can be considered for future work:

- The stirring time for the impregnation process may be prolonged as the regular distribution of MEA and DEA may be achieved.
- The heating time may be increased to ensure that the moisture content is zero especially for the high mixture ratio of MEA and DEA.
- The product must be kept in tightly container to prevent the reaction of impregnated activated carbon with air.

As for future works, the experiment of applying the newly modified activated carbon in real process of absorbing CO_2 must be conducted. More data can be collected from this work and the results will be the real measurement on how effective the adsorbent can be.

REFERENCES

Allwar. (2012). Characteristics of Micro- and Mesoporous Structure and Surface Chemistry of Activated Carbons Produced by Oil Palm Shell. *International Conference on Chemical, Ecology and Environmental Sciences.* Pg 138-141.

Aroua, M.K., Daud, W.M.A.W., Yin, C.Y. & Adinata, D. (2008). Adsorption Capacities of Carbon Dioxide, Oxygen, Nitrogen and Methane on Carbon Molecular Basket Derived from Polyethyleneimine Impregnation on Microporous Palm Shell Activated Carbon. *Separation and Purification Technology, 62 (3),* pp. 609-613.

Arshad, F. M., Alias, E. F., & Noh, K. M. (2011). Food Security: Self-Sufficiency of Rice in Malaysia. *IJMS 18(2),* 83-100.

Binkley, R., W. (1969). A Reexamination of the Effect of Benzophenone on Benzalazine Photochemistry. *The Journal of Organic Chemistry. Vol.24,* No. 10. 3218 - 3219.

Boonpoke, A., Chiarakorn, S., Laosiripojana, N., Towprayoon, S., & Chidthaisong, A. (2012).Investigation of CO_2 Adsorption by Bagasse-Based Activated Carbon. *Korean J. Chem. Eng.,* 2: 89-94.

Brotzel, F., & Mayr, H. (2007). Nucleophilicities of Amines, Amino Acids and Pyradines. *Chem. Eur. J. 2007, 13,* 336-345.

Bukalak, D., Kuceba, I. M., & Nowak, W. (2013). Assessment of the Sorption Capacity and Regeneration of Carbon Dioxide Sorbents using Thermogravimetric Methods. *J Therm Anal Calorim (2013), 113,* 157-160.

Cameron Carbon Incorporated. (2006). Activated Carbon: Manufacture, Structure & Properties. Retrieved on 1st November from www.cameroncarbon.com/documents/carbon_structure.pdf

Chen, Y., Zhu, Y., Wang, Z., Li, Y., Wang, L., Ding, L., Gao X., Ma, Y., & Guo, Y. (2011). Applications Studies of Activated Carbon Derived from Rice Husks Produced by Chemical-Thermal Process – A Review. *Advances in Colloid and Interface Science, Vol. 163, Issue 1,* 39-52.

Chien, C. C. (2013). Application Technology about Activated Carbon from Rice Husk. Retrieved on 6th October 2013 from www.itri.org.tw/eng/econtent/research/research05_02.aspx?sid=4

Dali, M. A., Ibrahem, A. S. & Hadi, A. (2012). General Study About Activated Carbon for Adsorption Carbon Dioxide. *Journal of Purity, Utility Reaction and Environment. Vol. 1 No. 5,* 236-251.

Deithorn, R. T. & Mazzoni, A. F. (2013). Activated Carbon: What is Activated Carbon and How Does It Work? Retrieved on 5th October 2013 from http://www.tigg.com/what-is-activated-carbon.html

Bezerra, D. P., Oliveira, R.S., Vieira, R. S., Jr, C. L. C. & Azevedo, D. S. C. (2010). Adsorption of CO_2 on Nitrogen-Enriched Activated Carbon and Zeolite 13X. *Adsorption 17:* 235-246.

Drage, T. C., Arenillas, A., Smith, K., & Snape, C. E. (2006). Comparison of Pre and Post-Combustion CO_2 Adsorbent Technologies. Retrieved on 29th September 2013 from http://www.geos.ed.ac.uk/ccs/Publications/Drage.pdf

Geankoplis, C. J. (2003). Transport Processes and Separation Process Principles. New Jersey: Pearson Education International.

Gregg, S. J. & Sing, K. S. W. (1982). Adsorption, Surface Area and Porosity. *Academic Press. First Ed.*

Havens, M. (1989). The Chemistry of Dissipative Plastics. *EOS/ESD Symposium of Cryovac Vol 28,* No. 3. 245-248.

Hayley, C. (2012) Direct Amide Formation Between Carboxylic Acids and Amines: Mechanism and Development of Novel Catalytic Solutions, Durham theses, Durham University.

Houshmand, A., Daud, W. M. A. W., Lee, M. G. & Shafeeyan, M. S. (2011). Carbon Dioxide Capture with Amine-Grafted Activated Carbon. *Water Air Soil Pollut*. Springer.

Jahangiri, M., Adl, J., Shahtaheri, S. J., Rashidi, A., Ghorbanali, A., Kakooe, H., Forushani, A. R., & Ganjali, M. R. (2013). Preparation of a New Adsorbent from Activated Carbon and Carbon nanofiber (AC/CNF) for Manufacturing Organic-Vapor Respirator Cartridge. Retrieved on 4th October 2013 from http://www.ijehse.com/content/10/1/15

Javed, S., H., Naveed, S., Feroze, N., Zafar, M., & Shafaq, M. (2010). Crystal and Amorphous Silica from $KMnO_4$ Treated and Untreated Rice Husk. *Journal of Quality and Technology Management. Vol 6*, 81-90.

Kangwanwatana, W., Saiwan, C., & Tontiwachwuthikul, P. (2013). Study of CO_2 Adsorption using Adsorbent Modified with Piperazine. *Chemical Engineering Transactions, 35,* 403-408.

Kermani, M., Pourmoghaddas, H., Bina, B., & Khazaei, Z. (2006). Removal of Phenol from Aqueous Solutions by Rice Husk Ash and Activated Carbon. *Pakistan Journal of Biological Sciences 9 (10).* 1905-1910.

Khalil, S. H., Aroua, M. K., & Daud, M. A. (2011). Impregnation of Commercial Palm Shell Activated Carbon with Monoethanolamine for Adsorbing CO_2 from Gas Mixture. *2011 International Conference on Biology, Environment and Chemistry IPCBEE vol.24*, 438-443.

Kim, Y., E., Lim, J., A., Jeong, S., K., Yoon, Y., I., Bae, S., T. & Nam, S., C. (2013). Comparison of Carbon Dioxide Absorption in Aqueous MEA, DEA, TEA, and AMP Solutions. *Bull. Korean Chem. Soc. 2013, Vol. 34*, No. 3, 783.

Kumar, A., Mohanta, K., Kumar, D., & Parkash, O. (2012). Properties and Industrial Applications of Rice Husk: A Review. *International Journal of Emerging Technology and Advanced Engineering. Vol 2, Issue 10*, 86-90.

Lee, S. C., Hsieh, C. C., Chen, C. H., & Chen, Y. S. (2013). CO_2 Adsorption by Y-Type Zeolite Impregnated with Amines in Indoor Air. *Aerosol and Air Quality Research, 13,* 360-366.

Liang, H., C. & Harrison, B., H. (1995). Organic Amine Impregnated Activated Carbon. Retrieved on 24th September 2013 from docs.google.com/viewer?url=patentimages.storage.googleapis.com/pdfs/US5462908.pdf

Lin, Y., Yan, Q., Kong, C., & Chen, L. (2013). Polyethyleneimine Incorporated Metal-Organic Frameworks Adsorbent for Highly Selective CO_2 Capture. Retrieved on 29th September 2013 from http://www.nature.com/srep/2013/130517/srep01859/full/srep01859.html

Meng, L., Cho, K. S. & Park, S. J. (2009). CO_2 Adsorption of Amine Functionalized Activated Carbons. *Carbon Letters, Vol 10, No. 3*, 221-224.

Mdoe, J. E. G. & Mkayula, L. L. (2002). Preparation and Characterization of Activated Carbons from Rice Husks and Shells of Palm Fruits. *Tanz. J. Sci. Vol. 28(2)*, 131-142.

Qi, G., Wang, Y., Estevez, L., Duan, X., Anako, N., Park, A. H. A., Li, W., Jones, C. W. & Giannelis, E. P. (2010). High Efficiency Nanocomposite Sorbents for CO_2 Capture Based on Amine-Functionalized Mesoporous Capsules. *Energy & Environmental Science, 4*, 444-452.

Ray, I. & Altshuer, B. (2013). Adsorption with Activated Carbon: Economical Removal of Malodorous and Toxic Organics. Retrieved on 5th October 2013 from http://www.enviroenergytek.com/upload/adsorption_activated_carbon.pdf

Scheiman, M. A. (1962). A Review of Monoethanolamine Chemistry. Surface Chemistry Branch Chemistry Division. U.S. Naval Research Laboratory, Washington D.C.

Shafeeyan, M., S., Daud, M. A., Houshmand, A., & Shamiri, A. (2010). A Review on Surface Modification of Activated Carbon for Carbon Dioxide. *Journal of Analytical and Applied Pyrolysis 89 (2010),* 143-151.

Shelke, V. R., Bhagade, S. S. & Mandavgane, S. A. (2010). Mesoporous Silica from Rice Husk Ash. *Bulletin of Chemical Reaction Engineering & Catalysis, 5 (2),* 63-67.

Snape, C. E., Smith, K. M., Arenillas, A., & Drage, T. C. (2004). Comparison of Two Different Approaches for Enhancement of CO_2 Removal by Adsorption on Carbons. *Prepr. Pap.-Am. Chem. Soc., Div. Fuel Chem. 2004, 49(2),* 685-687.

Spigarelli, B. P. & Kawatra, S. K. (2013). Opportunities and Challenges in Carbon Dioxide Capture. *Journal of CO_2 Utilization, 1,* 69-87.

Subki, R. & Rohasliney, H. (2011). Rice Husk as Biosorbent: A Review. *Health and the Environment Journal, 2012, Vol. 3, No. 1,* 89-95.

U. S. Department of State. (2007). Chapter 5: Projected Greenhouse Gas Emissions. Retrieved on 5th October from http://www.state.gov/documents/organization/140007.pdf

Wagner, A., Steen, B., Johansson, G., Zhanghellini, E., Jacobsson, P. & Johansson, P. (2013). Carbon Dioxide Capture from Ambient Air Using Amine-Grafted Mesoporous Adsorbents. *International Journal of Spectroscopy, Vol. 2013,* 1-8.

Wang, J., Chen, H., Zhou, H., Liu, X., Qiao, W., Long, D. & Ling, L. (2012). Carbon Dioxide Capture Using Polyethyleneimine-Loaded Mesoporous Carbons. *Journal of Environmental Sciences 25 (1),* 124-132.

Wang, Q., Luo, J., Zhong, Z., & Borgna, A. (2010). CO_2 Capture by Solid Adsorbents and Their Applications: Current Status and New Trends. *Energy Environ. Sci., 2011, 4,* 42-55.

Warudka. S. S. (2011). Comparison of Amine - Based Absorbents for Post - Combustion Carbon Capture. Retrieved on 6th October 2013 from http://www.aiche.org/cei/resources/chemeondemand/conference-presentations/comparison-amine-based-absorbents-post-combustion-carbon-capture

Yin, C. Y., Aroua, M. K. & Daud, W. M. A. W. (2007). Impregnation of Palm Shell Activated Carbon with Polyethylleneimine and its Effects on Cd^{+} Adsorption. *Colloids and Surfaces A: Physicochem. Eng. Aspects 307,* 128-136.

APPENDIX A

SAMPLE CALCULATION FOR PREPARATION OF STOCK SOLUTION DURING ACTIVATED CARBON PREPARATION

APPENDIX A

SAMPLE CALCULATION FOR PREPARATION OF STOCK SOLUTION DURING ACTIVATED CARBON PREPARATION

Type of amine: Monoethanolamine

Molecular weight: 61.08 g mol^{-1}

Purity: 99%

Density: 1.01 g mL^{-1}

Thus,

Concentration of monoethanolamine = $\frac{990\text{mL}}{1\text{L}} \times \frac{1.01\text{ g}}{\text{mL}} \times \frac{\text{mol}}{61.08\text{ g}} = 16.37\text{ mol/L}$

$= 16.37\text{M}$

For preparation of the **weight ratio 1:1**, the basis is 50 g of activated carbon is to 49.50 mL of MEA as the weight is divided by the density of MEA.

For concentration of 2M MEA,

$m_1v_1 = m_2v_2$

16.37M v_1 = 2M x 49.50 mL

v_1 = 6.0476 mL

Therefore, the volume of MEA needed for the preparation of 2M of MEA stock solution is 6.0476 mL while the balance which is 43.4524 mL is deionized water.

The calculation for the rest of stock solution according to the weight ratio and concentration is summarized in the table A1.

Table A1: The summary of the calculation of the stock solution according to the weight ratio and concentration.

Weight ratio	**Concentration of MEA**				
	2M	**4M**	**6M**	**8M**	**10M**
	Volume of MEA needed (mL)				
1:1 (50 g of activated carbon: 49.50 mL of stock solution)	6.0476	12.0953	18.1429	24.1906	30.2382
1:3 (50 g of activated carbon: 148.50 mL of stock solution)	18.1429	36.2859	54.4288	72.5718	90.7147
1:5 (50 g of activated carbon: 247.50 mL of stock solution)	30.2382	60.4765	90.7147	120.9530	151.1912

Type of amine: Diethanolamine

Molecular weight: 105.14 g mol^{-1}

Purity: 99%

Density: 1.097 g mL^{-1}

Thus,

Concentration of diethanolamine = $\frac{990\text{mL}}{1\text{L}} \times \frac{1.097\text{ g}}{\text{mL}} \times \frac{\text{mol}}{105.14\text{ g}} = 10.33\text{ mol/L}$

$= 10.33\text{M}$

For preparation of the **weight ratio 1:1**, the basis is 50 g of activated carbon is to 45.58 mL of DEA as the weight is divided by the density of DEA.

For concentration of 2M DEA,

$m_1v_1 = m_2v_2$

10.33M v_1 = 2M x 45.58 mL

v_1 = 8.8248 mL

Therefore, the volume of DEA needed for the preparation of 2M of DEA stock solution is 8.8248 mL while the balance which is 36.7552 mL is deionized water.

The calculation for the rest of stock solution according to the weight ratio and concentration is summarized in the table A2.

Table A2: The summary of the calculation of the stock solution according to the weight ratio and concentration.

Weight ratio	**Concentration of DEA**				
	2M	**4M**	**6M**	**8M**	**10M**
	Volume of DEA needed (mL)				
1:1 (50 g of activated carbon: 45.58 mL of stock solution)	8.8248 10.33	17.6496	26.4743	35.2991	44.1239
1:3 (50 g of activated carbon: 136.74 mL of stock solution)	26.4743	52.9487	79.4230	105.8974	132.3717
1:5 (50 g of activated carbon: 227.9 mL of stock solution)	44.1239	88.2478	132.3717	176.4956	220.6196

APPENDIX B

RESULTS & DISCUSSION

APPENDIX B-1

X-RAY DIFFRACTION (XRD) RESULTS

Analysis Results

General Information

Analysis date	4/24/2014 12:58:12 PM		
Sample name	XRD Analysis	Measured time	4/11/2014 9:42:23 AM
File name	1(non-impregnated activated carbon).raw	Operator	administrator
Comment	UMP		

Measurement profile

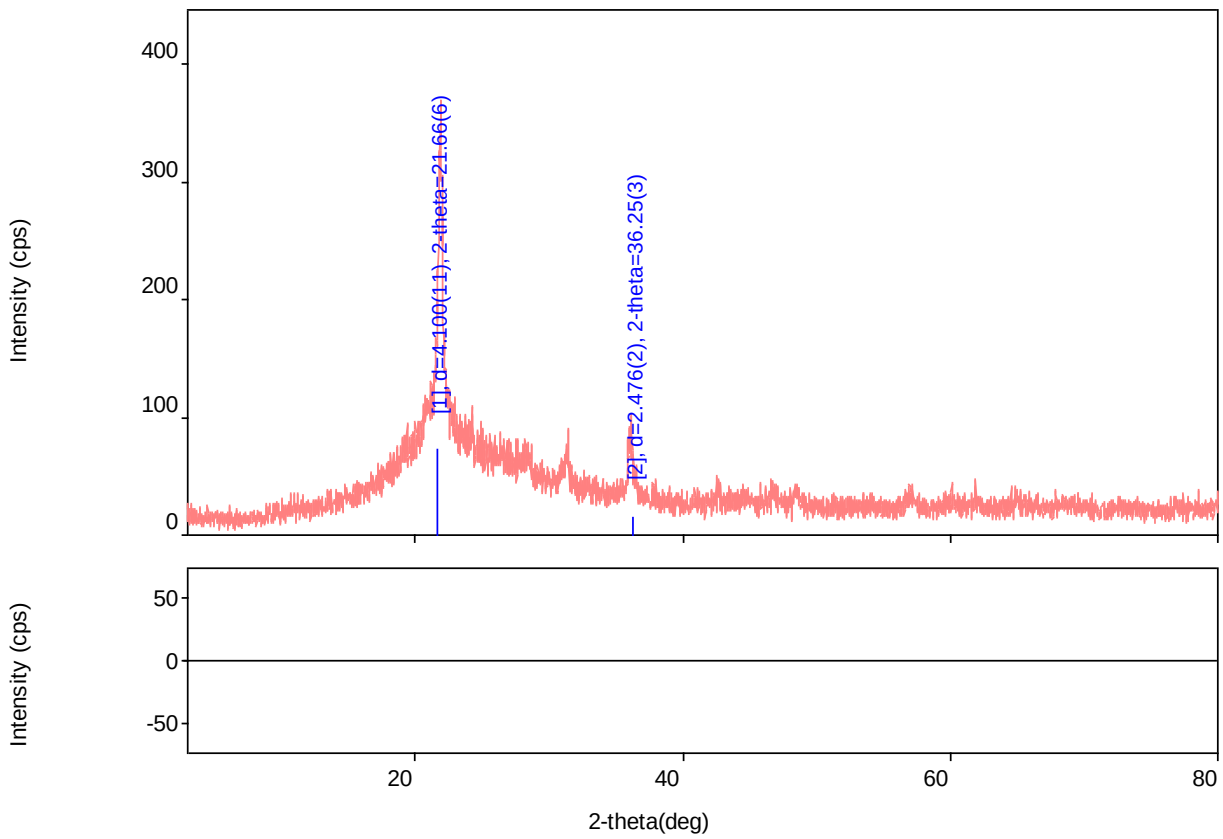
Intensity (cps)
400
300
200
100
0
[1], d=4.100(11), 2-theta=21.66(6)
[2], d=2.476(2), 2-theta=36.25(3)
Intensity (cps)
50
0
-50
20
40
60
80
2-theta(deg)

Measurement conditions

XG	Cu/30 kV/15 mA	Duration time / Scan speed	1 deg/min
Goniometer		Step / Sampling step	0.02 deg
Attachment	-	Measurement axis	2ƒÆ/ƒÆ
K-beta filter	-	Scan range	3-80 deg
Incident monochromator	-	Incident slit	-
Receiving monochromator	-	Vertical divergence slit	-
Counter	-	Receiving slit #1	-
		Receiving slit #2	-

Qualitative analysis results

Phase name	Formula	Figure of merit	ICDD
Pyrazole	C3 H4 N2	0.6216167956826982	211807 (ICDD)

Phase name	Formula	Space group	ICDD
Pyrazole	C3 H4 N2	33 : P21cn	211807 (ICDD)

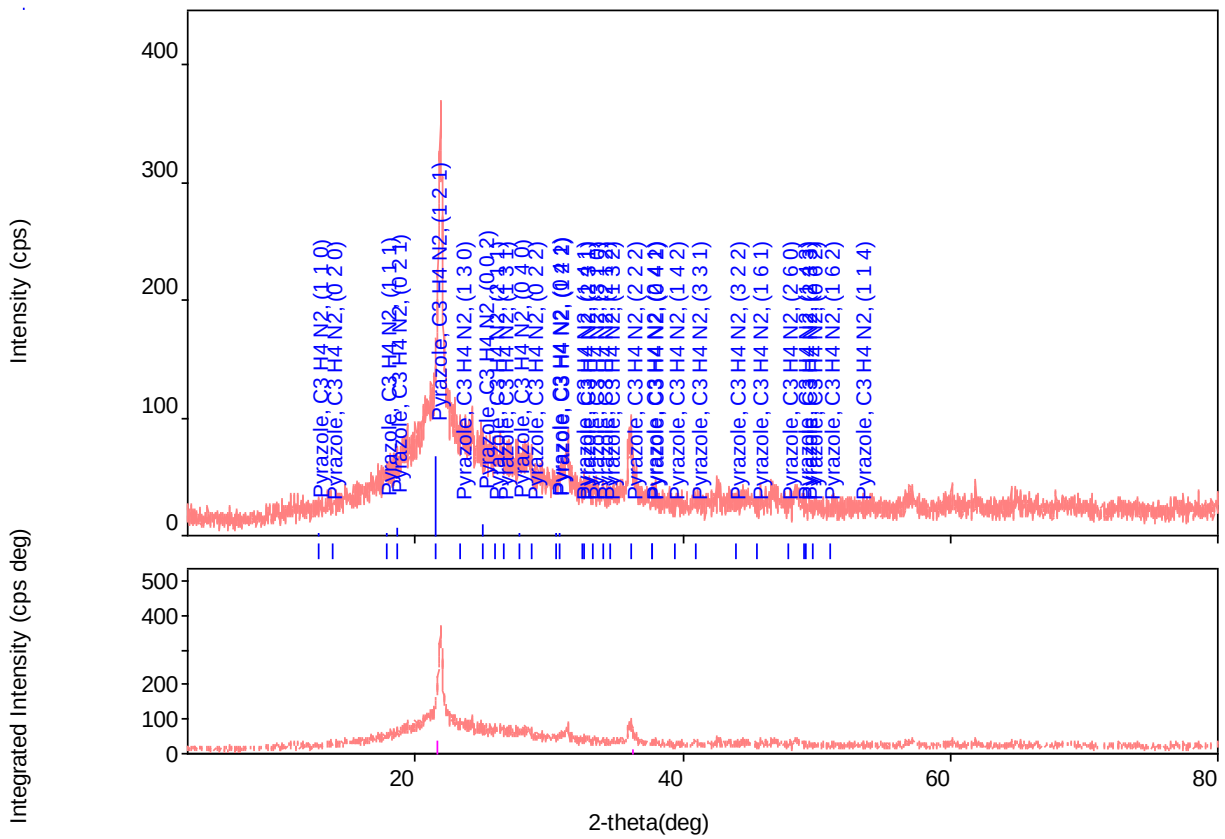

Peak list

2-theta (deg)	d (ang.)	Height (cps)	Int. I(cps¥deg)	FWHM(deg)	Size	Phase name
21.66(6)	4.100(11)	74(9)	395(7)	3.50(9)	24.1(6)	Pyrazole, (0,2,1)

36.25(3)	2.476(2)	17(4)	13.9(16)	0.54(11)	163(34)	Pyrazole, (2,2,2)

Parameters used for WPPF

Profile parameters

Common Parameter	Background	Data	1
		Function name	B-spline
		param0	8.592380539778109
		param1	19.81302420025243
		param2	51.94916682956907
		param3	9.22744629244418
		param4	29.49480799723946
		param5	17.61398298067857
		node0	3
		node1	28.66
		node2	54.32
		node3	80
Common Parameter	Peak shift		
		Function name	Shift axial displacement
		param0	0.02897139653371736
		param1	0
		param2	0
Pyrazole	Scale factor	s	5.53(12)
	FWHM	U	0.0000
		V	0.0000
		W	10.0000
	Asym. Factor	A0	-0.3525
		A1	0.0000
	Extinction coefficient	etaL0/mL0	0.9531
		etaL1/mL1	0.0000
		etaH0/mH0	0.8878

	etaH1/mH1	0.0000
Preferred orientationMarch-Dollase	h	0
	k	0
	l	0
	March coefficient	1.000000

Structure parameters

Data set name	Phase Name	Element	X	y	z	Occupancy	Temperature factor

File name	Rwp	Rp	Re	S	Chi^2	Maximum shift/e.s.d.
1	0	0	0	0	0	0

Lattice constants

Angular correction

No correction
Use External standard parameters
Use internal standard data

Analysis results

File name	a (ang.)	b (ang.)	c (ang.)	alpha (deg)	beta (deg)	gamma (deg)
1	8.248000	12.841000	7.096000	90.000000	90.000000	90.000000

Phase name	a (ang.)	b (ang.)	c (ang.)	alpha (deg)	beta (deg)	gamma (deg)
Pyrazole	8.248000	12.841000	7.096000	90.000000	90.000000	90.000000

Analysis Results

General Information

Analysis date	4/24/2014 1:06:20 PM		
Sample name	XRD Analysis	Measured time	4/11/2014 11:02:52 AM
File name	2(4M MEA).raw	Operator	administrator
Comment	UMP		

Measurement profile

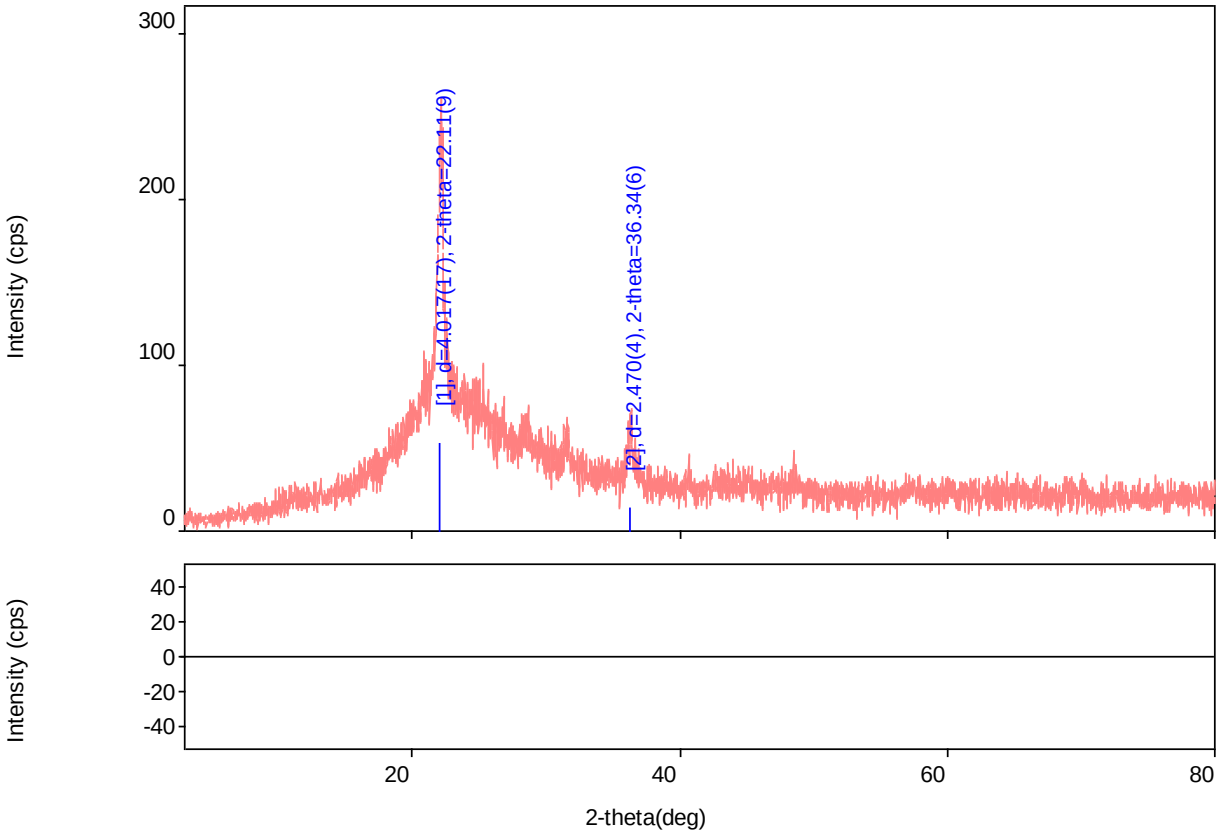
Intensity (cps)
300
200
100
0
[1], d=4.017(17), 2-theta=22.11(9)
[2], d=2.470(4), 2-theta=36.34(6)
Intensity (cps)
40
20
0
-20
-40
20
40
60
80
2-theta(deg)

Measurement conditions

XG	Cu/30 kV/15 mA	Duration time / Scan speed	1 deg/min
Goniometer		Step / Sampling step	0.02 deg
Attachment	-	Measurement axis	2ƒÆ/ƒÆ
K-beta filter	-	Scan range	3-80 deg
Incident monochromator	-	Incident slit	-
Receiving monochromator	-	Vertical divergence slit	-
Counter	-	Receiving slit #1	-
		Receiving slit #2	-

Qualitative analysis results

Phase name	Formula	Figure of merit	ICDD
Pyrazole	C3 H4 N2	0.4296309058563116	211807 (ICDD)
Ethanolamine phosphoric acid	C2 H7 N O · H3 P O4	0.6820043079691741	50203 (ICDD)

Phase name	Formula	Space group	ICDD
Pyrazole	C3 H4 N2	33 : P21cn	211807 (ICDD)
Ethanolamine phosphoric acid	C2 H7 N O · H3 P O4	-	50203 (ICDD)

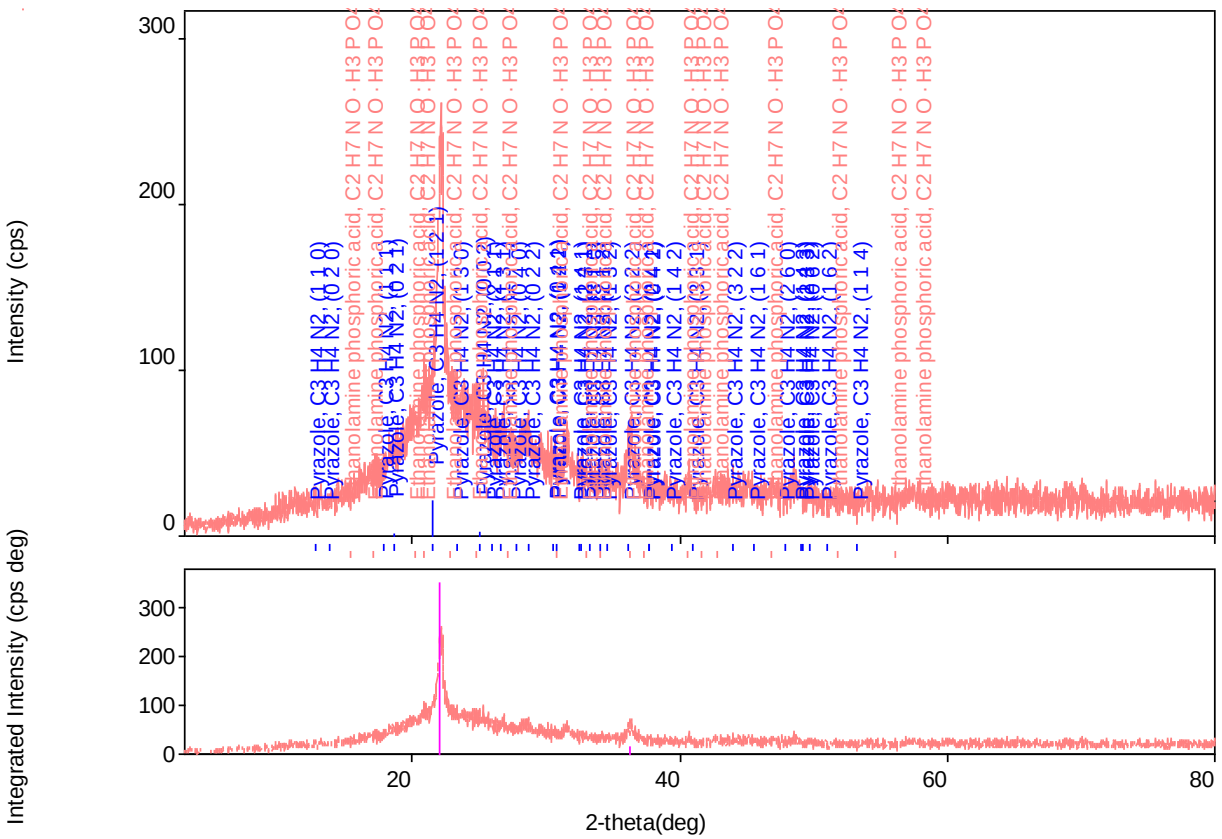
Intensity (cps)
Integrated Intensity (cps deg)
2-theta(deg)
300
200
100
0
20
40
60
80

Peak list

2-theta (deg)	d (ang.)	Height (cps)	Int. I(cps¥deg)	FWHM(deg)	Size	Phase name
22.11(9)	4.017(17)	54(7)	460(6)	5.81(14)	14.6(3)	Pyrazole, (1,1,1), Ethanolamine phosphoric acid, (-512,-512,-512)
36.34(6)	2.470(4)	15(4)	13.3(16)	0.60(9)	145(22)	Pyrazole, (2,2,2), Ethanolamine phosphoric acid, (-512,-512,-512)

Parameters used for WPPF

Profile parameters

Common Parameter	Background	Data	2
		Function name	B-spline
		param0	0.8771662190690904
		param1	30.86105276695256
		param2	24.11446322233912
		param3	17.84888055238357
		param4	19.91664841882044
		node0	3
		node1	41.5
		node2	80
Common Parameter	Peak shift		

		Function name	Shift axial displacement
		param0	0.1
		param1	0
		param2	0
Pyrazole	Scale factor	s	4.37(14)
	FWHM	U	0.0000
		V	0.0000
		W	10.0000
	Asym. Factor	A0	-0.4588
		A1	0.0000
	Extinction coefficient	etaL0/mL0	0.7329
		etaL1/mL1	0.0000
		etaH0/mH0	0.9459
		etaH1/mH1	0.0000
	Preferred orientationMarch-Dollase	h	0
		k	0
		l	0
		March coefficient	1.000000
Ethanolamine phosphoric acid	Scale factor	s	0.16(5)
	FWHM	U	0.0000
		V	0.0000
		W	10.0000
	Asym. Factor	A0	-0.4588
		A1	0.0000
	Extinction coefficient	etaL0/mL0	0.7329
		etaL1/mL1	0.0000
		etaH0/mH0	0.9459
		etaH1/mH1	0.0000
	Preferred orientationMarch-Dollase	h	0
		k	0
		l	0
		March coefficient	1.000000

Structure parameters

Data set name	Phase Name	Element	X	y	z	Occupancy	Temperature factor

File name	Rwp	Rp	Re	S	Chi^2	Maximum shift/e.s.d.
2	0	0	0	0	0	0

Lattice constants

Angular correction

No correction
Use External standard parameters
Use internal standard data

Analysis results

File name	a (ang.)	b (ang.)	c (ang.)	alpha (deg)	beta (deg)	gamma (deg)
2	8.248000	12.841000	7.096000	90.000000	90.000000	90.000000

Phase name	a (ang.)	b (ang.)	c (ang.)	alpha (deg)	beta (deg)	gamma (deg)
Pyrazole	8.248000	12.841000	7.096000	90.000000	90.000000	90.000000

Analysis Results

General Information

Analysis date	4/24/2014 1:08:57 PM		
Sample name	XRD Analysis	Measured time	4/11/2014 12:15:35 PM
File name	3(10M MEA).raw	Operator	administrator
Comment	UMP		

Measurement profile

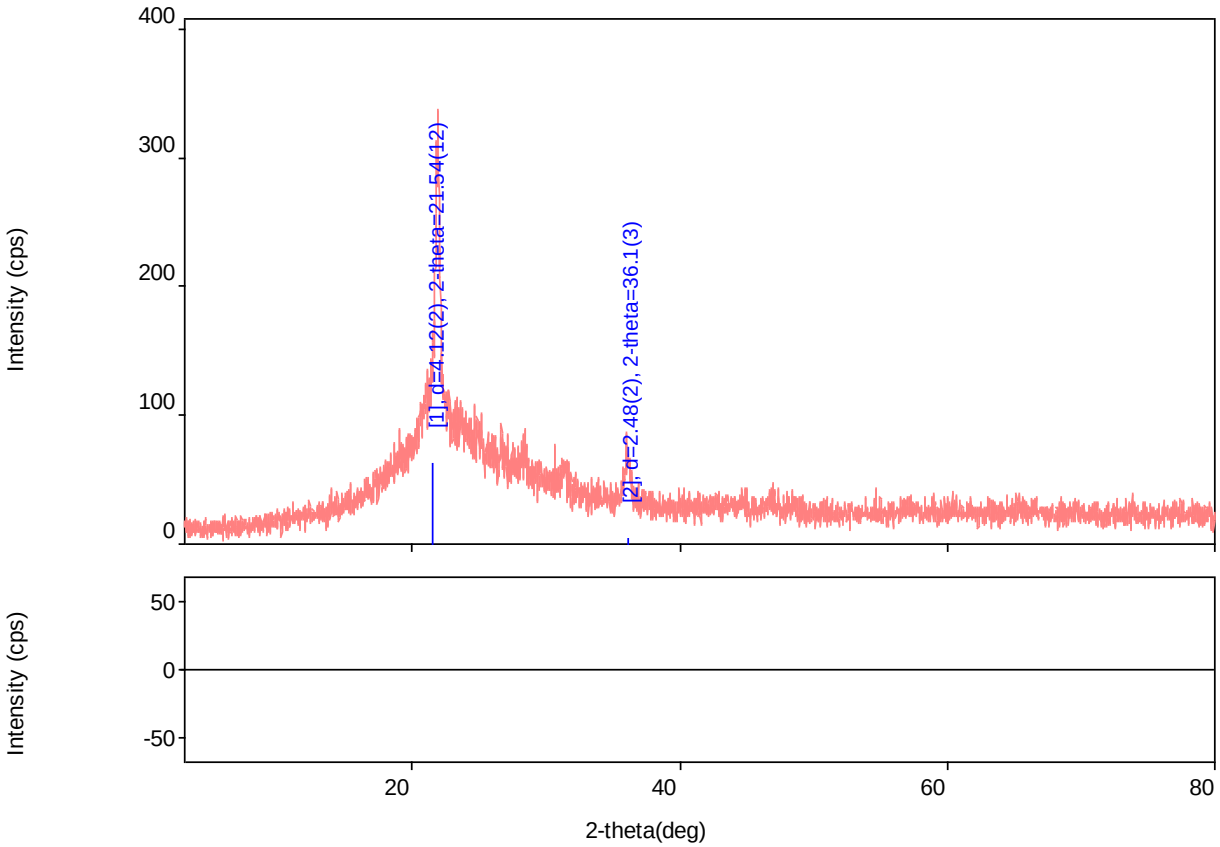
400
300
200
100
0
Intensity (cps)
[1], d=4.12(2), 2-theta=21.54(12)
[2], d=2.48(2), 2-theta=36.1(3)
50
0
-50
Intensity (cps)
20
40
60
80
2-theta(deg)

Measurement conditions

XG	Cu/30 kV/15 mA	Duration time / Scan speed	1 deg/min
Goniometer		Step / Sampling step	0.02 deg
Attachment	-	Measurement axis	2ƒÆ/ƒÆ
K-beta filter	-	Scan range	3-80 deg
Incident monochromator	-	Incident slit	-
Receiving monochromator	-	Vertical divergence slit	-
Counter	-	Receiving slit #1	-
		Receiving slit #2	-

Qualitative analysis results

Phase name	Formula	Figure of merit	ICDD
2,6-Diaminopyridine	C5 H7 N3	0.5200719385594721	411765 (ICDD)
Ethanolamine phosphoric acid	C2 H7 N O · H3 P O4	0.6600053948394827	50203 (ICDD)

Phase name	Formula	Space group	ICDD
2,6-Diaminopyridine	C5 H7 N3	19 : P212121	411765 (ICDD)
Ethanolamine phosphoric acid	C2 H7 N O · H3 P O4	-	50203 (ICDD)

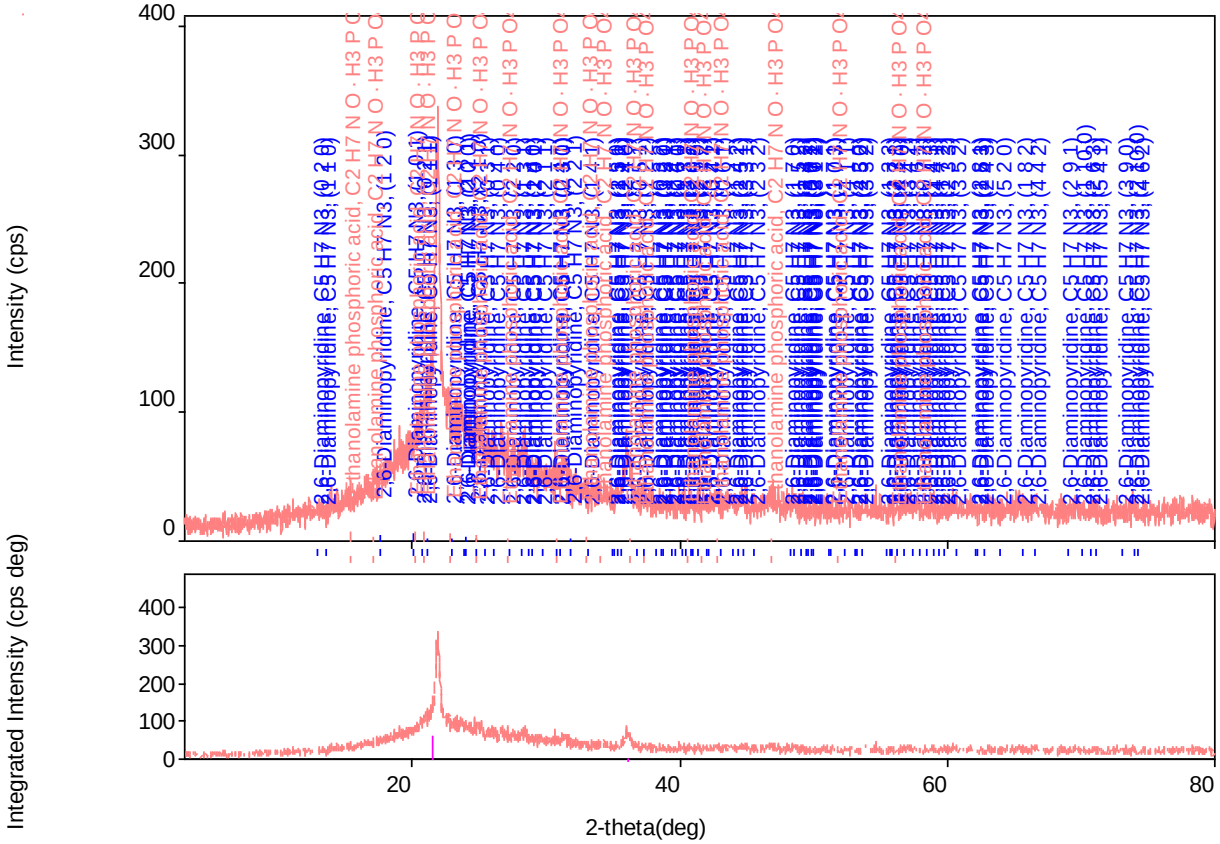
Intensity (cps)
Integrated Intensity (cps deg)
2-theta(deg)
0
100
200
300
400
20
40
60
80

Peak list

2-theta (deg)	d (ang.)	Height (cps)	Int. I(cps¥deg)	FWHM(deg)	Size	Phase name
21.54(12)	4.12(2)	63(8)	509(8)	5.42(15)	15.6(4)	2,6-Diaminopyridine, (1,2,0), Ethanolamine phosphoric acid, (-512,-512,-512)
36.1(3)	2.48(2)	5(2)	12(3)	1.7(5)	51(15)	2,6-Diaminopyridine, (1,5,0), Ethanolamine phosphoric acid, (-512,-512,-512)

Parameters used for WPPF

Profile parameters

Common Parameter	Background	Data	3
		Function name	B-spline
		param0	4.086220117088405
		param1	36.79860510650259
		param2	23.8651289811744
		param3	21.1444692456109
		param4	20.93180132502829
		node0	3
		node1	41.5
		node2	80
Common Parameter	Peak shift		

		Function name	Shift axial displacement
		param0	0.1
		param1	0
		param2	0
2,6-Diaminopyridine	Scale factor	s	1.61(7)
	FWHM	U	0.0000
		V	0.0000
		W	10.0000
	Asym. Factor	A0	-0.6228
		A1	0.0000
	Extinction coefficient	etaL0/mL0	0.7200
		etaL1/mL1	0.0000
		etaH0/mH0	0.9663
		etaH1/mH1	0.0000
	Preferred orientationMarch-Dollase	h	0
		k	0
		l	0
		March coefficient	1.000000
Ethanolamine phosphoric acid	Scale factor	s	0.39(7)
	FWHM	U	0.0000
		V	0.0000
		W	10.0000
	Asym. factor	A0	-0.6228
		A1	0.0000
	Extinction coefficient	etaL0/mL0	0.7200
		etaL1/mL1	0.0000
		etaH0/mH0	0.9663
		etaH1/mH1	0.0000
	Preferred orientationMarch-Dollase	h	0
		k	0
		l	0
		March coefficient	1.000000

Structure parameters

Data set name	Phase Name	Element	x	y	z	Occupancy	Temperature factor

File name	Rwp	Rp	Re	S	Chi^2	Maximum shift/e.s.d.
3	0	0	0	0	0	0

Lattice constants

Angular correction

	No correction
	Use External standard parameters
	Use internal standard data

Analysis results

File name	a (ang.)	b (ang.)	c (ang.)	alpha (deg)	beta (deg)	gamma (deg)
3	7.441500	13.640000	5.493500	90.000000	90.000000	90.000000

Phase name	a (ang.)	b (ang.)	c (ang.)	alpha (deg)	beta (deg)	gamma (deg)
2,6-Diaminopyridine	7.441500	13.640000	5.493500	90.000000	90.000000	90.000000

Analysis Results

General Information

Analysis date	4/24/2014 1:10:58 PM		
Sample name	XRD Analysis	Measured time	4/11/2014 2:43:06 PM
File name	4(4M DEA).raw	Operator	administrator
Comment	UMP		

Measurement profile

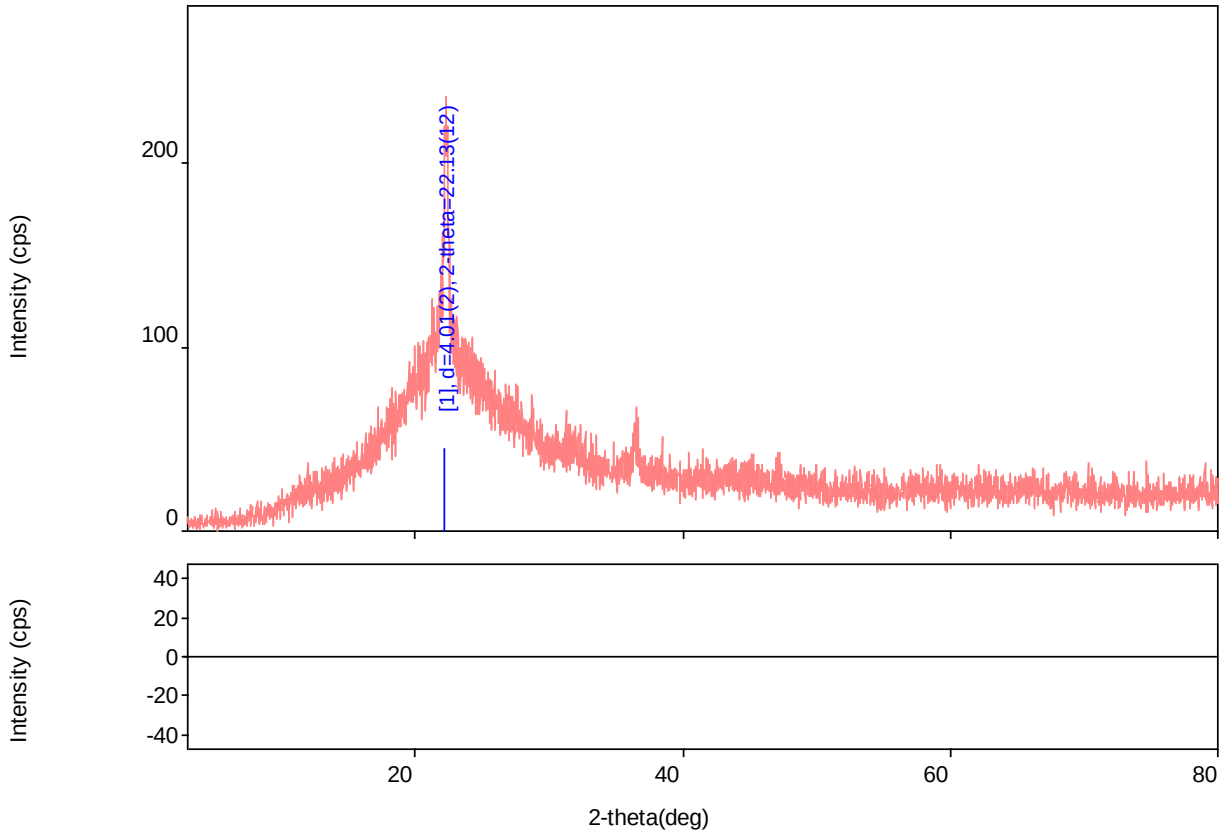
Intensity (cps)
200
100
0
[1], d=4.017(2), 2-theta=22.13(12)
Intensity (cps)
40
20
0
-20
-40
20
40
60
80
2-theta(deg)

Measurement conditions

XG	Cu/30 kV/15 mA	Duration time / Scan speed	1 deg/min
Goniometer		Step / Sampling step	0.02 deg
Attachment	-	Measurement axis	2ƒÆ/ƒÆ
K-beta filter	-	Scan range	3-80 deg
Incident monochromator	-	Incident slit	-
Receiving monochromator	-	Vertical divergence slit	-
Counter	-	Receiving slit #1	-
		Receiving slit #2	-

Qualitative analysis results

Phase name	Formula	Figure of merit	ICDD
4-aminopyridine	C5 H6 N2	0.8552583670852438	301518 (ICDD)
Diethanolamine 3,5-dinitrobenzoic acid	C11 H15 N3 O8	2.813118381793835	421742 (ICDD)

Phase name	Formula	Space group	ICDD
4-aminopyridine	C5 H6 N2	19 : P212121	301518 (ICDD)
Diethanolamine 3,5-dinitrobenzoic acid	C11 H15 N3 O8	1 : P1	421742 (ICDD)

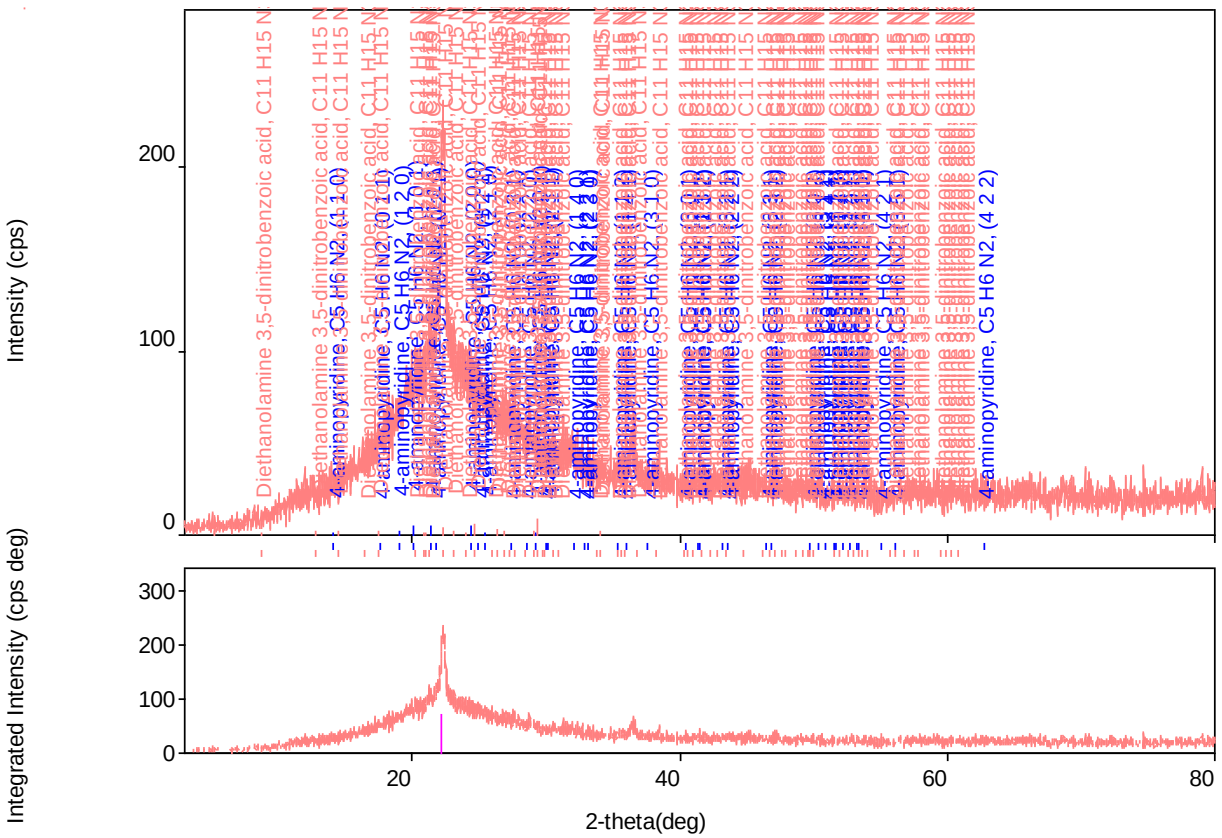
Intensity (cps)
Integrated Intensity (cps deg)
2-theta(deg)
Diethanolamine 3,5-dinitrobenzoic acid, C11 H15 N
4-aminopyridine, C5 H6 N2, (1 1 0)
4-aminopyridine, C5 H6 N2, (0 1 1)
4-aminopyridine, C5 H6 N2, (1 2 0)
4-aminopyridine, C5 H6 N2, (1 0 1)
4-aminopyridine, C5 H6 N2, (2 0 0)
4-aminopyridine, C5 H6 N2, (2 1 0)
4-aminopyridine, C5 H6 N2, (2 2 0)
4-aminopyridine, C5 H6 N2, (3 1 0)
4-aminopyridine, C5 H6 N2, (4 2 2)

Peak list

2-theta (deg)	d (ang.)	Height (cps)	Int. I(cps¥deg)	FWHM(deg)	Size	Phase name
22.13(12)	4.01(2)	46(7)	327(5)	6.43(11)	13.1(2)	4-aminopyridine, (0,1,1), Diethanolamine 3,5-dinitrobenzoic acid, (0,1,1)

Parameters used for WPPF

Profile parameters

Common Parameter	Background	Data	4
		Function name	B-spline
		param0	-0.2349106534931104
		param1	16.24590976125642
		param2	58.10094368404177
		param3	5.383614965818457
		param4	27.1529058103773
		param5	16.40252851279522
		node0	3
		node1	28.66
		node2	54.32
		node3	80
Common Parameter	Peak shift		
		Function name	Shift axial displacement
		param0	0
		param1	0

		param2	0
4-aminopyridine	Scale factor	s	1.07(4)
	FWHM	U	0.0000
		V	0.0000
		W	10.0000
	Asym. factor	A0	-0.0117
		A1	0.0000
	Extinction coefficient	etaL0/mL0	0.1402
		etaL1/mL1	0.0000
		etaH0/mH0	0.0955
		etaH1/mH1	0.0000
	Preferred orientationMarch-Dollase	h	0
		k	0
		l	0
		March coefficient	1.000000
Diethanolamine 3,5-dinitrobenzoic acid	Scale factor	s	0.20(4)
	FWHM	U	0.0000
		V	0.0000
		W	10.0000
	Asym. factor	A0	-0.0117
		A1	0.0000
	Extinction coefficient	etaL0/mL0	0.1402
		etaL1/mL1	0.0000
		etaH0/mH0	0.0955
		etaH1/mH1	0.0000
	Preferred orientationMarch-Dollase	h	0
		k	0
		l	0
		March coefficient	1.000000

Structure parameters

Data set name	Phase Name	Element	x	y	z	Occupancy	Temperature factor

File name	Rwp	Rp	Re	S	Chi^2	Maximum shift/e.s.d.
4	0	0	0	0	0	0

Lattice constants

Angular correction

	No correction
	Use External standard parameters
	Use internal standard data

Analysis results

File name	a (ang.)	b (ang.)	c (ang.)	alpha (deg)	beta (deg)	gamma (deg)
4	7.307000	12.076000	5.547000	90.000000	90.000000	90.000000
4	4.518628	7.267647	10.478431	95.529999	98.750000	104.290001

Phase name	a (ang.)	b (ang.)	c (ang.)	alpha (deg)	beta (deg)	gamma (deg)
4-aminopyridine	7.307000	12.076000	5.547000	90.000000	90.000000	90.000000
Diethanolamine 3,5-	4.518628	7.267647	10.478431	95.529999	98.750000	104.290001

Analysis Results

General Information

Analysis date	4/24/2014 1:12:37 PM		
Sample name	XRD Analysis	Measured time	4/11/2014 5:11:47 PM
File name	5(10M DEA).raw	Operator	administrator
Comment	UMP		

Measurement profile

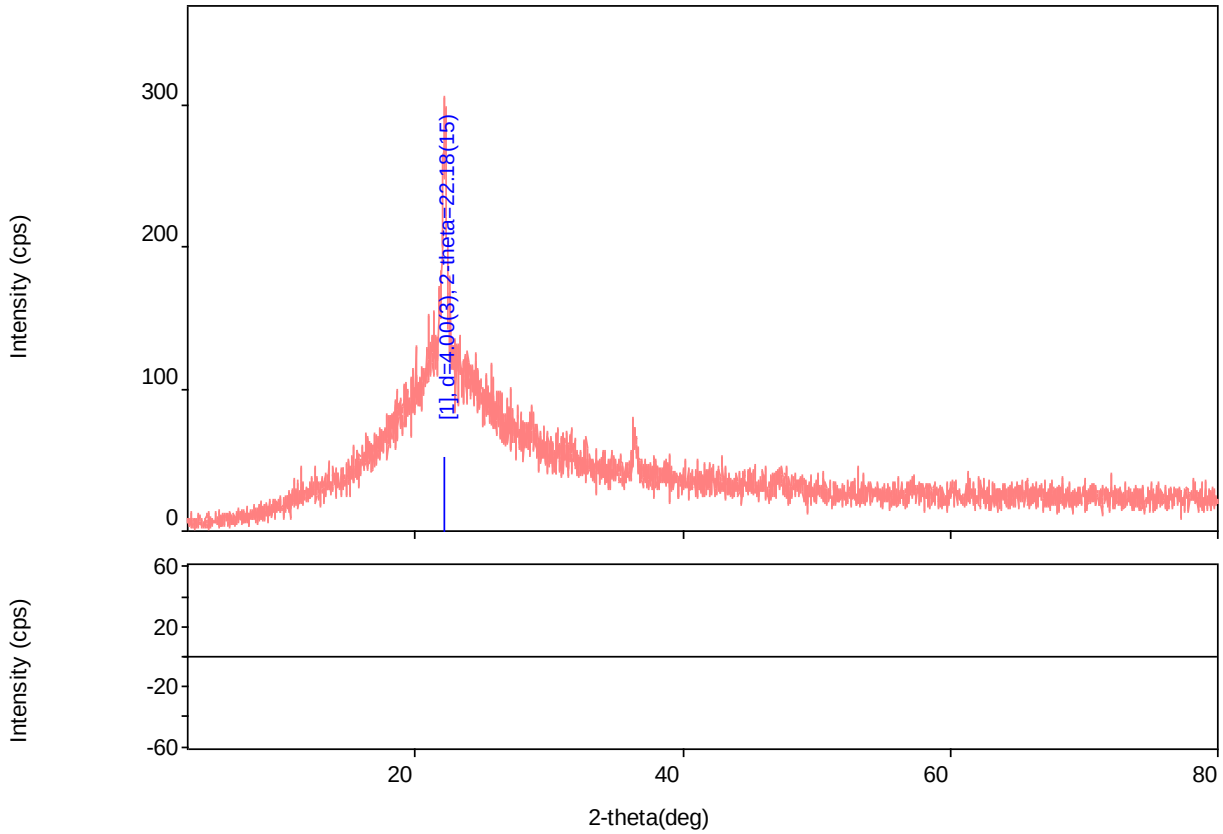
Intensity (cps)
300
200
100
0
[1] d=4.00(3), 2-theta=22.18(15)
Intensity (cps)
60
20
-20
-60
20
40
60
80
2-theta(deg)

Measurement conditions

XG	Cu/30 kV/15 mA	Duration time / Scan speed	1 deg/min
Goniometer		Step / Sampling step	0.02 deg
Attachment	-	Measurement axis	2ƒÆ/ƒÆ
K-beta filter	-	Scan range	3-80 deg
Incident monochromator	-	Incident slit	-
Receiving monochromator	-	Vertical divergence slit	-
Counter	-	Receiving slit #1	-
		Receiving slit #2	-

Qualitative analysis results

Phase name	Formula	Figure of merit	ICDD
Benzalazine	C14 H12 N2	0.8371575333831237	541540 (ICDD)
Diethanolamine 3,5-dinitrobenzoic acid	C11 H15 N3 O8	0.8133905442523594	421742 (ICDD)

Phase name	Formula	Space group	ICDD
Benzalazine	C14 H12 N2	60 : Pbcn	541540 (ICDD)
Diethanolamine 3,5-dinitrobenzoic acid	C11 H15 N3 O8	1 : P1	421742 (ICDD)

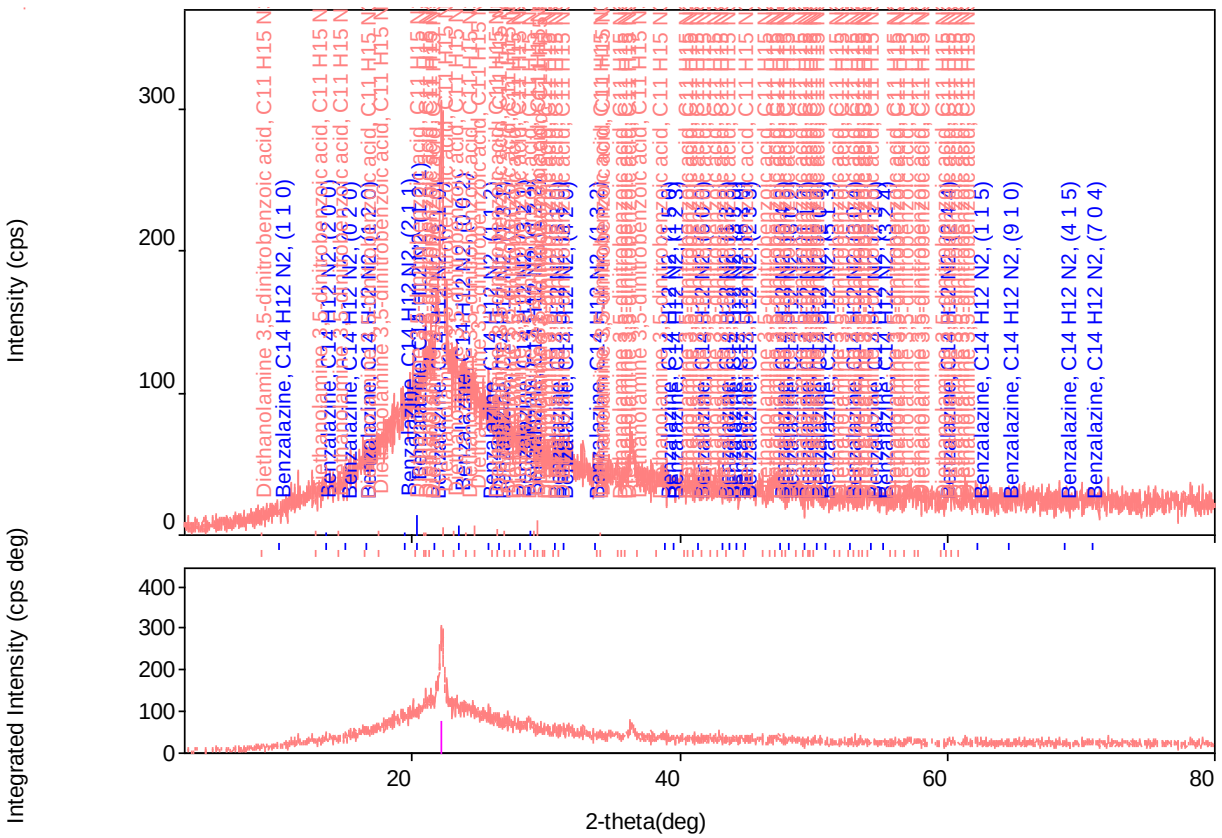
Intensity (cps)
Integrated Intensity (cps deg)
2-theta(deg)
Diethanolamine 3,5-dinitrobenzoic acid, C11 H15 N
Benzalazine, C14 H12 N2, (1 1 0)
Benzalazine, C14 H12 N2, (2 0 0)
Benzalazine, C14 H12 N2, (0 2 0)
Benzalazine, C14 H12 N2, (1 2 0)
Benzalazine, C14 H12 N2, (0 0 2)
Benzalazine, C14 H12 N2, (2 1 1)
Benzalazine, C14 H12 N2, (1 2 1)
Benzalazine, C14 H12 N2, (3 1 1)
Benzalazine, C14 H12 N2, (2 2 1)
Benzalazine, C14 H12 N2, (1 3 1)
Benzalazine, C14 H12 N2, (4 2 0)
Benzalazine, C14 H12 N2, (1 3 2)
Benzalazine, C14 H12 N2, (3 3 1)
Benzalazine, C14 H12 N2, (2 3 2)
Benzalazine, C14 H12 N2, (4 2 2)
Benzalazine, C14 H12 N2, (1 5 0)
Benzalazine, C14 H12 N2, (4 3 1)
Benzalazine, C14 H12 N2, (0 4 2)
Benzalazine, C14 H12 N2, (5 1 1)
Benzalazine, C14 H12 N2, (3 4 1)
Benzalazine, C14 H12 N2, (1 1 5)
Benzalazine, C14 H12 N2, (9 1 0)
Benzalazine, C14 H12 N2, (4 1 5)
Benzalazine, C14 H12 N2, (7 0 4)
0
100
200
300
400
20
40
60
80

Peak list

2-theta (deg)	d (ang.)	Height (cps)	Int. I(cps¥deg)	FWHM(deg)	Size	Phase name
22.18(15)	4.00(3)	53(7)	321(9)	5.66(13)	14.9(3)	Benzalazine, (2,1,1), Diethanolamine 3,5-dinitrobenzoic acid, (0,0,2)

Parameters used for WPPF

Profile parameters

Common Parameter	Background	Data	5
		Function name	B-spline
		param0	-0.434985780159952
		param1	26.12045997919789
		param2	74.86744362717926
		param3	3.909602887577147
		param4	33.02165407463478
		param5	17.82736311851985
		node0	3
		node1	28.66
		node2	54.32
		node3	80
Common Parameter	Peak shift		
		Function name	Shift axial displacement
		param0	0
		param1	0

		param2	0
Benzalazine	Scale factor	s	2.34(9)
	FWHM	U	0.0000
		V	0.0000
		W	10.0000
	Asym. factor	A0	0.0157
		A1	0.0000
	Extinction coefficient	etaL0/mL0	0.0000
		etaL1/mL1	0.0000
		etaH0/mH0	0.0000
		etaH1/mH1	0.0000
	Preferred orientationMarch-Dollase	h	0
		k	0
		l	0
		March coefficient	1.000000
Diethanolamine 3,5-dinitrobenzoic acid	Scale factor	s	0.53(4)
	FWHM	U	0.0000
		V	0.0000
		W	10.0000
	Asym. factor	A0	0.0157
		A1	0.0000
	Extinction coefficient	etaL0/mL0	0.0000
		etaL1/mL1	0.0000
		etaH0/mH0	0.0000
		etaH1/mH1	0.0000
	Preferred orientationMarch-Dollase	h	0
		k	0
		l	0
		March coefficient	1.000000

Structure parameters

Data set name	Phase Name	Element	x	y	z	Occupancy	Temperature factor

File name	Rwp	Rp	Re	S	Chi^2	Maximum shift/e.s.d.
5	0	0	0	0	0	0

Lattice constants

Angular correction

	No correction
	Use External standard parameters
	Use internal standard data

Analysis results

File name	a (ang.)	b (ang.)	c (ang.)	alpha (deg)	beta (deg)	gamma (deg)
5	13.080000	11.750000	7.560000	90.000000	90.000000	90.000000
5	4.518628	7.267647	10.478431	95.529999	98.750000	104.290001

Phase name	a (ang.)	b (ang.)	c (ang.)	alpha (deg)	beta (deg)	gamma (deg)
Benzalazine	13.080000	11.750000	7.560000	90.000000	90.000000	90.000000
Diethanolamine 3,5-	4.518628	7.267647	10.478431	95.529999	98.750000	104.290001

Analysis Results

General Information

Analysis date	5/8/2014 11:12:36 AM		
Sample name	XRD Analysis	Measured time	4/11/2014 9:42:23 AM
File name	1(Combine).raw	Operator	administrator
Comment	UMP		

Measurement profile

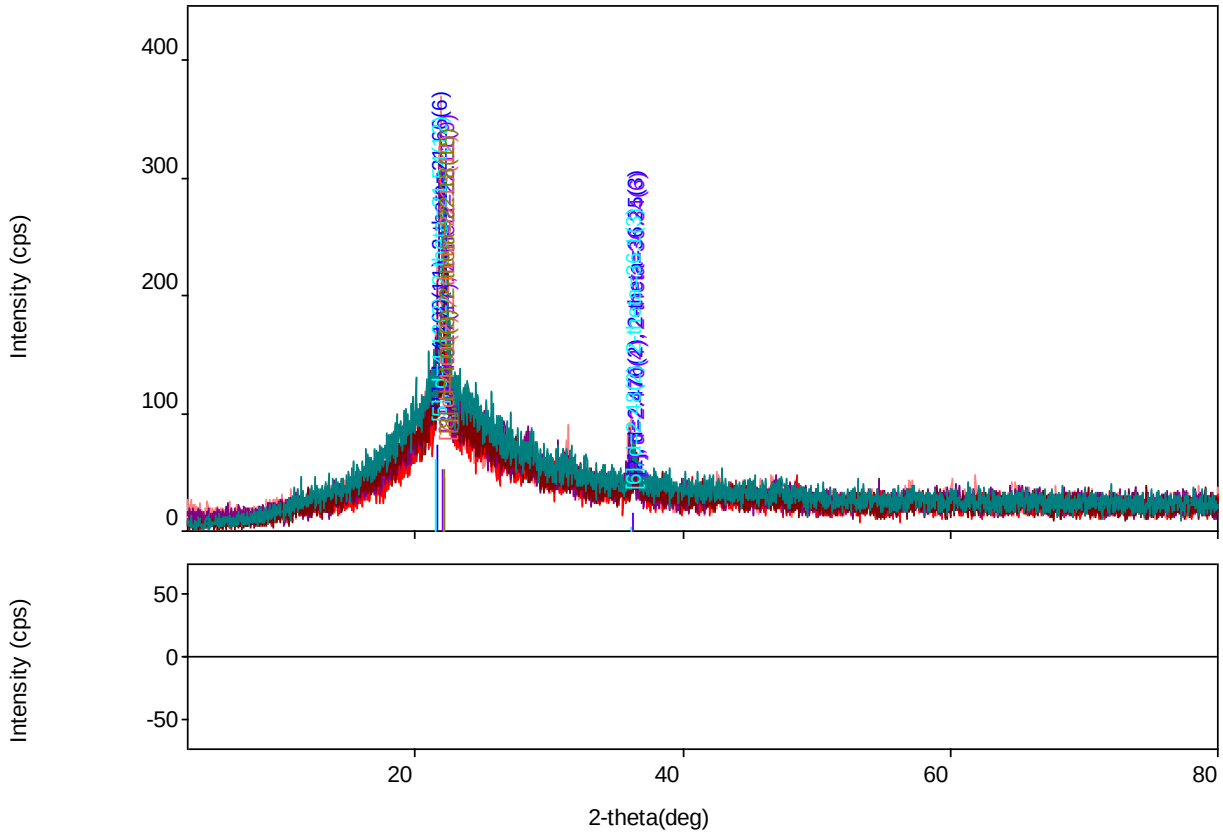
Intensity (cps)
400
300
200
100
0
Intensity (cps)
50
0
-50
20
40
60
80
2-theta(deg)

Measurement conditions

XG	Cu/30 kV/15 mA	Duration time / Scan speed	1 deg/min
Goniometer		Step / Sampling step	0.02 deg
Attachment	-	Measurement axis	2ƒÆ/ƒÆ
K-beta filter	-	Scan range	3-80 deg
Incident monochromator	-	Incident slit	-
Receiving monochromator	-	Vertical divergence slit	-
Counter	-	Receiving slit #1	-
		Receiving slit #2	-

Qualitative analysis results

Phase name	Formula	Figure of merit	ICDD

Phase name	Formula	Space group	ICDD

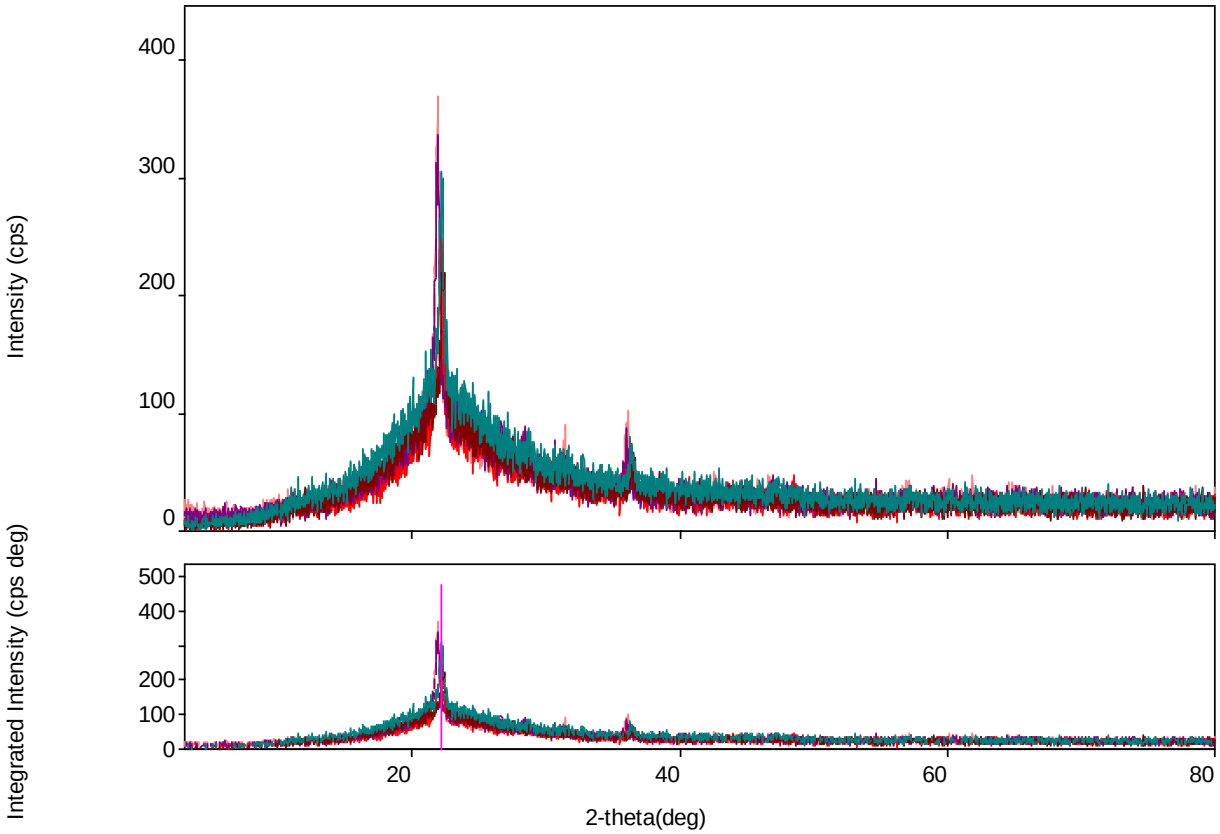
Intensity (cps)
400
300
200
100
0
Integrated Intensity (cps deg)
500
400
200
100
0
20
40
60
80
2-theta(deg)

Peak list

2-theta (deg)	d (ang.)	Height (cps)	Int. I(cps¥deg)	FWHM(deg)	Size	Phase name
21.66(6)	4.100(11)	74(9)	395(7)	3.50(9)	24.1(6)	Unknown,
36.25(3)	2.476(2)	17(4)	13.9(16)	0.54(11)	163(34)	Unknown,
22.11(9)	4.017(17)	54(7)	460(6)	5.81(14)	14.6(3)	Unknown,
36.34(6)	2.470(4)	15(4)	13.3(16)	0.60(9)	145(22)	Unknown,
21.54(12)	4.12(2)	63(8)	509(8)	5.42(15)	15.6(4)	Unknown,
36.1(3)	2.48(2)	5(2)	12(3)	1.7(5)	51(15)	Unknown,
22.13(12)	4.01(2)	46(7)	327(5)	6.43(11)	13.1(2)	Unknown,
22.18(15)	4.00(3)	53(7)	321(9)	5.66(13)	14.9(3)	Unknown,

APPENDIX B-2

BRUNAUER, EMMETT AND TELLER (BET) RESULTS

Extended Report

Filename: C:\Surfer\result\Aishah\METHOD MESOPORE BAM-PM-102_060314_2.iso
Mass: 0.3874 g

Analytical Conditions

Blank done with: Helium

Adsorbate:	Nitrogen		
Equilibrium time [min:s]	0:00	0:00	0:00
Pre run time:	0:00 min		

Desorption	1st	2nd
Equilibrium time [min:s]	0:00	0:00

Adsorption Data

#	V_{dos} [cm^3]	p_{load} [Torr]	p_{equi} [Torr]	t_{equi} [min:s]	p^0 [Torr]	p/p^0	V_{ads} [cm^3g^{-1}]	n_{ads} [mmol g^{-1}]
1						0.0032	0.0103	0.0012
2						0.006	0.0594	0.0068
3						0.063	-0.046	-0.0054
4						0.1211	0.1626	0.0187
5						0.1787	0.4027	0.0464
6						0.2343	0.6376	0.0734
7						0.2926	0.8957	0.1032
8						0.3526	1.1926	0.1373
9						0.4097	1.5101	0.1739
10						0.4661	1.8172	0.2093
11						0.5262	2.1915	0.2524
12						0.5864	2.5916	0.2985
13						0.6412	2.9788	0.3431
14						0.6976	3.3996	0.3915
15						0.7551	3.8462	0.443
16						0.8136	4.3366	0.4994
17						0.8732	4.889	0.5631

Desorption Data

#	V_{dos} [cm^3]	p_{equi} [Torr]	t_{equi} [min:s]	p^0 [Torr]	p/p^0	V_{ads} [cm^3g^{-1}]	n_{ads} [mmol g^{-1}]
18					0.8631	5.0542	0.5821
19					0.853	4.9432	0.5693
20					0.7971	4.4708	0.5149
21					0.7418	3.9933	0.4599
22					0.6861	3.5648	0.4105
23					0.6309	3.1569	0.3636
24					0.5747	2.7672	0.3187
25					0.5192	2.4161	0.2783
26					0.4631	2.0702	0.2384
27					0.407	1.7579	0.2024
28					0.3515	1.443	0.1662
29					0.2955	1.1642	0.1341
30					0.2403	0.8906	0.1026
31					0.1848	0.6427	0.074
32					0.1299	0.4027	0.0464

Isotherm

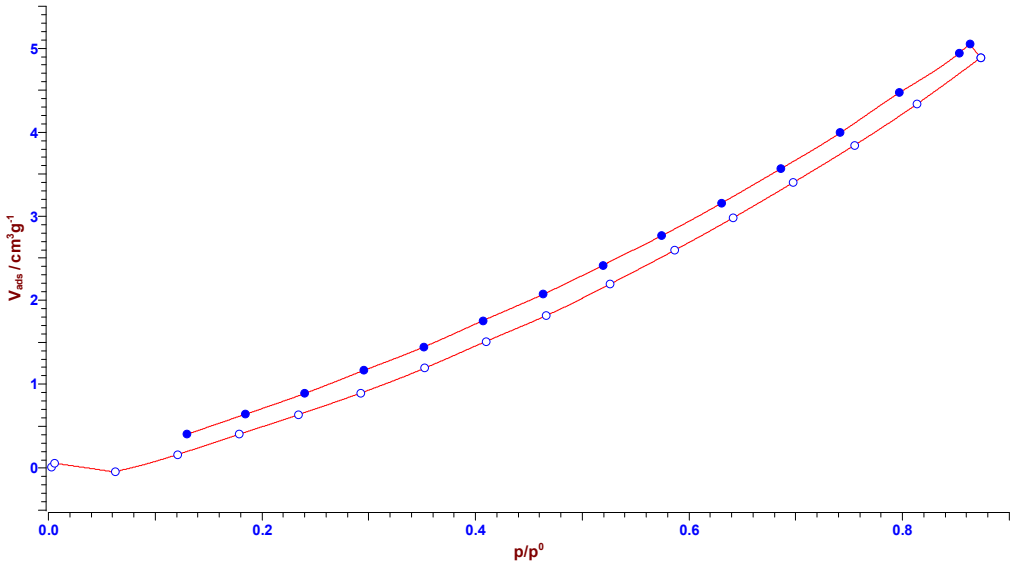

Pore volume (Gurvich) at p/p^0 0.95 is 0.0086 cm^3g^{-1}

Surface Area (Langmuir)

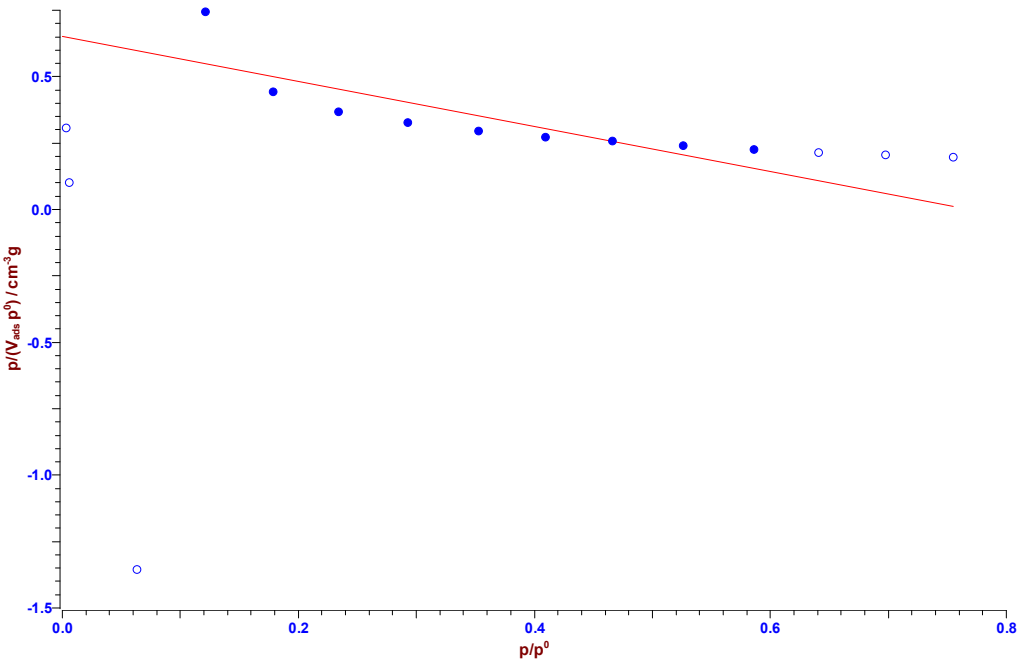

Linear regression from p/p^0	0.1 to 0.6
Offset:	0.65045497 ± 0.08212982
Slope:	-0.8467632 ± 0.21468438
R:	-0.8304659
Monoloayer volume	-1.181 cm^3g^{-1}
Monoloayer amount:	-0.053 mmol g^{-1}
B:	-1.302
Calculation with a molecular area of	16.2 $Å^2$
Surface area was:	-5.14 m^2g^{-1}

Surface Area (B.E.T.) 2 Parameters Line

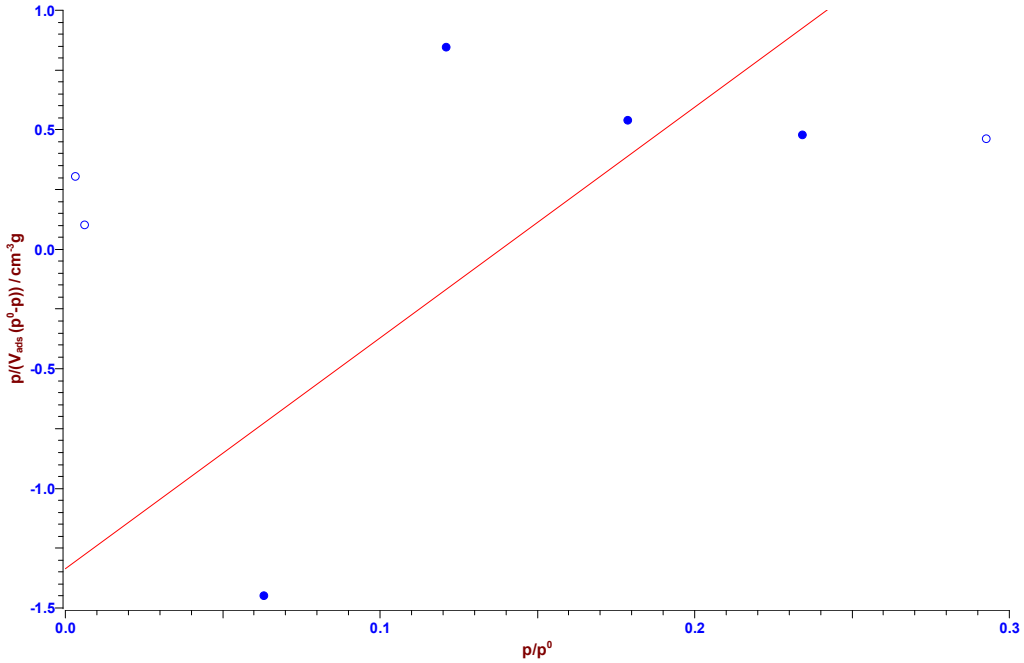

Linear regression from p/p^0	0.05 to 0.25
Offset:	-1.335876 ± 1.19443998
Slope:	9.65442298 ± 7.35757771
R:	0.68016597
Monoloayer volume	0.1202 cm^3g^{-1}
Monoloayer amount:	0.0054 mmol g^{-1}
C:	-6.227
Calculation with a molecular area of	16.2 $Å^2$
Surface area was:	0.5232 m^2g^{-1}

Surface Area (B.E.T.) 3 Parameters Fit

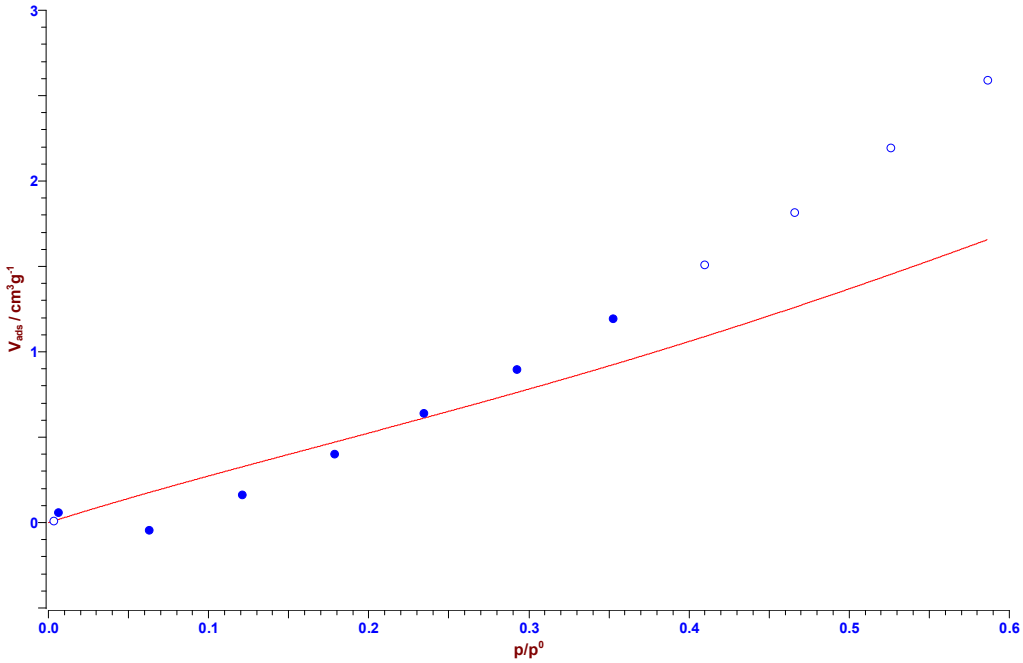

Simplex fit from p/p^0	0.005 to 0.4
r^2:	0.88465674
Monoloayer volume	0.968 cm^3g^{-1}
Monoloayer amount:	0.0432 mmol g^{-1}
C:	3.0648
N:	5.6482
Calculation with a molecular area of	16.2 $Å^2$
Surface area was:	4.2134 m^2g^{-1}

Mesopores (B.J.H.)

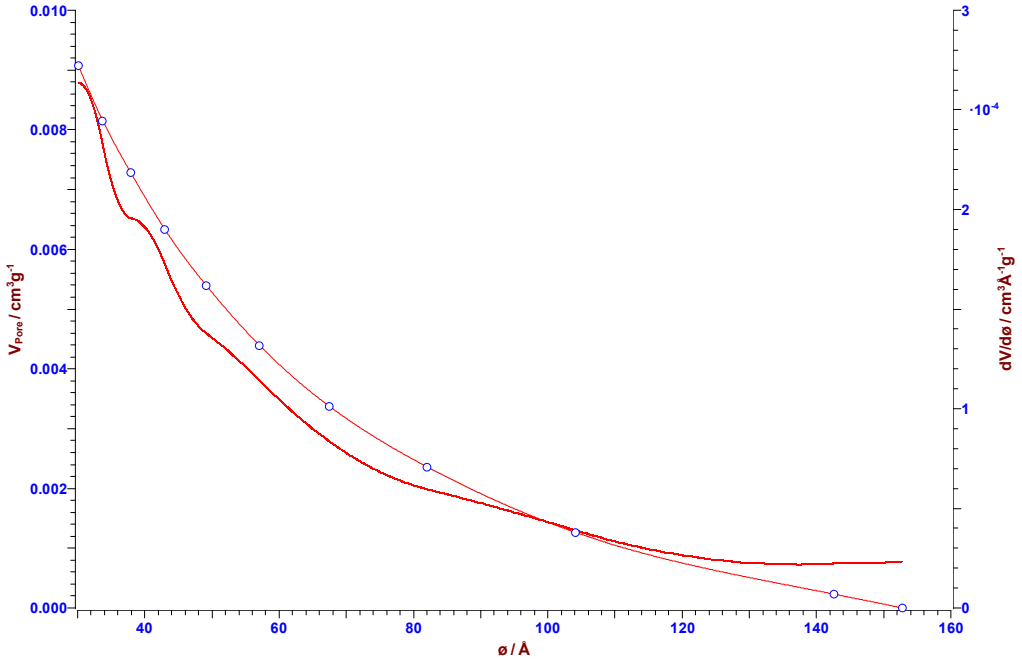

Calculations used Desorption Branch from p/p^0 0.3 to 0.95

with standard isotherm: Universal (Halsey)

from literature: ASTM Standards Designation: D 4641-87

Calculation with a molecular area of	16.2 $Å^2$
molecular weight of	28.01 g/mol
liquid density of	0.8086 g cm^{-3}
and surface tension of	8.85 Dyne cm^{-1}
Median pore diameter	55.821 Å
Maximum pore diameter	30.114 Å
Cumulative pore volume	0.0091 cm^3g^{-1}
Cumulative pore area	6.7359 m^2g^{-1}

Mesopores (Cranston and Inkley)

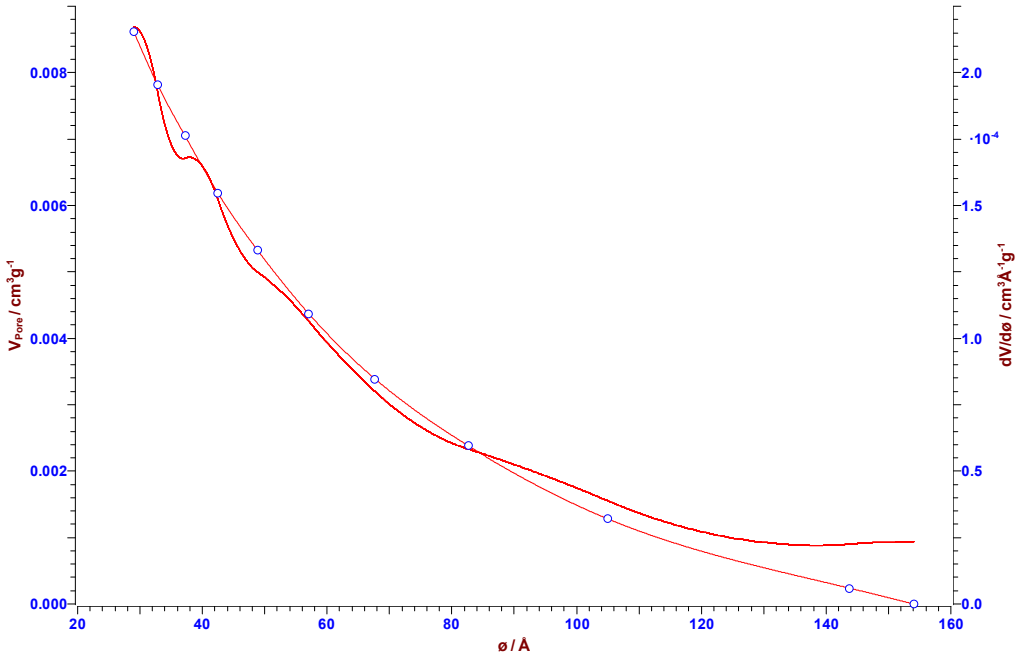

Calculations used Desorption Branch from p/p^0 0.3 to 0.95
with standard isotherm: Universal (Harkins,Jura)
from literature: ASTM Standards Designation: D 4641-87

Calculation with a molecular area of	16.2 $Å^2$
molecular weight of	28.01 g/mol
liquid density of	0.8086 g cm^{-3}
and surface tension of	8.85 Dyne cm^{-1}
Median pore diameter	57.62 Å
Maximum pore diameter	29.028 Å
Cumulative pore volume	0.0086 cm^3g^{-1}
Cumulative pore area	6.3217 m^2g^{-1}

Mesopores (Modelless)

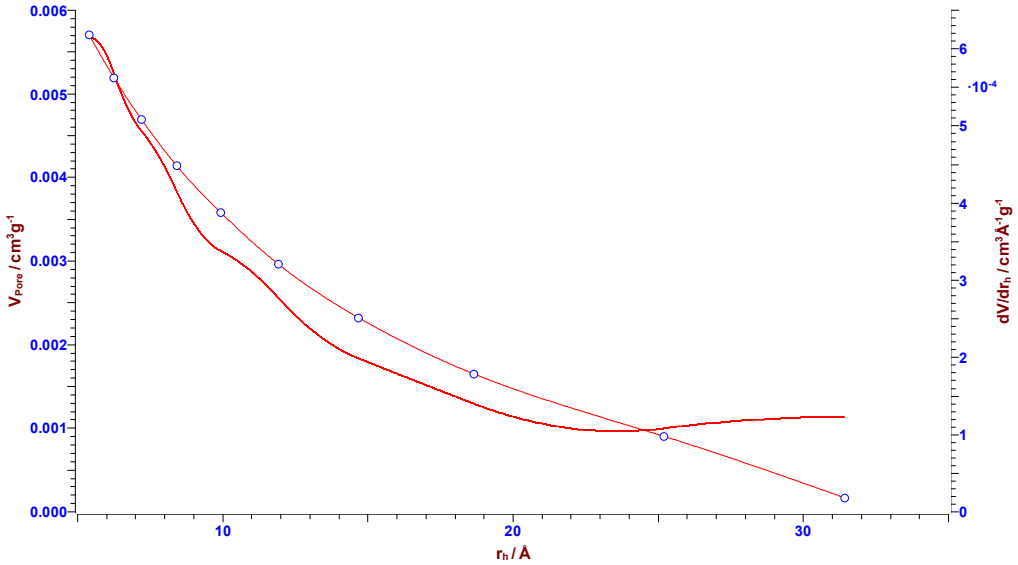

Calculations used Desorption Branch from p/p^0 0.3 to 0.95
with standard isotherm: Universal (Harkins,Jura)
from literature: ASTM Standards Designation: D 4641-87

Calculation with a molecular area of	16.2 $Å^2$
molecular weight of	28.01 g/mol
and liquid density of	0.8086 g cm^{-3}
Median hydraulic radius	9.0137 Å
Maximum hydraulic radius	5.4002 Å
Cumulative pore volume	0.0078 cm^3g^{-1}
Cumulative pore area	5.5416 m^2g^{-1}

Micropores (Horvath and Kawazoe)

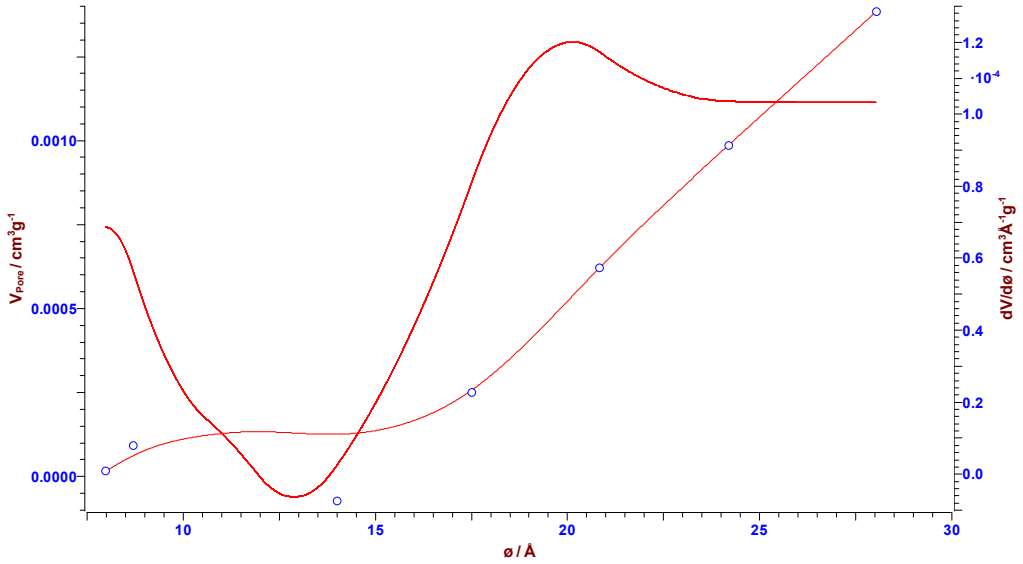

Calculations from p/p^0 0 to 0.35

with potential function: Nitrogen on Graphite @77.3 K
from literature: G. Horvath, K. Kawazoe, J. Chem. Eng. Japan, 16, 6(1983), 470-475

Calculation with a molecular area of	16.2 $Å^2$
molecular weight of	28.01 g/mol
and liquid density of	0.8086 g cm^{-3}
Median pore diameter	21.472 Å
Maximum pore diameter	20.127 Å
Cumulative pore volume	0.0014 cm^3g^{-1}
Cumulative pore area	1.2908 m^2g^{-1}

Extended Report

Filename: C:\Surfer\result\Aishah\METHOD MESOPORE BAM-PM-102_070314_2.iso
Mass: 0.3824 g

Analytical Conditions

Blank done with: Helium

Adsorbate:	Nitrogen		
Equilibrium time [min:s]	0:00	0:00	0:00
Pre run time:	0:00 min		

Desorption	1st	2nd
Equilibrium time [min:s]	0:00	0:00

Adsorption Data

#	V_{dos} [cm^3]	p_{load} [Torr]	p_{equi} [Torr]	t_{equi} [min:s]	p^0 [Torr]	p/p^0	V_{ads} [cm^3g^{-1}]	n_{ads} [mmol g^{-1}]
1						0.0035	0.0026	0.00031
2						0.0066	0.0157	0.0018
3						0.0627	-0.175	-0.02
4						0.1214	-0.016	-0.0018
5						0.1793	0.1412	0.0165
6						0.2357	0.3373	0.0394
7						0.2935	0.557	0.065
8						0.3482	0.7767	0.0906
9						0.4051	1.0303	0.1202
10						0.4637	1.3075	0.1526
11						0.5228	1.6344	0.1907
12						0.5781	1.9456	0.227
13						0.6343	2.2908	0.2673
14						0.6918	2.6621	0.3106
15						0.7512	3.0675	0.3579
16						0.8116	3.5173	0.4104
17						0.8714	3.9749	0.4638

Desorption Data

#	V_{dos} [cm^3]	p_{equi} [Torr]	t_{equi} [min:s]	p^0 [Torr]	p/p^0	V_{ads} [cm^3g^{-1}]	n_{ads} [mmol g^{-1}]
18					0.8607	4.1553	0.4848
19					0.8505	4.0717	0.4751
20					0.7943	3.6428	0.425
21					0.7389	3.2296	0.3768
22					0.684	2.8556	0.3332
23					0.6285	2.5026	0.292
24					0.5734	2.1679	0.2529
25					0.5178	1.8567	0.2166
26					0.4624	1.5769	0.184
27					0.4072	1.3049	0.1522
28					0.3518	1.0669	0.1245
29					0.2967	0.8421	0.0982
30					0.2411	0.6224	0.0726
31					0.1849	0.4079	0.0476
32					0.1299	0.2275	0.0265

Isotherm

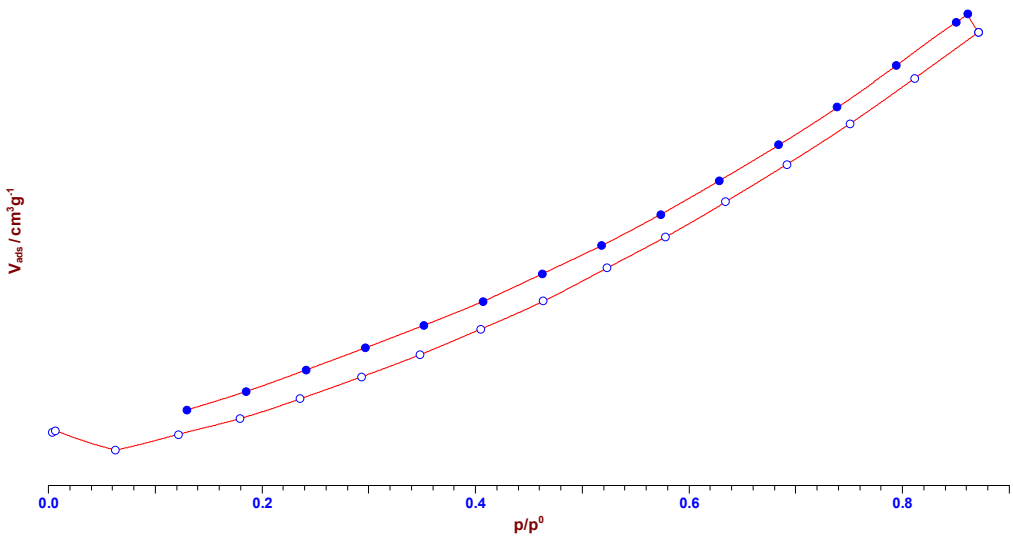

Pore volume (Gurvich) at p/p^0 0.95 is 0.0071 cm^3g^{-1}

Surface Area (Langmuir)

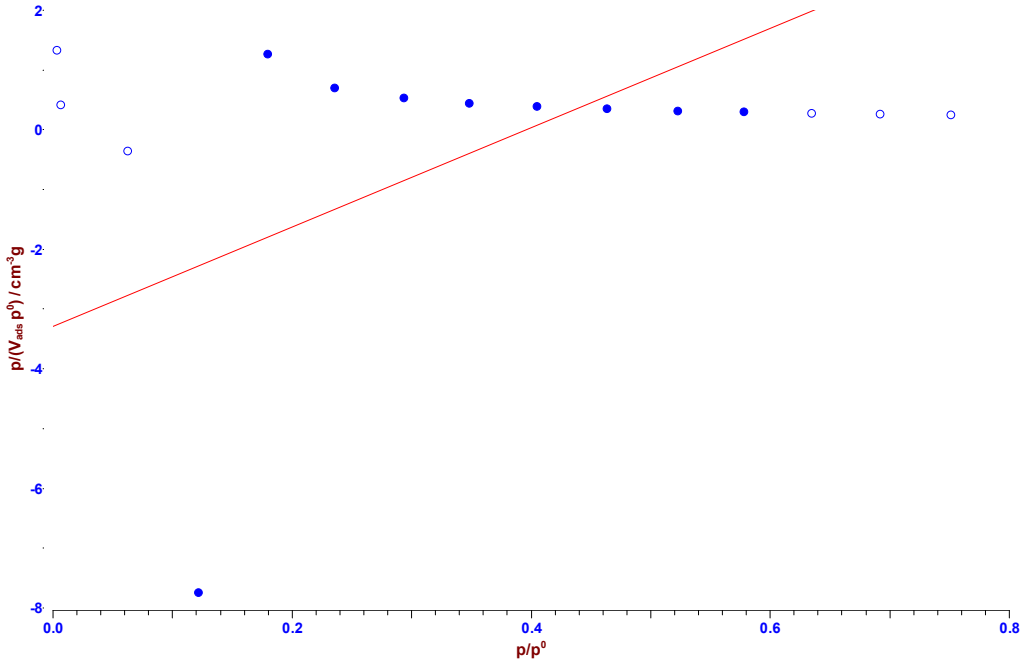

Linear regression from p/p^0	0.1 to 0.6
Offset:	-3.2898461 ± 2.25046136
Slope:	8.31617432 ± 5.92945108
R:	0.46836452
Monoloayer volume	0.1202 cm^3g^{-1}
Monoloayer amount:	0.0054 mmol g^{-1}
B:	-2.528
Calculation with a molecular area of	16.2 $Å^2$
Surface area was:	0.5234 m^2g^{-1}

Surface Area (B.E.T.) 2 Parameters Line

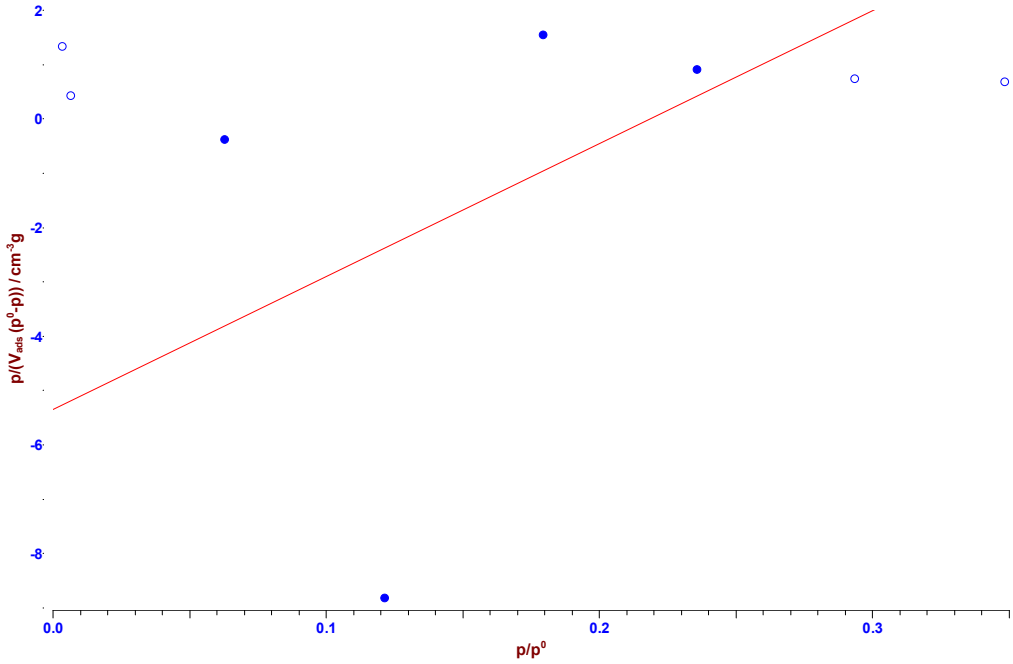

Linear regression from p/p^0	0.05 to 0.25
Offset:	-5.3476534 ± 6.90691129
Slope:	24.4701834 ± 42.3543767
R:	0.37818798
Monoloayer volume	0.0523 cm^3g^{-1}
Monoloayer amount:	0.0023 mmol g^{-1}
C:	-3.576
Calculation with a molecular area of	16.2 $Å^2$
Surface area was:	0.2276 m^2g^{-1}

Surface Area (B.E.T.) 3 Parameters Fit

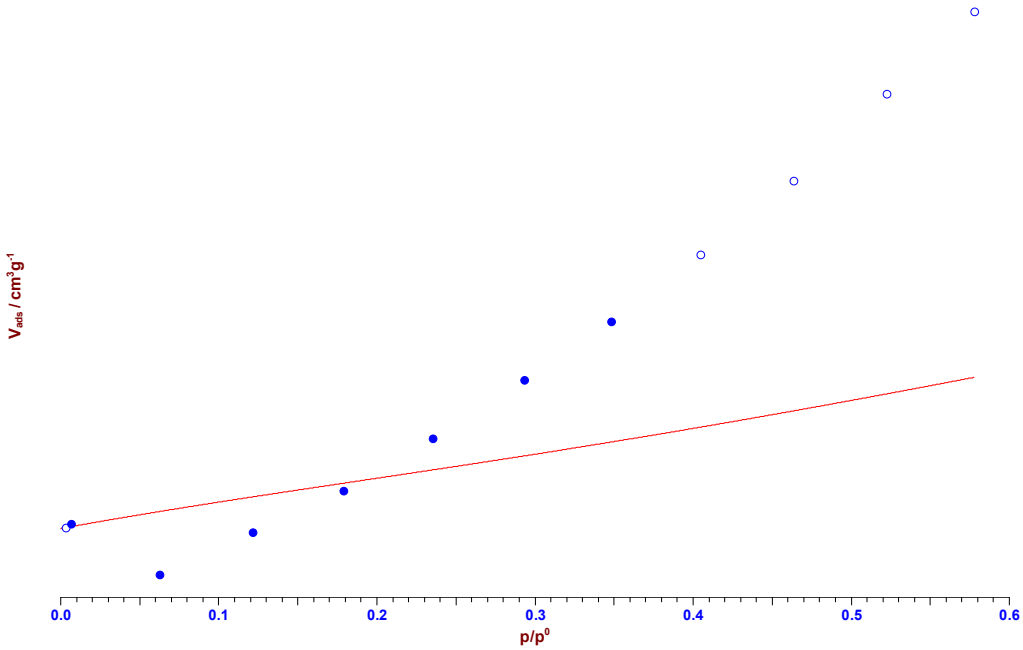

Simplex fit from p/p^0	0.005 to 0.4
r^2:	0.66815381
Monoloayer volume	0.3394 cm^3g^{-1}
Monoloayer amount:	0.0151 mmol g^{-1}
C:	3.2343
N:	5.4189
Calculation with a molecular area of	16.2 $Å^2$
Surface area was:	1.4774 m^2g^{-1}

Mesopores (B.J.H.)

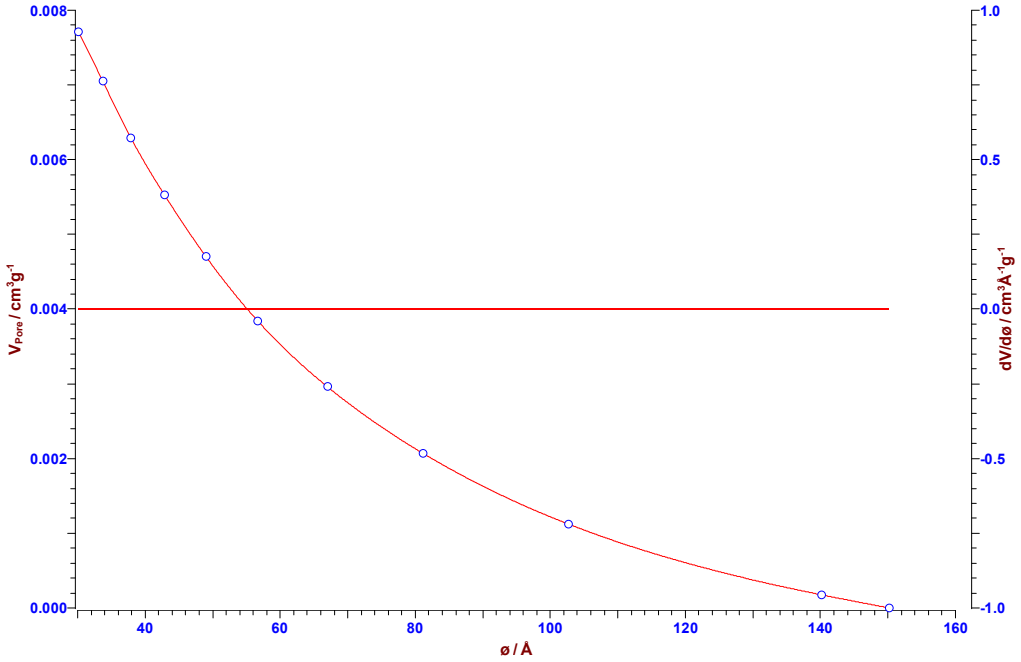

Calculations used Desorption Branch from p/p^0 0.3 to 0.95

with standard isotherm: Universal (Halsey)

from literature: ASTM Standards Designation: D 4641-87

Calculation with a molecular area of	16.2 $Å^2$
molecular weight of	28.01 g/mol
liquid density of	0.8086 g cm^{-3}
and surface tension of	8.85 Dyne cm^{-1}
Median pore diameter	56.49 Å
Maximum pore diameter	34.288 Å
Cumulative pore volume	0.0077 cm^3g^{-1}
Cumulative pore area	5.665 m^2g^{-1}

Mesopores (Cranston and Inkley)

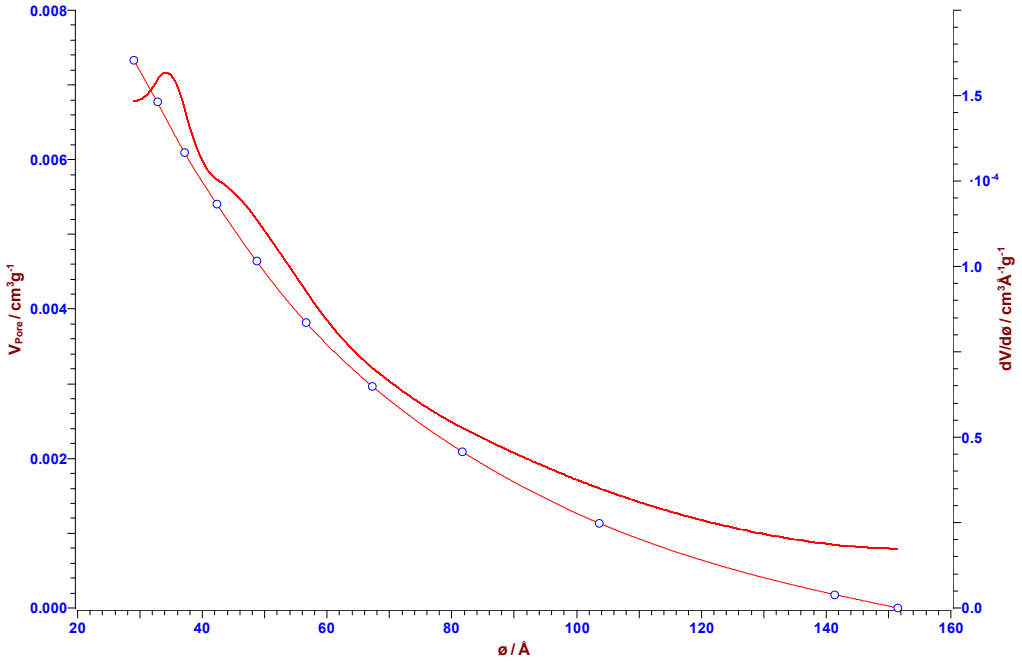

Calculations used Desorption Branch from p/p^0 0.3 to 0.95
with standard isotherm: Universal (Harkins,Jura)
from literature: ASTM Standards Designation: D 4641-87

Calculation with a molecular area of	16.2 $Å^2$
molecular weight of	28.01 g/mol
liquid density of	0.8086 g cm^{-3}
and surface tension of	8.85 Dyne cm^{-1}
Median pore diameter	58.343 Å
Maximum pore diameter	34.178 Å
Cumulative pore volume	0.0073 cm^3g^{-1}
Cumulative pore area	5.313 m^2g^{-1}

Mesopores (Modelless)

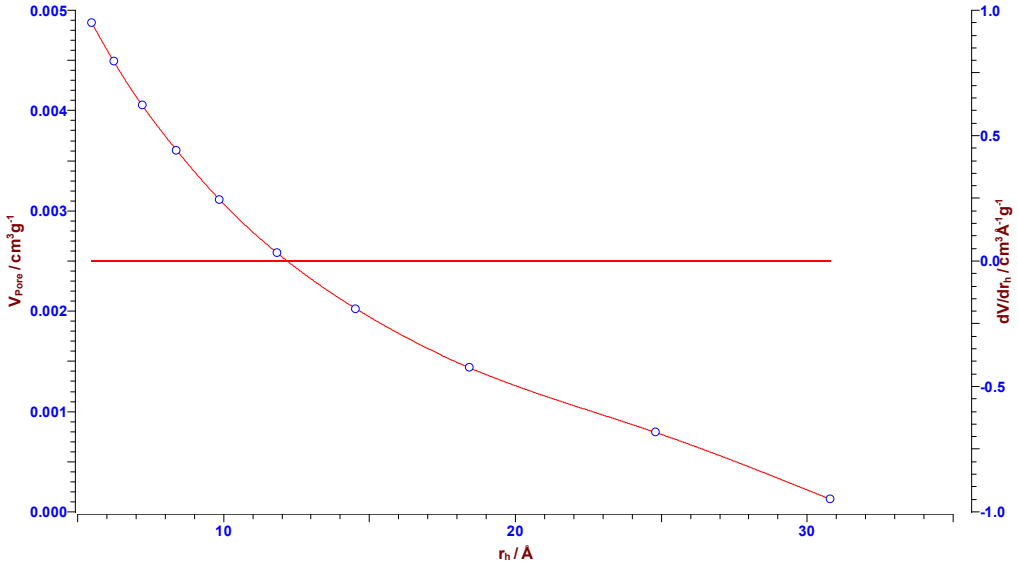

Calculations used Desorption Branch from p/p^0 0.3 to 0.95
with standard isotherm: Universal (Harkins,Jura)
from literature: ASTM Standards Designation: D 4641-87

Calculation with a molecular area of	16.2 $Å^2$
molecular weight of	28.01 g/mol
and liquid density of	0.8086 g cm^{-3}
Median hydraulic radius	9.5516 Å
Maximum hydraulic radius	5.4761 Å
Cumulative pore volume	0.0064 cm^3g^{-1}
Cumulative pore area	4.6916 m^2g^{-1}

Micropores (Horvath and Kawazoe)

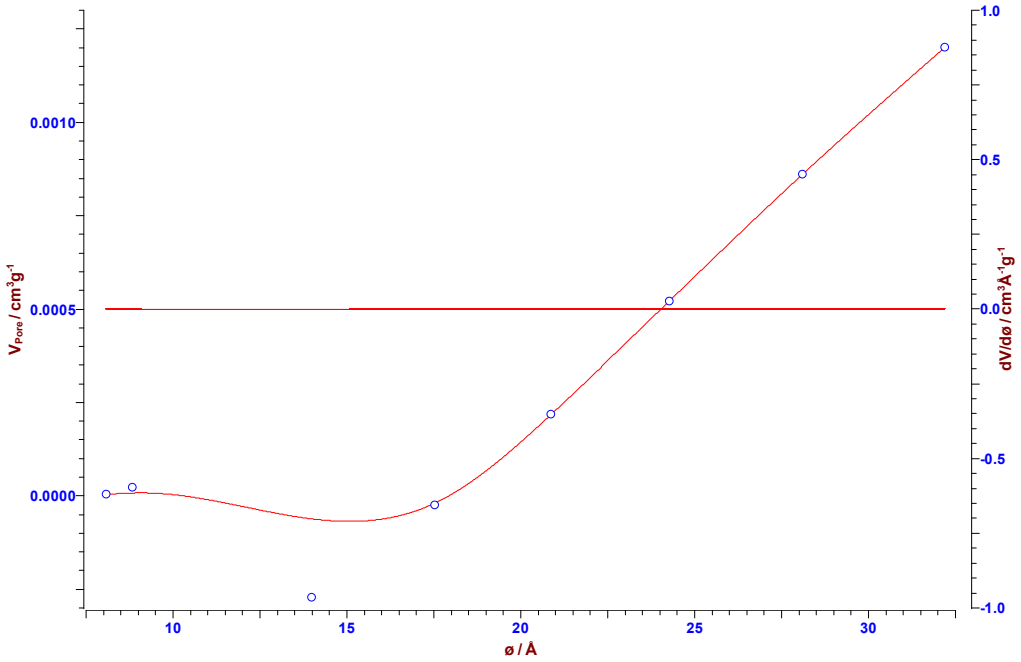

Calculations from p/p^0 0 to 0.35

with potential function: Nitrogen on Graphite @77.3 K
from literature: G. Horvath, K. Kawazoe, J. Chem. Eng. Japan, 16, 6(1983), 470-475

Calculation with a molecular area of	16.2 $Å^2$
molecular weight of	28.01 g/mol
and liquid density of	0.8086 g cm^{-3}
Median pore diameter	25.166 Å
Maximum pore diameter	24.207 Å
Cumulative pore volume	0.0012 cm^3g^{-1}
Cumulative pore area	0.85 m^2g^{-1}

Extended Report

Filename: C:\Surfer\result\Aishah\METHOD MESOPORE BAM-PM-102_110314_2.iso
Mass: 0.3023 g

Analytical Conditions

Blank done with: Helium

Adsorbate:	Nitrogen		
Equilibrium time [min:s]	0:00	0:00	0:00
Pre run time:	0:00 min		

Desorption	1st	2nd
Equilibrium time [min:s]	0:00	0:00

Adsorption Data

#	V_{dos} [cm^3]	p_{load} [Torr]	p_{equi} [Torr]	t_{equi} [min:s]	p^0 [Torr]	p/p^0	V_{ads} [cm^3g^{-1}]	n_{ads} [mmol g^{-1}]
1						9.2E-5	4.2607	0.6288
2						0.00016	7.2445	1.0692
3						0.0045	12.445	1.8367
4						0.0263	14.367	2.1203
5						0.0735	16.073	2.3722
6						0.1224	17.201	2.5387
7						0.1726	18.111	2.673
8						0.2201	18.846	2.7814
9						0.2731	19.573	2.8888
10						0.3242	20.232	2.9859
11						0.3719	20.824	3.0733
12						0.4274	21.449	3.1656
13						0.4842	22.124	3.2652
14						0.5371	22.789	3.3633
15						0.5849	23.391	3.4522
16						0.6331	24.032	3.5469
17						0.6825	24.747	3.6523
18						0.7327	25.514	3.7656
19						0.7898	26.474	3.9072
20						0.8471	27.668	4.0834

Desorption Data

#	V_{dos} [cm^3]	p_{equi} [Torr]	t_{equi} [min:s]	p^0 [Torr]	p/p^0	V_{ads} [cm^3g^{-1}]	n_{ads} [mmol g^{-1}]
21					0.8389	28.148	4.1542
22					0.8286	28.022	4.1357
23					0.7808	27.307	4.0302
24					0.7355	26.58	3.9228
25					0.6906	25.968	3.8325
26					0.6459	25.399	3.7485
27					0.6004	24.856	3.6685
28					0.5548	24.35	3.5938
29					0.5095	23.86	3.5215
30					0.4643	23.358	3.4473
31					0.4191	22.607	3.3365
32					0.3736	22.061	3.2559
33					0.3289	21.601	3.1881
34					0.2837	21.128	3.1182
35					0.2381	20.619	3.0431
36					0.1921	20.04	2.9576
37					0.147	19.444	2.8697
38					0.1029	18.74	2.7657

Isotherm

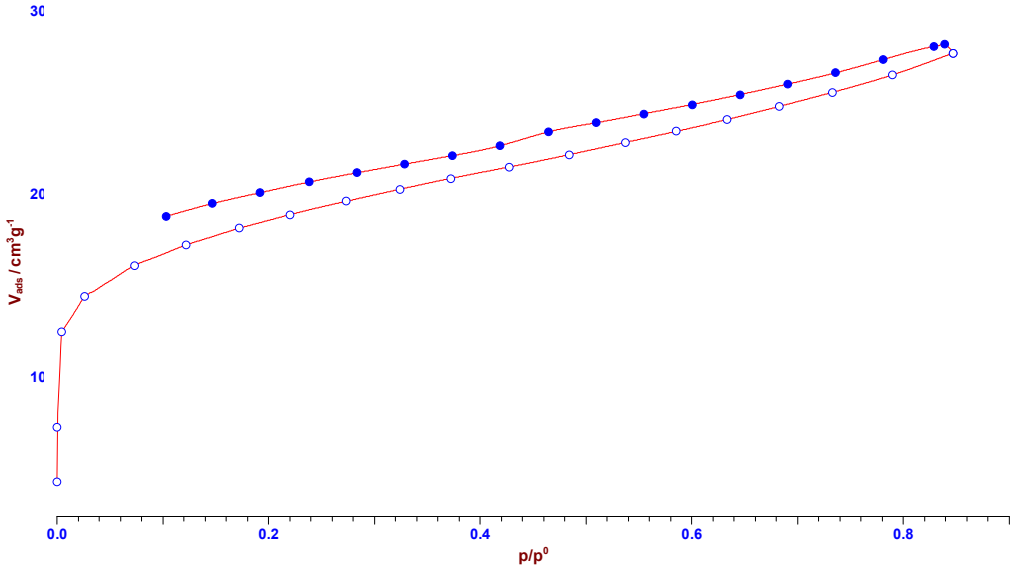

Pore volume (Gurvich) at p/p^0 0.95 is 0.0458 cm^3g^{-1}

Surface Area (Langmuir)

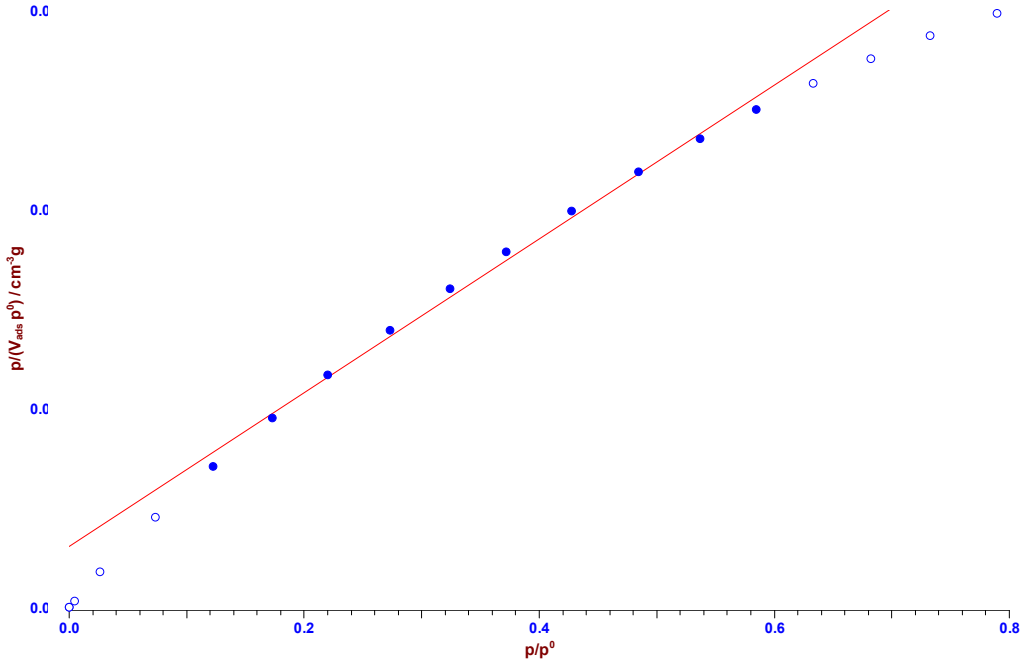

Linear regression from p/p^0	0.1 to 0.6
Offset:	0.00307987 ± 0.00036569
Slope:	0.03858877 ± 0.00095741
R:	0.99754682
Monoloayer volume	25.914 cm^3g^{-1}
Monoloayer amount:	1.1562 mmol g^{-1}
B:	12.529
Calculation with a molecular area of	16.2 $Å^2$
Surface area was:	112.8 m^2g^{-1}

Surface Area (B.E.T.) 2 Parameters Line

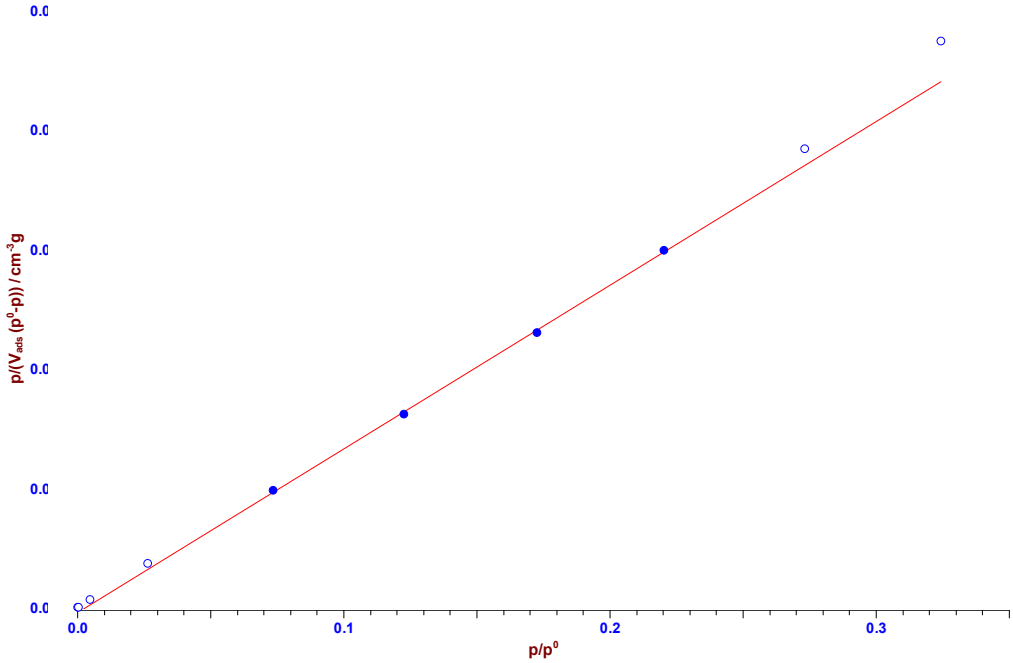

Linear regression from p/p^0	0.05 to 0.25
Offset:	-0.000183 ± 0.00019342
Slope:	0.06841617 ± 0.0012317
R:	0.99967605
Monoloayer volume	14.656 cm^3g^{-1}
Monoloayer amount:	0.6539 mmol g^{-1}
C:	-372.8
Calculation with a molecular area of	16.2 $Å^2$
Surface area was:	63.791 m^2g^{-1}

Surface Area (B.E.T.) 3 Parameters Fit

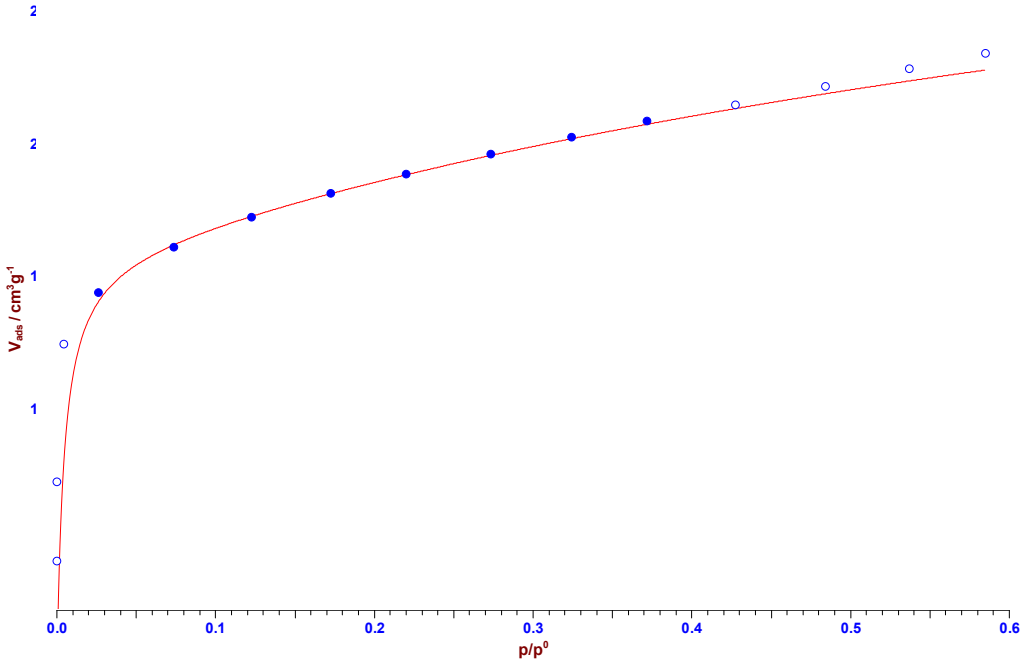

Simplex fit from p/p^0	0.005 to 0.4
r^2:	0.99782746
Monoloayer volume	15.908 cm^3g^{-1}
Monoloayer amount:	0.7098 mmol g^{-1}
C:	227.37
N:	2.2112
Calculation with a molecular area of	16.2 $Å^2$
Surface area was:	69.242 m^2g^{-1}

Mesopores (B.J.H.)

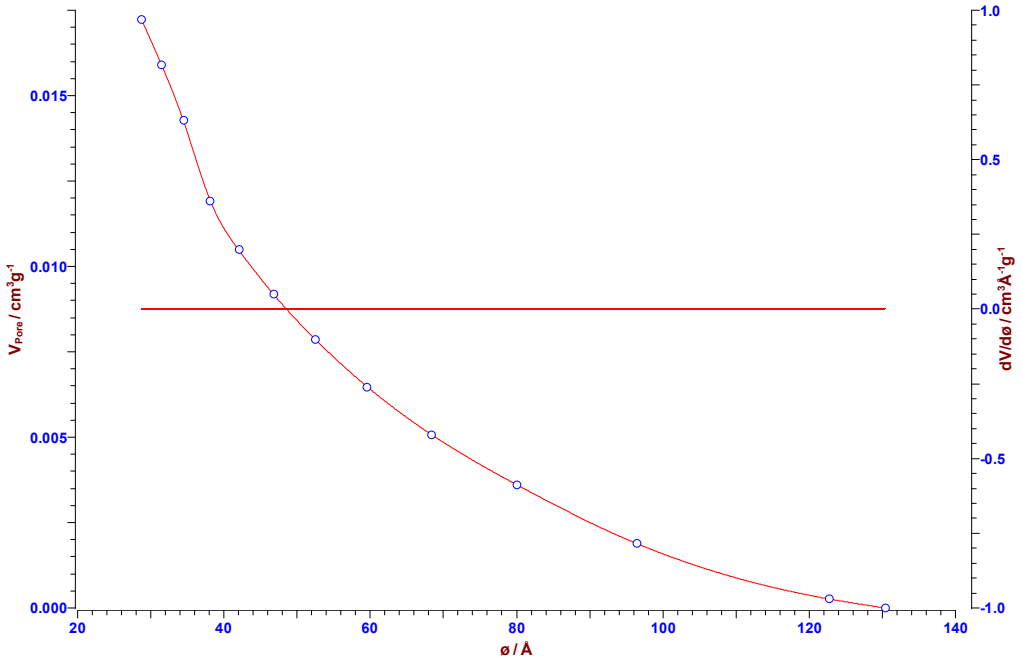

Calculations used Desorption Branch from p/p^0 0.3 to 0.95

with standard isotherm: Universal (Halsey)

from literature: ASTM Standards Designation: D 4641-87

Calculation with a molecular area of	16.2 $Å^2$
molecular weight of	28.01 g/mol
liquid density of	0.8086 g cm^{-3}
and surface tension of	8.85 Dyne cm^{-1}
Median pore diameter	49.106 Å
Maximum pore diameter	35.858 Å
Cumulative pore volume	0.0172 cm^3g^{-1}
Cumulative pore area	14.159 m^2g^{-1}

Mesopores (Cranston and Inkley)

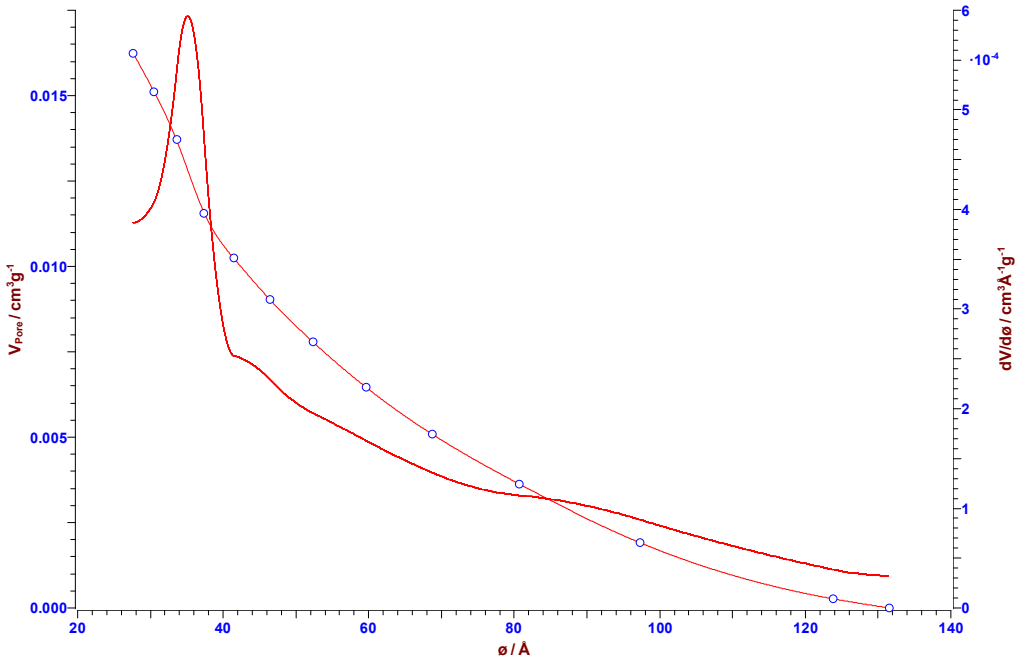

Calculations used Desorption Branch from p/p^0 0.3 to 0.95
with standard isotherm: Universal (Harkins,Jura)
from literature: ASTM Standards Designation: D 4641-87

Calculation with a molecular area of	16.2 $Å^2$
molecular weight of	28.01 g/mol
liquid density of	0.8086 g cm^{-3}
and surface tension of	8.85 Dyne cm^{-1}
Median pore diameter	50.64 Å
Maximum pore diameter	35.134 Å
Cumulative pore volume	0.0162 cm^3g^{-1}
Cumulative pore area	13.26 m^2g^{-1}

Mesopores (Modelless)

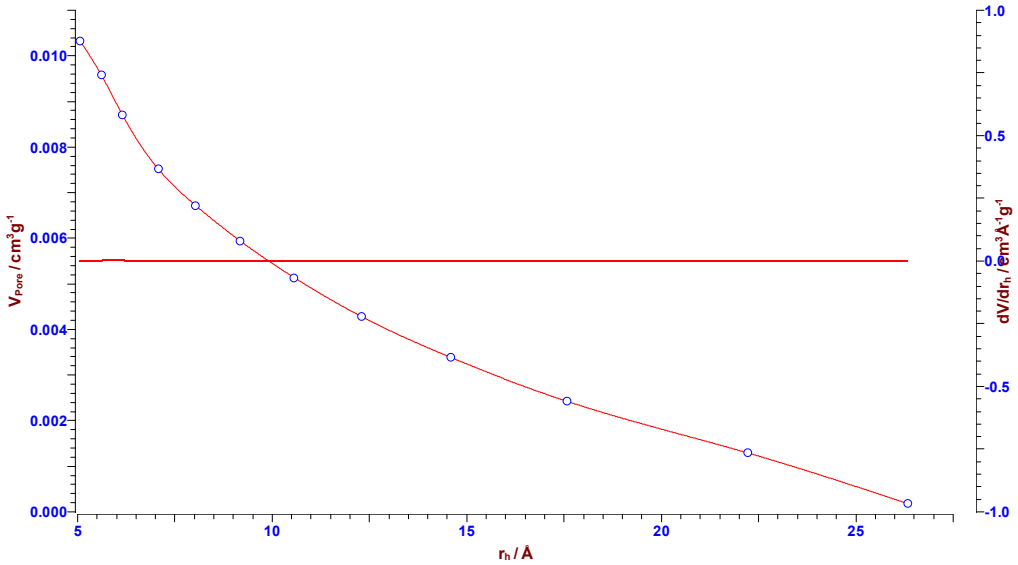

Calculations used Desorption Branch from p/p^0 0.3 to 0.95
with standard isotherm: Universal (Harkins,Jura)
from literature: ASTM Standards Designation: D 4641-87

Calculation with a molecular area of	16.2 $Å^2$
molecular weight of	28.01 g/mol
and liquid density of	0.8086 g cm^{-3}
Median hydraulic radius	89.938 Å
Maximum hydraulic radius	5.9138 Å
Cumulative pore volume	0.0435 cm^3g^{-1}
Cumulative pore area	11.359 m^2g^{-1}

Micropores (Horvath and Kawazoe)

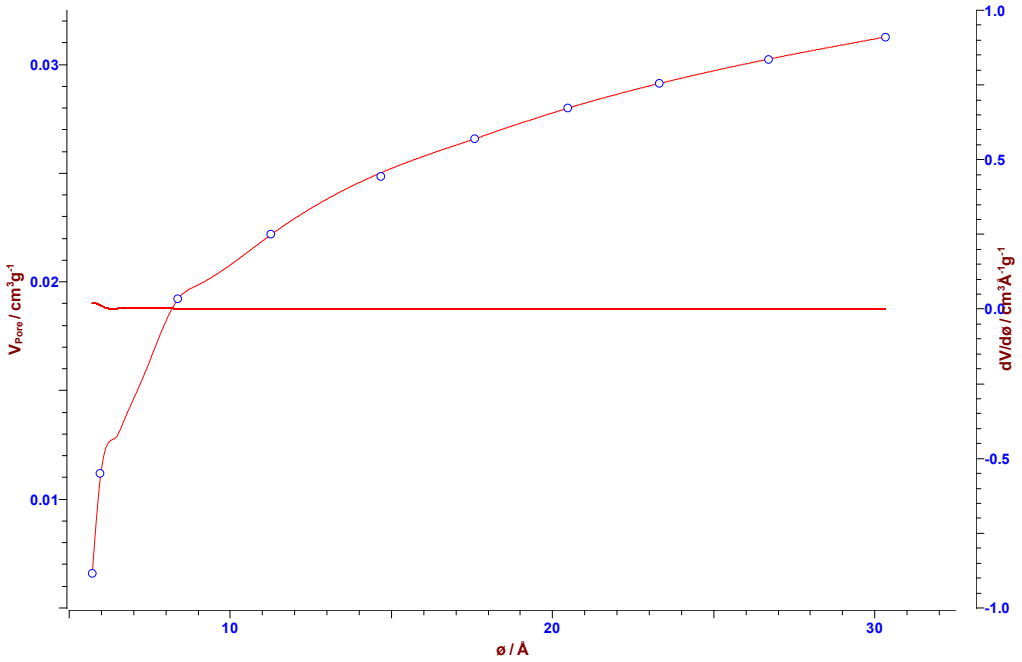

Calculations from p/p^0 0 to 0.35

with potential function: Nitrogen on Graphite @77.3 K
from literature: G. Horvath, K. Kawazoe, J. Chem. Eng. Japan, 16, 6(1983), 470-475

Calculation with a molecular area of	16.2 $Å^2$
molecular weight of	28.01 g/mol
and liquid density of	0.8086 g cm^{-3}
Median pore diameter	6.8115 Å
Maximum pore diameter	7.5813 Å
Cumulative pore volume	0.0313 cm^3g^{-1}
Cumulative pore area	72.441 m^2g^{-1}